

9-3-2014

# Advances in molecular quantum chemistry contained in the Q-Chem 4 program package

Shervin Fatehi

*University of Texas Rio Grande Valley*, shervin.fatehi@utrgv.edu

Follow this and additional works at: [https://scholarworks.utrgv.edu/chem\\_fac](https://scholarworks.utrgv.edu/chem_fac)

 Part of the [Chemistry Commons](#)

---

## Recommended Citation

Y. Shao et al., *Mol. Phys.* 113, 184 (2015)

This Article is brought to you for free and open access by the College of Sciences at ScholarWorks @ UTRGV. It has been accepted for inclusion in Chemistry Faculty Publications and Presentations by an authorized administrator of ScholarWorks @ UTRGV. For more information, please contact [justin.white@utrgv.edu](mailto:justin.white@utrgv.edu).

To appear in *Molecular Physics*  
Vol. 00, No. 00, Month 2014, 1–48

## ORIGINAL ARTICLE

### *Advances in molecular quantum chemistry contained in the Q-Chem 4 program package*

Yihan Shao<sup>a</sup>, Zhengting Gan<sup>a</sup>, Evgeny Epifanovsky<sup>a,b,c</sup>, Andrew T. B. Gilbert<sup>d</sup>, Michael Wormit<sup>e</sup>, Joerg Kussmann<sup>f</sup>, Adrian W. Lange<sup>g</sup>, Andrew Behn<sup>c</sup>, Jia Deng<sup>d</sup>, Xintian Feng<sup>b</sup>, Debashree Ghosh<sup>b,ca</sup>, Matthew Goldey<sup>c</sup>, Paul R. Horn<sup>c</sup>, Leif D. Jacobson<sup>g</sup>, Ilya Kaliman<sup>h</sup>, Rustam Z. Khaliullin<sup>c</sup>, Tomasz Kuś<sup>b</sup>, Arie Landau<sup>b,cb</sup>, Jie Liu<sup>i,g</sup>, Emil I. Proynov<sup>a,cc</sup>, Young Min Rhee<sup>c,cd</sup>, Ryan M. Richard<sup>g</sup>, Mary A. Rohrdanz<sup>g,ce</sup>, Ryan P. Steele<sup>j</sup>, Eric J. Sundstrom<sup>c</sup>, H. Lee Woodcock III<sup>ad</sup>, Paul M. Zimmerman<sup>c,k</sup>, Dmitry Zuev<sup>b</sup>, Ben Albrecht<sup>l</sup>, Ethan Alguire<sup>s</sup>, Brian Austin<sup>c</sup>, Gregory J. O. Beran<sup>m</sup>, Yves A. Bernard<sup>b</sup>, Eric Berquist<sup>l</sup>, Kai Brandhorst<sup>c,cf</sup>, Ksenia B. Bravaya<sup>b,cg</sup>, Shawn T. Brown<sup>a,ch</sup>, David Casanova<sup>c,n</sup>, Chung-Min Chang<sup>a</sup>, Yunqing Chen<sup>k</sup>, Siu Hung Chien<sup>a</sup>, Kristina D. Closser<sup>a</sup>, Deborah L. Crittenden<sup>d,ci</sup>, Michael Diedenhofen<sup>o</sup>, Robert A. DiStasio Jr.<sup>c</sup>, Hainam Do<sup>p</sup>, Anthony D. Dutoi<sup>q</sup>, Richard G. Edgar<sup>r</sup>, Shervin Fatehi<sup>s,j</sup>, Laszlo Fusti-Molnar<sup>a,cj</sup>, An Ghysels<sup>t,ek</sup>, Anna Golubeva-Zadorozhnaya<sup>b</sup>, Joseph Gomes<sup>c</sup>, Magnus W.D. Hanson-Heine<sup>p</sup>, Philipp H. P. Harbach<sup>e</sup>, Andreas W. Hauser<sup>c</sup>, Edward G. Hohenstein<sup>u</sup>, Zachary C. Holden<sup>g</sup>, Thomas-C. Jagau<sup>b</sup>, Hyunjun Ji<sup>v</sup>, Ben Kaduk<sup>w</sup>, Kirill Khistyayev<sup>b</sup>, Jaehoon Kim<sup>v</sup>, Jihan Kim<sup>c,cl</sup>, Rollin A. King<sup>x</sup>, Phil Klunzinger<sup>y</sup>, Dmytro Kosenkov<sup>h,cu</sup>, Tim Kowalczyk<sup>w,cv</sup>, Caroline M. Krauter<sup>e</sup>, Ka Un Lao<sup>g</sup>, Adèle Laurent<sup>b,cm</sup>, Keith V. Lawler<sup>c,cn</sup>, Sergey V. Levchenko<sup>b,co</sup>, Ching Yeh Lin<sup>d</sup>, Fenglai Liu<sup>al</sup>, Ester Livshits<sup>z</sup>, Rohini C. Lochan<sup>c</sup>, Arne Luenser<sup>f</sup>, Prashant Manohar<sup>b,cp</sup>, Samuel F. Manzer<sup>c</sup>, Shan-Ping Mao<sup>aa</sup>, Narbe Mardirossian<sup>c</sup>, Aleksandr V. Marenich<sup>ab</sup>, Simon A. Maurer<sup>f</sup>, Nicholas J. Mayhall<sup>c</sup>, C. Melania Oana<sup>b</sup>, Roberto Olivares-Amaya<sup>r,ac</sup>, Darragh P. O'Neill<sup>d</sup>, Eric Neuscammann<sup>c</sup>, John A. Parkhill<sup>c,cq</sup>, Trilisa M. Perrine<sup>k,cr</sup>, Roberto Peverati<sup>ab,c</sup>, Alexander Prociuk<sup>k</sup>, Dirk R. Rehn<sup>e</sup>, Edina Rosta<sup>b,cs</sup>, Nicholas J. Russ<sup>a</sup>, Shaama M. Sharada<sup>c</sup>, Sandeep Sharma<sup>ac</sup>, David W. Small<sup>c</sup>, Alexander Sodt<sup>c,t</sup>, Tamar Stein<sup>z,ce</sup>, David Stück<sup>c</sup>, Yu-Chuan Su<sup>aa</sup>, Alex J. W. Thom<sup>c,ct</sup>, Takashi Tsuchimochi<sup>w</sup>, Vitalii Vanovschi<sup>b</sup>, Leslie Vogt<sup>r</sup>, Oleg Vydrov<sup>w</sup>, Tao Wang<sup>b</sup>, Mark A. Watson<sup>ac,r</sup>, Jan Wenzel<sup>e</sup>, Alec White<sup>c</sup>, Christopher F. Williams<sup>g</sup>, Jun Yang<sup>ac</sup>, Sina Yeganeh<sup>w</sup>, Shane R. Yost<sup>c,w</sup>, Zhi-Qiang You<sup>as,g</sup>, Igor Ying Zhang<sup>af</sup>, Xing Zhang<sup>g</sup>, Yan Zhao<sup>ab</sup>, Bernard R. Brooks<sup>t</sup>, Garnet K. L. Chan<sup>ac</sup>, Daniel M. Chipman<sup>ag</sup>, Christopher J. Cramer<sup>ab</sup>, William A. Goddard III<sup>ah</sup>, Mark S. Gordon<sup>ai</sup>, Warren J. Hehre<sup>y</sup>, Andreas Klamt<sup>o</sup>, Henry F. Schaefer III<sup>aj</sup>, Michael W. Schmidt<sup>ai</sup>, C. David Sherrill<sup>u</sup>, Donald G. Truhlar<sup>ab</sup>, Arieh Warshel<sup>b</sup>, Xin Xu<sup>af</sup>, Alán Aspuru-Guzik<sup>r</sup>, Roi Baer<sup>z</sup>, Alexis T. Bell<sup>c</sup>, Nicholas A. Besley<sup>p</sup>, Jeng-Da Chai<sup>aa</sup>, Andreas Dreuw<sup>e</sup>, Barry D. Dunietz<sup>ak</sup>, Thomas R. Furlani<sup>al</sup>, Steven R. Gwaltney<sup>am</sup>, Chao-Ping Hsu<sup>ae</sup>, Yousung Jung<sup>v</sup>, Jing Kong<sup>a,cc</sup>, Daniel S. Lambrecht<sup>l</sup>, WanZhen Liang<sup>i</sup>, Christian Ochsenfeld<sup>f</sup>, Vitaly A. Rassolov<sup>an</sup>, Lyudmila V. Slipchenko<sup>h</sup>, Joseph E. Subotnik<sup>s</sup>, Troy Van Voorhis<sup>w</sup>, John M. Herbert<sup>g</sup>, Anna I. Krylov<sup>b</sup>, Peter M. W. Gill<sup>d</sup>, and, Martin Head-Gordon<sup>c\*</sup>

<sup>a</sup>*Q-Chem Inc, 6601 Owens Drive, Suite 105, Pleasanton, California 94588, USA;*

<sup>b</sup>*Department of Chemistry, University of Southern California, Los Angeles, California 90089, USA;*

<sup>c</sup>*Department of Chemistry, University of California, Berkeley, California 94720, USA;*

<sup>d</sup>*Research School of Chemistry, Australian National University, Canberra, Australia;*

- <sup>e</sup> *Interdisciplinary Center for Scientific Computing, Ruprecht-Karls University, Im Neuenheimer Feld 368, 69120 Heidelberg, Germany;*
- <sup>f</sup> *Department of Chemistry, University of Munich (LMU), Butenandtstr. 7, D-81377 München, Germany;*
- <sup>g</sup> *Department of Chemistry and Biochemistry, The Ohio State University, Columbus, Ohio 43210, USA;*
- <sup>h</sup> *Department of Chemistry, Purdue University, West Lafayette, Indiana 47907, USA;*
- <sup>i</sup> *Department of Chemistry, Xiamen University, Xiamen 361005, China;*
- <sup>j</sup> *Department of Chemistry, The University of Utah, Salt Lake City, Utah 84112, USA;*
- <sup>k</sup> *Department of Chemistry, University of Michigan, Ann Arbor, Michigan 48109, USA;*
- <sup>l</sup> *Department of Chemistry, University of Pittsburgh, Pittsburgh, Pennsylvania 15260, USA;*
- <sup>m</sup> *Department of Chemistry, University of California, Riverside, California 92521, USA;*
- <sup>n</sup> *IKERBASQUE - Basque Foundation for Science & Donostia International Physics Center (DIPC) & Kimika Fakultatea, Euskal Herriko Unibertsitatea (UPV/EHU) 20080 Donostia, Euskadi (Spain);*
- <sup>o</sup> *COSMOlogic GmbH & Co. KG, Imbacher Weg 46, D-51379 Leverkusen, Germany;*
- <sup>p</sup> *School of Chemistry, The University of Nottingham, University Park, Nottingham NG7 2RD, United Kingdom;*
- <sup>q</sup> *Department of Chemistry, University of the Pacific, 3601 Pacific Ave., Stockton, California 95211, USA;*
- <sup>r</sup> *Department of Chemistry and Chemical Biology, Harvard University, Cambridge, Massachusetts 02138, USA;*
- <sup>s</sup> *Department of Chemistry, University of Pennsylvania, Philadelphia, Pennsylvania 19104, USA;*
- <sup>t</sup> *Computational Biophysics Section, Heart, Lung, and Blood Institute, National Institutes of Health, Bethesda, Maryland 20892, USA;*
- <sup>u</sup> *School of Chemistry and Biochemistry, Georgia Institute of Technology, Atlanta, Georgia 30332, USA;*
- <sup>v</sup> *Graduate School of EEWS, KAIST, Daejeon 305-701, Republic of Korea;*
- <sup>w</sup> *Department of Chemistry, Massachusetts Institute of Technology, Cambridge, Massachusetts 02139, USA;*
- <sup>x</sup> *Department of Chemistry, Bethel University, 3900 Bethel Drive, St. Paul, Minnesota 55112, USA;*
- <sup>y</sup> *Wavefunction Inc., 18401 Von Karman Avenue, Suite 370, Irvine, California 92612 USA;*
- <sup>z</sup> *The Chaim Weizmann Institute of Chemistry, and the Fritz Haber Research Center for Molecular Dynamics, The Hebrew University of Jerusalem, Jerusalem 91904, Israel;*
- <sup>aa</sup> *Department of Physics, National Taiwan University, No. 1, Sec. 4, Roosevelt Road, Taipei 10617, Taiwan;*
- <sup>ab</sup> *Department of Chemistry, University of Minnesota, Minneapolis, Minnesota 55455, USA;*
- <sup>ac</sup> *Department of Chemistry, Princeton University, Princeton, New Jersey 08544, USA;*
- <sup>ad</sup> *Department of Chemistry, University of South Florida, Tampa, Florida 33620, USA;*
- <sup>ae</sup> *Institute of Chemistry, Academia Sinica, Nankang, Taipei 115, Taiwan;*
- <sup>af</sup> *Department of Chemistry, Fudan University, 220 Handan Road, Shanghai, 200433, China;*
- <sup>ag</sup> *Radiation Laboratory, University of Notre Dame, Notre Dame, Indiana 46556, USA;*
- <sup>ah</sup> *Materials and Process Simulation Center, California Institute of Technology, Pasadena, California 91125, USA;*
- <sup>ai</sup> *Department of Chemistry, Iowa State University, Ames, Iowa 50011, USA;*
- <sup>aj</sup> *Department of Chemistry, University of Georgia, Athens, Georgia 30602, USA;*

To appear in *Molecular Physics*

Vol. 00, No. 00, Month 2014, 3-18  
 Department of Chemistry and Biochemistry, Kent State University, Kent, Ohio 44242,  
 USA;

<sup>al</sup> Center for Computational Research, SUNY at Buffalo, Buffalo, New York, 14203, USA;

<sup>am</sup> Department of Chemistry, Mississippi State University, Mississippi State, Mississippi  
 39762, USA;

<sup>an</sup> Department of Chemistry and Biochemistry, University of South Carolina, Columbia,  
 South Carolina 29208, USA;

<sup>ca</sup> Current address: Physical and Materials Chemistry Division, CSIR-National Chemical  
 Laboratory, Pune 411008, India;

<sup>cb</sup> Current address: Faculty of Chemistry, Technion - Israel Institute of Technology,  
 Technion City, Haifa 3200008, Israel;

<sup>cc</sup> Current address: Department of Chemistry, Middle Tennessee State University, 1301  
 East Main Street, Murfreesboro, TN 37132, USA;

<sup>cd</sup> Current address: Department of Chemistry, Pohang University of Science and  
 Technology (POSTECH), Pohang, 790-784, Republic of Korea;

<sup>ce</sup> Current address: Department of Chemistry, Rice University, Houston, TX 77251, USA;

<sup>cf</sup> Current address: Institut für Anorganische und Analytische Chemie, Technische  
 Universität Braunschweig, 38106 Braunschweig, Germany;

<sup>cg</sup> Current address: Department of Chemistry, Boston University, Boston, MA 02215,  
 USA;

<sup>ch</sup> Current address: Pittsburgh Supercomputing Center, 300 S. Craig Street, Pittsburgh,  
 PA 15213, USA;

<sup>ci</sup> Current address: Department of Chemistry, University of Canterbury, Christchurch,  
 New Zealand;

<sup>cj</sup> Current address: OpenEye Scientific Software, 9 Bisbee Court, Suite D, Santa Fe, NM  
 87508, USA;

<sup>ck</sup> Current address: Center for Molecular Modeling, QCMM Alliance Ghent-Brussels,  
 Ghent University, Technologiepark 903, B-9052 Zwijnaarde, Belgium;

<sup>cl</sup> Current address: Department of Chemical and Biomolecular Engineering, KAIST,  
 Daejeon 305-701, Republic of Korea;

<sup>cm</sup> Current address: University of Nantes, CEISAM UMR 6230 2 rue de la Houssinière,  
 44322 Nantes Cedex 1, France;

<sup>cn</sup> Current address: Department of Chemistry, University of Nevada, Las Vegas, NV  
 89154, USA;

<sup>co</sup> Current address: Fritz-Haber-Institut der Max-Planck-Gesellschaft, Faradayweg 4-6,  
 D-14195 Berlin, Germany;

<sup>cp</sup> Current address: Birla Institute of Technology and Science, Pilani 333031, Rajasthan,  
 India;

<sup>cq</sup> Current address: Department of Chemistry & Biochemistry, University of Notre Dame,  
 Notre Dame, IN 46556, USA;

<sup>cr</sup> Current address: Department of Chemistry and Biochemistry, Ohio Northern  
 University, Ada, OH 45810, USA;

<sup>cs</sup> Current address: Department of Chemistry, Kings College London, London SE1 1DB,  
 United Kingdom;

<sup>ct</sup> Current address: Department of Chemistry, Cambridge University, Lensfield Road,  
 Cambridge CB2 1EW, United Kingdom;

<sup>cu</sup> Current address: Department of Chemistry and Physics, Monmouth University, West  
 Long Branch, New Jersey, 07764, USA;

<sup>cv</sup> Current address: Department of Chemistry, Western Washington University, 516 High  
 St, Bellingham, WA 98225., USA;

(Revised version: July 29, 2014)

1 A summary of the technical advances that are incorporated in the fourth major release of  
2 the Q-CHEM quantum chemistry program is provided, covering approximately the last seven  
3 years. These include developments in density functional theory methods and algorithms, NMR  
4 property evaluation, coupled cluster and perturbation theories, methods for electronically ex-  
5 cited and open-shell species, tools for treating extended environments, algorithms for walking  
6 on potential surfaces, analysis tools, energy and electron transfer modeling, parallel comput-  
7 ing capabilities, and graphical user interfaces. In addition, a selection of example case studies  
8 that illustrate these capabilities are given. These include extensive benchmarks of the compar-  
9 ative accuracy of modern density functionals for bonded and non-bonded interactions, tests  
10 of attenuated MP2 methods for intermolecular interactions, a variety of parallel performance  
11 benchmarks, and tests of the accuracy of implicit solvation models. Some specific chemical ex-  
12 amples include calculations on the strongly correlated Cr<sub>2</sub> dimer, exploring zeolite-catalyzed  
13 ethane dehydrogenation, energy decomposition analysis of a charged ter-molecular complex  
14 arising from glycerol photoionization, and natural transition orbitals for a Frenkel exciton  
15 state in a 9-unit model of a self-assembling nanotube.

16 **Keywords:** quantum chemistry; software; electronic structure theory; density functional  
17 theory; electron correlation; computational modeling; Q-Chem

## 18 1. Introduction

19 Quantum chemistry is a vigorous branch of theoretical chemistry, which is con-  
20 cerned with the development of practical theory, algorithms and software, based  
21 on approximations to the fundamental principles of quantum mechanics. Whilst  
22 the electronic Schrodinger equation offers an in-principle exact description of the  
23 behavior of electrons in molecules, subject to neglect of relativistic effects and  
24 nuclear motion, it is intractable to solve for realistic systems without approxi-  
25 mations. Several fundamental approaches to developing such approximations have  
26 been followed. The predominant methods for present-day applications to larger  
27 molecules are based on the framework of density functional theory (DFT). For  
28 smaller molecules, accuracy that is higher can be achieved by the use of wave func-  
29 tion theory (WFT) approaches such as perturbation theory, and coupled cluster  
30 theories. The optimal model for a given problem depends on the accuracy required,  
31 the computational resources available, and the size of the system under consider-  
32 ation. In general, useful electronic structure methods trade off accuracy against  
33 computational feasibility over a very wide range.

34 All of the approximate methods of quantum chemistry provide models by which  
35 the electronic potential energy of a molecule,  $E(\mathbf{R})$ , can be evaluated as a function  
36 of the clamped nuclear positions,  $\mathbf{R}$ . Walking on the potential energy surface down-  
37 wards to local minima leads to stable molecular structures, whose relative energies  
38 may be evaluated to predict reaction energies, and thus the thermodynamics of  
39 chemical transformations. Walking downhill in all directions but one (the reaction  
40 coordinate), and walking uphill in that direction leads to the first-order saddle  
41 points that separate reactants from products, and often play a major role in de-  
42 termining the kinetics of chemical reactions. Multistep reaction mechanisms can  
43 in principle be identified this way, with the aid of appropriate surface-walking al-  
44 gorithms. The spectroscopic methods that experimentally characterize molecular  
45 properties may also be evaluated from quantum chemical models as derivatives of  
46 the energy with respect to applied perturbations, such as electric fields or magnetic  
47 fields.

48 Putting together a useful range of quantum chemical models that offer differ-  
49 ent tradeoffs between achievable accuracy and computational effort for a range of  
50

---

51 \*Corresponding author. Email: mhg@cchem.berkeley.edu



1 molecular sizes is a non-trivial matter. Things are further complicated by the need  
2 to evaluate a range of responses of the energy to such key perturbations as moving  
3 the atoms, and applying fields. Therefore the realization of electronic structure sim-  
4 ulations through useful software has evolved over the past five decades into team  
5 science of increasingly large scale. Early efforts such as Gaussian 70 represented  
6 essentially the work of a single group (Sir John Pople's group). Today, there are  
7 roughly a dozen or so leading electronic structure codes in chemistry, all of which  
8 represent the end result of delocalized collaborations amongst many groups. In  
9 addition to Q-CHEM, and its collaborator, Spartan ([www.wavefun.com](http://www.wavefun.com)), leading  
10 commercial programs are represented by the ADF program [1], the Gaussian pro-  
11 gram [2], Jaguar [3], MolCAS [4], the Molpro package [5], and the TURBOMOLE  
12 program [6, 7]. Additionally there are a range of non-commercial programs which  
13 also represent the result of substantial collaborations. These include ACES III [8],  
14 CFOUR [9] Dalton [10], GAMESS US [11] and UK [12], NWChem [13], Psi [14].  
15 Many other related codes exist in the condensed matter physics community, where  
16 periodic rather than molecular systems are typically the primary focus.  
17

18  
19 Some 21 years ago, in late 1992, Peter Gill, then a postdoctoral researcher with  
20 John Pople, began writing the first lines of a then-new quantum chemistry pro-  
21 gram, called Q-CHEM, over his Christmas vacation. This paper marks the fourth  
22 major release of the resulting software, which now is over 3 million lines of code,  
23 and contains a very wide range of functionality for calculating the structure and  
24 properties of molecules using methods based on the principles of quantum me-  
25 chanics. The technical developments prior to 2000 were summarized in a first ma-  
26 jor review on Q-CHEM version 2 [15], whose author list also illustrates the rapid  
27 growth in the number of contributors, which included not only members of the early  
28 founders' groups, but also many new groups including most famously the 1998 No-  
29 bel Laureate, Sir John Pople [16]. Subsequent advances between 2000 and 2006  
30 were contained in Q-CHEM version 3.0, and were also documented in a review [17].  
31

32 A very recent overview of Q-CHEM [18] provides some further details of the his-  
33 torical development and evolution of the package, as well as a high-level summary  
34 of its capabilities. Today Q-CHEM serves the needs of a very large number of users  
35 (over 50,000 including both direct users, and the very large number of users who  
36 access its capabilities as the back-end of the widely used Spartan modeling pack-  
37 age). Q-CHEM also serves the needs of one of the larger development communities  
38 in quantum chemistry, currently consisting of over 200 developers spread across a  
39 large number of research groups, primarily in academia. For the developers of the  
40 code, Q-CHEM is an open team-ware project, where the source code is provided  
41 freely, and distributed and updated through a central code repository. The rights  
42 of other developers and the company itself are protected through a straightfor-  
43 ward non-disclosure agreement that places no restrictions on a developer's ability  
44 to publish research describing new theory or algorithms. The activity of the devel-  
45 oper community is the key driver behind technical advances in Q-CHEM software,  
46 so that this is very much a symbiotic relationship.  
47

48  
49 This paper summarizes the fourth major release of Q-CHEM, and seeks to ac-  
50 complish three principal purposes. The first purpose is to review a selection of  
51 the technical advances that have occurred in quantum chemistry over the past 7  
52 years or so which are incorporated into the Q-CHEM 4. The review is, by necessity,  
53 relatively non-technical, with a focus on the physical content of the methods and  
54 algorithms. We provide brief overviews of the strengths and weaknesses of a large  
55 and diverse selection of new methods from the perspective of utility in chemical  
56 applications. Complete citations are given to the original literature for readers who  
57 are still hungry for further detail. The second purpose is to provide some example  
58  
59  
60

1 case studies of the new methods, particularly those that are not widely used as  
2 yet. Such studies provide some specific illustrations of the utility of the methods  
3 described in this work for particular chemical applications.

4 The third purpose of the paper is to serve as the literature citation for release  
5 4 of the Q-CHEM quantum chemistry software package. This purpose is useful  
6 because it leads via the technical review to full literature citations for the key  
7 algorithms contained in the program, at the moment in time when this version is  
8 current. By contrast, web sites are continually updated (and archival material is  
9 continually removed), and an author list is an “empty citation” that does not give  
10 the researcher any direct path to further information. The author list of this paper  
11 comprises the scientists who have contributed to Q-CHEM in either release 3 or  
12 release 4. Authors of earlier versions who have not subsequently contributed may  
13 be seen in the reviews describing release 2 [15] and release 3 [17].

14 The remainder of this paper addresses the challenge of reviewing the science  
15 and presenting selected examples under the following organization. The main areas  
16 where methodological advances have been made within our code are reviewed  
17 together with a variety of example calculations that illustrate accuracy and/or  
18 computational performance, and a selection of chemical case studies. The sequence  
19 of topics begins with general purpose electronic structure methods. We treat density  
20 functional theory (DFT), which is the most widely used family of electronic  
21 structure methods, in Sec. 2, and discuss recently added functionals for improved  
22 accuracy, and algorithmic improvements. Developments in wave function based  
23 methods are reviewed in Sec. 3. They have the great strength of systematic im-  
24 provability, particularly at the level of coupled cluster theory, where object-oriented  
25 design is vital to facilitate development and implementation of new methods. Sup-  
26 port for parallel and GPU computing environments is summarized in Sec. 4, with  
27 some example timings.

28 The standard (and many non-standard) electronic structure methods can be used  
29 in a great many ways, starting with recent developments in moving around on the  
30 resulting potential energy surfaces, which are discussed in Sec. 5. We turn next to  
31 the problem of treating extended environments in Sec. 6, which is important for  
32 modeling molecules in solution, large clusters, or active sites abstracted from com-  
33 plex systems such as proteins or heterogeneous solids. Energy and electron transfer  
34 capabilities are discussed in Sec. 7, followed by methods for chemical analysis of  
35 (at least some classes of) calculations in Sec. 8. As appropriate for a review of a  
36 “back-end” code, as Q-CHEM fundamentally is, we then finish with a short discus-  
37 sion of the available “front-ends” that provide input to the back-end, and visualize  
38 the resulting output.

## 44 2. Density functional theory

### 45 2.1. *Functionals*

46 Kohn-Sham density functional theory [19] and its extensions provide a foundation  
47 for the development of model functionals, but no prescription for how such devel-  
48 opment should be accomplished. Accordingly, this is an area of great activity. The  
49 full range of density functionals supported in Q-CHEM is too large to comfortably  
50 list here, and includes functionals ranging from vintage to brand new. Furthermore,  
51 assessing the strengths and weaknesses of different functionals is a major ongoing  
52 effort that involves the entire community of both developers and applications spe-  
53 cialists. An overview paper cannot summarize this effort, although we can provide  
54 a few leading references to comparative studies [20–23] and the main issues [24, 25].

1 We shall discuss some of the new functionals added to Q-CHEM over recent years  
2 by considering the current main directions for improved physical content over the  
3 predominant density functional for chemistry, which during the last decade was  
4 certainly the global hybrid, B3LYP [26].

- 5  
6 (1) *Meta-GGA and hybrid meta-GGA functionals*: Including the kinetic energy  
7 density,  $\tau$ , gives flexibility beyond global hybrids, and therefore is used in  
8 many modern density functionals, including M06-L, M06, M06-2X, and M06-  
9 HF [27], as well as the recently introduced M11 and M11-L functionals [28,  
10 29]. These functionals often yield improved accuracy for thermochemistry  
11 and noncovalent interactions relative to functionals that do not depend on  
12  $\tau$ . M06-L and M11-L have the considerable computational advantage of not  
13 requiring exact exchange, although there is reduced accuracy, particularly for  
14 reaction barrier heights. Other meta-GGA functionals include the constraint-  
15 based TPSS [30], as well as its 1-parameter hybrid cousin, TPSSH [30].
- 16 (2) *Range-separated hybrid functionals*: Self-interaction error (SIE), where an  
17 electron artificially sees a fraction of itself, is a well-known defect of standard  
18 density functionals, and causes artifacts that include spurious delocalization  
19 of unpaired electrons [31, 32], and charge-transfer excited states that can be  
20 drastically too low [33, 34]. Whilst very difficult to remove fully, SIE can  
21 be significantly reduced by including 100% exact (wave function) exchange  
22 at large electron-electron distances, and a much smaller fraction at short  
23 distances, where DFT exchange functionals are effective. Examples of func-  
24 tionals of this type include the LC- $\omega$ PBE family of methods [35–38], the  
25  $\omega$ B97 functionals [39–42], M11 [28], as well as tuned functionals of the BNL  
26 type [43, 44], where the range-separation parameter can be chosen for the  
27 problem at hand based on physical criteria [45, 46]. Another option is to in-  
28 clude 100% HF exchange at *all* inter-electronic distances, as in the M06-HF  
29 functional [47]. SIE at short inter-electronic distances also affects TDDFT  
30 predictions of core excitation energies and near-edge X-ray absorption fine  
31 structure (NEXAFS) spectra. These short-range SIE errors can be substan-  
32 tially reduced by short-range corrected functionals [48], which are available  
33 in Q-CHEM.
- 34 (3) *Non-bonded interactions*: Noncovalent interactions, particularly van der  
35 Waals forces, involve nonlocal correlation effects that are very difficult to  
36 treat within a standard correlation functional. Thus, the characteristic  $R^{-6}$   
37 long-range interaction potential is absent in traditional local and semi-local  
38 density functionals [49]. Whilst it is quite often possible to still obtain an  
39 accurate result at the van der Waals minimum without including the long-  
40 range  $R^{-6}$  behavior (e.g. with M06-2X or M06-L), several viable methods  
41 have emerged that recover the correct long-range behavior [50]:
- 42 • A vast range of dispersion-corrected functionals that include damped  
43  $C_6/R^6$  atom-atom potentials, based on either the Grimme -D2 [51] or  
44 -D3 [52] parameterizations are available. Computationally virtually free,  
45 but not actually density functionals at all, these methods represent the  
46 simplest possible treatment of dispersion.
  - 47 • Becke’s exchange dipole model (XDM) [53, 54] is a novel and accurate  
48 method for treating dispersion which has been implemented in Q-CHEM  
49 in an efficient and numerically stable form [55].
  - 50 • van der Waals density functionals, which numerically integrate a non-  
51 local correlation functional that depends simultaneously on  $\rho(\mathbf{r})$  and  
52  $\rho(\mathbf{r}')$ , are a soundly based approach. Examples include vdW-DF-04 [56],  
53 vdW-DF-10 [57], VV09 [58], and VV10 [59]. The VV10 form is also used  
54  
55  
56  
57  
58  
59  
60



1 in the very recently developed  $\omega$ B97X-V functional [42], a 10 parameter  
2 semi-empirical functional that is a further evolution of the  $\omega$ B97 fam-  
3 ily that reduces the number of empirical parameters, while improving  
4 physical content.  
5

- 6 (4) *Double hybrid functionals*: Based on Görling-Levy perturbation theory as  
7 well as semi-empirical considerations, functionals that include second-order  
8 perturbation theory (PT2) corrections to a Kohn-Sham reference can yield  
9 improved accuracy for both bonded and non-bonded interactions, albeit with  
10 increased computational cost and a need for larger basis sets. Q-CHEM con-  
11 tains numerous double hybrids, including B2PLYP [60] and B2PLYP-D [61],  
12 XYG3 [62],  $\omega$ B97X-2 [41], and PBE0-2 [63]. XYGJ-OS is an opposite spin  
13 double hybrid [64], which scales as only  $O(M^4)$ , for which the analytical  
14 gradient is also available [65].  
15 (5) *Becke post-SCF functionals*: The semi-empirical B05 post-SCF functional[66,  
16 67] uses the Becke-Roussel exchange model[68] to compute a local analogue  
17 to the exact exchange hole. The extent of delocalization of the exact exchange  
18 hole is used as a parameter for capturing both same-spin and opposite-spin  
19 nondynamical correlation within a single determinant framework. Coupled  
20 with the modified Bc88 correlation functional (BR94)[69, 70] to capture dy-  
21 namical correlation, the performance of the 6-parameter B05 functional paral-  
22 lels the performance of existing hybrid meta-GGA functionals for atomization  
23 energies and barrier heights. A self-consistent version of the B05 functional  
24 has been efficiently implemented[71] into Q-CHEM 4, including a resolution-  
25 of-the-identity (RI) version that greatly reduces the cost of computing the  
26 exact exchange energy density[72].  
27  
28

29 To provide just a glimpse of the comparative performance of some of the stan-  
30 dard functionals available in Q-CHEM, Table 1 shows the RMS errors associated  
31 with a variety of density functionals on some established test sets for bonded and  
32 non-bonded interactions. Of the 10 datasets, the first 4 (TAE, Alk19, DBH24, and  
33 G21IP) correspond to thermochemistry (TC) datapoints (203 total), while the lat-  
34 ter 6 (HW30, S22, S66, A24, X40, and DS14) correspond to noncovalent interactions  
35 (NC) datapoints (196 total). Computational details and specific dataset informa-  
36 tion can be found in Reference [42]; comparisons of GGA functionals trained on  
37 the same data with different choices of non-local exchange and correlation have  
38 also been presented recently [73].  
39

40 For the bonded interactions, it is clear that exact exchange is very useful, as  
41 the two best functionals are the range-separated hybrid GGA  $\omega$ B97X-V functional  
42 and the global hybrid meta-GGA M06-2X functional, with RMS errors around 3  
43 kcal/mol. In comparison, the best local functional for thermochemistry (M06-L)  
44 has an RMS error that is nearly double that of the best hybrid functional. For  
45 non-bonded interactions, the range-separated hybrid GGA  $\omega$ B97X-V functional  
46 outperforms the next best density functional by almost a factor of 2. However, local  
47 meta-GGA functionals like M06-L can compete with well-established dispersion-  
48 corrected hybrid functionals such as  $\omega$ B97X-D. On the popular S22 dataset, the  
49 three best density functionals are  $\omega$ B97X-V,  $\omega$ B97X-D, and M06-L, with RMS  
50 errors of 0.23, 0.41, and 0.43 kcal/mol, respectively. For a more comprehensive  
51 assessment of these density functionals on a dataset of over 2400 datapoints, the  
52 reader is referred to Table 6 in Reference [42].  
53  
54  
55  
56  
57  
58  
59  
60

Functional datapoints	#	TAE 124	Alk19 19	DBH24 24	G2IP 36	HW30 30	S22 22	S66 66	A24 24	X40 40	DS14 14	TC 203	NC 196
PBE-D2	1	16.94	26.21	10.37	4.81	0.71	0.70	0.63	0.59	0.74	0.57	16.01	0.67
PBE-D3	2	16.85	20.93	10.27	4.81	0.48	0.60	0.46	0.41	0.59	0.47	15.20	0.50
B3LYP-D2	4	5.28	0.64	5.28	4.86	0.53	0.74	0.62	0.39	0.47	0.28	4.95	0.55
B3LYP-D3	5	5.23	5.50	5.23	4.86	0.35	0.50	0.43	0.23	0.34	0.23	5.19	0.38
B3LYP-NL	4	5.92	14.74	6.01	4.35	0.21	0.68	0.46	0.27	0.43	0.24	7.03	0.43
B97-D2	11	4.06	9.28	4.36	3.48	0.35	0.60	0.36	0.26	0.43	0.25	4.74	0.39
B97-D	10	5.18	10.48	7.18	4.47	0.40	0.54	0.52	0.32	0.59	0.37	6.03	0.49
VV10	2	12.46	5.85	9.86	5.43	0.43	0.63	0.52	0.41	0.63	0.52	10.71	0.53
LC-VV10	3	5.30	19.04	3.02	5.23	0.30	0.51	0.31	0.15	0.41	0.12	7.55	0.34
$\omega$ B97X	14	3.50	2.84	2.33	3.79	0.45	0.95	0.50	0.40	0.54	0.36	3.38	0.55
$\omega$ B97X-D	15	3.65	2.90	2.07	3.82	0.35	0.41	0.52	0.15	0.49	0.18	3.47	0.43
$\omega$ B97X-V	10	3.34	0.71	1.81	3.57	0.20	0.23	0.18	0.09	0.21	0.05	3.09	0.18
M06-L	34	5.54	8.11	5.38	5.60	0.35	0.43	0.36	0.23	0.48	0.25	5.82	0.38
M06	30	3.94	4.63	2.97	3.78	0.33	0.77	0.53	0.25	0.57	0.34	3.88	0.51
M06-2X	33	3.24	5.27	1.12	3.49	0.46	0.47	0.29	0.28	0.28	0.20	3.37	0.34
M11-L	43	6.62	29.35	3.54	4.50	0.48	0.91	0.81	0.46	1.23	0.59	10.60	0.84
M11	40	4.37	3.94	1.48	4.64	0.38	0.58	0.41	0.27	0.54	0.30	4.15	0.44

Table 1. RMS errors in kcal/mol for 17 density functionals available in Q-CHEM on 10 datasets comprised of 399 datapoints. The first 4 datasets contain bonded interactions, representative of thermochemistry (TC), evaluated using the aug-cc-pVQZ basis. The latter 6 datasets contain noncovalent (NC) interactions, which are evaluated using the aug-cc-pVTZ basis, except for the X40 data, which used the def2-TZVPPD basis set. The TC datasets are (i) non-multireference total atomization energies (TAE) [74], (ii) atomization energies of  $n=1-8$  alkanes (Alk19) [75], (iii) diverse barrier heights (DBH24) [76–78], (iv) adiabatic ionization potentials (G21P) [79, 80], (v) weak hydrocarbon-water interactions (HW30) [81], (vi) hydrogen-bonded and dispersion-bonded complexes (S22) [82, 83], (vii) interaction energies of relevant biomolecular structures (S66) [84, 85], (viii) small noncovalent complexes (A24) [86], (ix) noncovalent interactions of halogenated molecules (X40) [87], and (x) interactions of complexes containing divalent sulfur (DS14) [88]. The final two columns give the overall RMS errors for the 4 TC datasets and 6 NC datasets.

## 2.2. Electric and magnetic molecular properties

The calculation of molecular properties provides an important link to experiment and many linear-scaling methods have been developed over recent years that allow to compute molecular systems with more than 1000 atoms (see, e.g., Refs. [89–92]). The Q-CHEM program package allows the computation of a wide range of properties at the Hartree-Fock and Kohn-Sham density functional theory level. Apart from determining geometries, vibrational spectra, and electronic excitations, the new version of Q-CHEM offers several new and improved efficient linear-scaling methods to evaluate different electric and magnetic response properties for large systems. These range from the calculation of NMR chemical shieldings using density matrix-based coupled-perturbed SCF (D-CPSCF) theory [93, 94] (also for large basis sets with up to  $g$  functions in the new version) to electric response properties [95, 96] by an implementation of the density matrix-based time-dependent SCF algorithm (D-TDSCF) [97] that allows for calculating static and dynamic polarizabilities and first hyperpolarizabilities. Here, an overall asymptotic linear-scaling behavior can be reached by employing  $\mathcal{O}(N)$  integral evaluations based on CFMM [98] and LinK [99, 100] in combination with efficient sparse algebra routines [93].

Furthermore, the combination of linear-scaling QM methods for calculating molecular properties with simple MM schemes (QM/MM) have proven to be a very valuable tool for studying complex molecular systems. The linear-scaling methods allow to systematically converge the property with the chosen QM sphere and convergence for QM/MM schemes is typically clearly faster than in pure QM calculations, since in complex systems long-range electrostatics are accounted for (see, e.g., Refs. [92, 101, 102]).

As another new feature, the calculation of indirect nuclear spin-spin coupling constants ( $J$ -coupling) [103, 104] is introduced. The implementation uses the LinK scheme [99, 100] for the construction of exchange-type matrices for nonmetallic systems. A fully density matrix-based algorithm is currently in development [105]. Basis functions with angular momenta up to  $g$  are supported. Predictions of good accuracy for  $J$ -couplings can be obtained [106, 107] especially when using specialized basis sets [108–111], several of which have been added to the basis set library.

The  $J$ -based configurational analysis [112] is a robust technique for the structural elucidation of even large organic molecules [113]. In the past, analyses of

1  $J$ -couplings have mostly utilized the Karplus equations [114–116], which relates  
2  $^3J$ -coupling constants to the dihedral angle between atoms. Moving from empirical  
3 equations to predictions from first principles, for example with DFT, is desirable  
4 not only because the predictions are expected to be more reliable, but also be-  
5 cause it expands their applicability. Long-range  $J$ -couplings [117], or even couplings  
6 through hydrogen bonds [118], neither of which are tractable with current empiri-  
7 cal methods, can naturally be studied by computational chemistry if an adequate  
8 level of electronic structure theory is selected.  
9

### 10 11 12 13 **2.3. Algorithm developments**

14 A great variety of algorithmic improvements for DFT calculations have been incor-  
15 porated into Q-CHEM. Those to do with parallel computing are covered separately  
16 in Sec. 4.

17 *Resolution-of-the-identity methods:* For large AO basis sets in particular, resolu-  
18 tion of the identity (RI) methods offer substantially improved performance relative  
19 to exact evaluation of two-electron integrals with nearly negligible loss of accuracy,  
20 if appropriately optimized auxiliary basis sets are employed. The Karlsruhe group  
21 associated with TurboMole has been amongst the leading developers of such ba-  
22 sis sets. The standard RI method may be further enhanced by performing local  
23 fitting of a density or function pair element. This is the basis of the atomic-RI  
24 method (ARI), which has been developed for both Coulomb (J) matrix [119] and  
25 exchange (K) matrix evaluation [120]. In ARI, only nearby auxiliary functions  $K(r)$   
26 are employed to fit the target function. This reduces the asymptotic scaling of the  
27 matrix-inversion step as well as that of many intermediate steps in the digestion of  
28 RI integrals. Briefly, atom-centered auxiliary functions on nearby atoms are only  
29 used if they are within the outer radius ( $R_1$ ) of the fitting region. Between  $R_1$  and  
30 the inner radius ( $R_0$ ), the amplitude of interacting auxiliary functions is smoothed  
31 by a function that goes from zero to one and has continuous derivatives. To op-  
32 timize efficiency, the van der Waals radius of the atom is included in the cutoff  
33 so that smaller atoms are dropped from the fitting radius sooner. Energies and  
34 gradients are available.  
35

36 *Multiresolution exchange-correlation (MrXC) quadrature:* MrXC [121–123] can  
37 accelerate the numerical quadrature associated with computation of the XC energy  
38 and the XC matrix needed in the SCF procedure. It is an algorithm for seamlessly  
39 combining the standard atom-centered grid of quantum chemistry, with a cubic grid  
40 of uniform spacing by placing the calculation of the smooth part of the density and  
41 XC matrix onto the uniform grid. The computation associated with the smooth  
42 fraction of the electron density is the major bottleneck of the XC part of a DFT  
43 calculation and can be done at a much faster rate on the cubic grid due to its low  
44 resolution. Fast Fourier transform and B-spline interpolation are employed for the  
45 accurate transformation between the two types of grids such that the final results  
46 remain the same as they would be on the atom-centered grid alone. By this means,  
47 a speed-up of several times for the calculations of the XC matrix is achieved. The  
48 smooth part of the calculation with mrXC can also be combined with the Fourier  
49 transform coulomb method [124] to achieve even higher efficiency, particularly for  
50 calculations using large basis sets and diffuse functions.  
51

52 *TDDFT gradients and Hessians:* A recent implementation of TDDFT analyti-  
53 cal gradients (also in the Tamm-Dancoff approximation [125]) is available [126],  
54 with parallel capabilities. A more distinctive capability is the availability of an  
55 implementation of TDDFT analytical frequencies (greatly extending an existing  
56 analytical CIS frequency code [127]), both in the Tamm-Dancoff approximation  
57  
58  
59  
60

[128] and for full TDDFT [129]. Additionally analytical TDDFT gradients and frequencies have been extended [130] to include the smooth polarizable continuum models for solvation that are discussed in Sec. 6.1. Compared to numerical differentiation, analytical second derivatives of the excitation energy yield higher precision and need much less computer time, but require much more memory. The memory usage is mainly dominated by the geometric derivatives of the MO coefficients and transition amplitudes, which is dealt with by solving the coupled-perturbed equations in segments. To ensure high precision, a fine grid for numerical integration should be used, since up to fourth-order functional derivatives with respect to the density variables as well as their derivatives with respect to the nuclear coordinates are needed.

*Dual basis methods:* An effective method for reducing the computational cost of SCF calculations is to perform the SCF calculation in a small (“primary”) basis set, and subsequently correct that result in a larger (“secondary”) basis set, using perturbation theory. Q-CHEM contains two related approaches for performing dual basis calculations. Both energies and analytical gradients are available for the dual basis approach of Head-Gordon and co-workers [131, 132], who have also developed dual basis pairings for the Dunning cc-pVXZ [133] and aug-cc-pVXZ [134] basis sets. From a good reference, the Hartree-Fock perturbation theory (HFPT) approach [135, 136] provides more accurate corrections even at first order, and is also applicable to DFT calculations. Not only jumps in basis set, but also in the choice of quadrature grid, and density functional itself are possible via the “triple jumping” approach [137].

*Metadynamics and non-orthogonal configuration interaction:* SCF metadynamics [138] allows one to find alternative minima within the SCF framework either (HF or KS-DFT). Alternative minima are obtained by applying a bias in density matrix space at the locations of previously found minima and using standard convergence algorithms DIIS/GDM/RCA on this modified potential energy surface. It is then possible to perform Non-Orthogonal Configuration Interaction (NOCI) [139, 140] using the resulting non-orthogonal determinants as a basis. One then builds and diagonalizes the Hamiltonian in this, which is general non-orthogonal. Q-CHEM supports the use of general and complex HF orbitals for this purpose. While calculation of the Hamiltonian is more complicated than in orthogonal CI, it has been shown for some systems that the number of determinants to obtain qualitatively accurate results for ground and excited states of challenging systems such as polyenes is rather small (less than 100 or so) [140].

#### 2.4. Case study: Relative and binding energies of 10 $F^-(H_2O)_{10}$ isomers

In a recent paper [141], Herbert and coworkers discovered that halide-water clusters present a challenge for density functionals such as LC-VV10,  $\omega$ B97X-D, and M06-2X. In particular, the binding energies of 10 isomers of  $F^-(H_2O)_{10}$  proved to be the most notorious case. Using the same geometries and reference values, 9 density functionals available in Q-CHEM were benchmarked on these 10 isomers, and the results, calculated in the aug-cc-pVTZ basis set with a (99,590) grid, are provided in Table 2 and Figure 1. Table 2 confirms that a majority of these density functionals are unable to accurately predict the binding energies of these isomers. However, the newly-developed  $\omega$ B97X-V functional performs at least 2 times better than the next best functional, which is (surprisingly) PBE. In order to identify if the functionals in question are underbinding or overbinding the clusters, it is useful to consider Figure 1. Besides PBE and B3LYP, all of the density functionals overbind the isomers, with B3LYP-D2, M06-2X, and PBE-D2 overbinding more severely

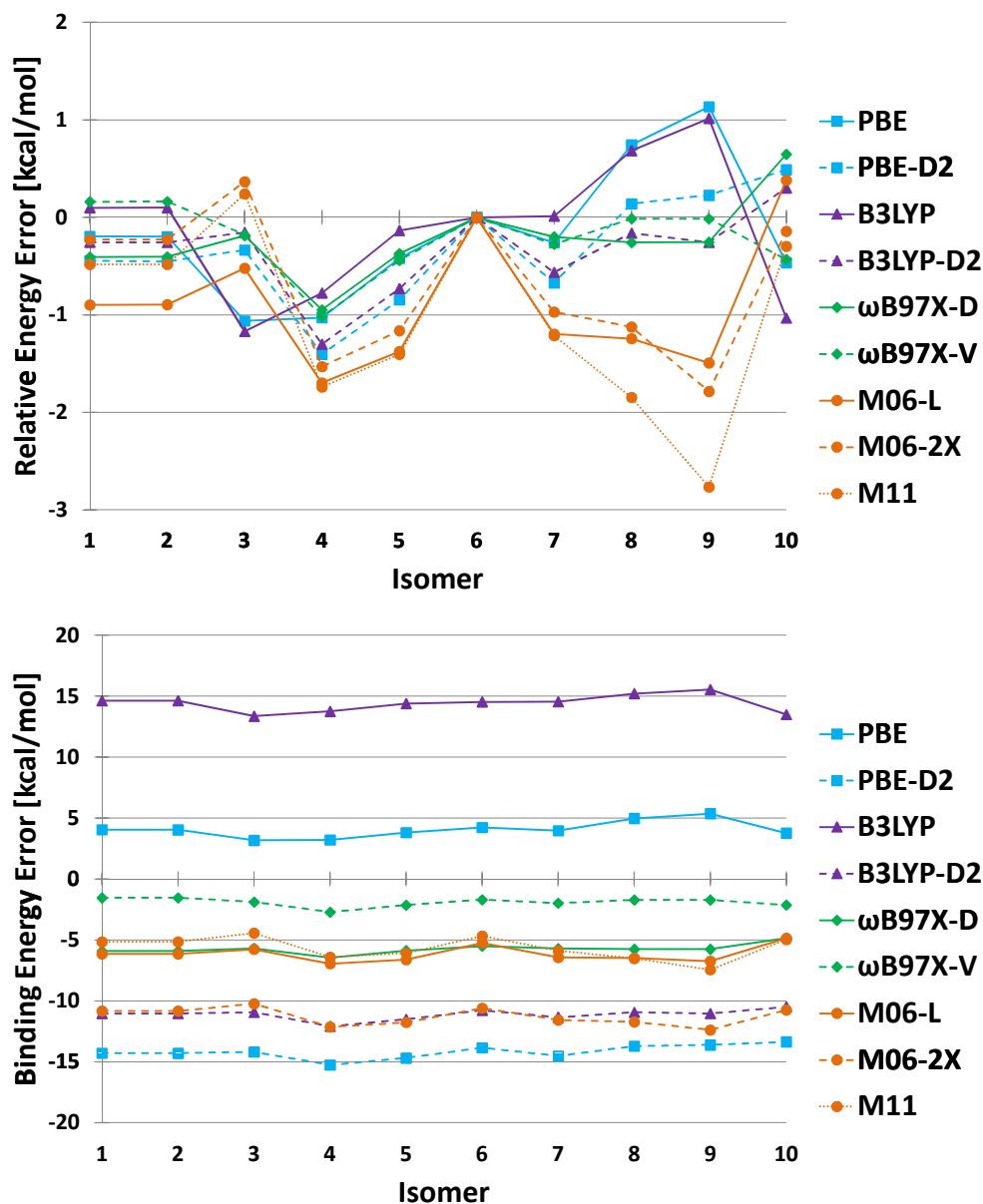


Figure 1. Relative and binding energy errors for 10 isomers of  $F^-(H_2O)_{10}$  with respect to RI-CCSD(T)/CBS benchmark values.

than the rest.  $\omega$ B97X-D, M06-L, and M11 overbind considerably as well, though by approximately 5 kcal/mol instead of more than 10 kcal/mol. For the relative energies of the clusters, the Minnesota functionals perform poorly, with errors larger than 1 kcal/mol. The two best functionals are  $\omega$ B97X-V and  $\omega$ B97X-D, with RMS errors of 0.40 and 0.45 kcal/mol, respectively.

RMSD	PBE	PBE-D2	B3LYP	B3LYP-D2	$\omega$ B97X-D	$\omega$ B97X-V	M06-L	M06-2X	M11
Relative Energy	0.68	0.63	0.68	0.54	0.45	0.40	1.10	0.97	1.35
Binding Energy	4.11	14.19	14.42	11.13	5.76	1.94	6.17	11.30	5.74

Table 2. Relative and binding energy RMS errors in kcal/mol for 10 isomers of  $F^-(H_2O)_{10}$  with respect to RI-CCSD(T)/CBS benchmark values.



System	# basis functions	RI-MP2		RI-CDD-MP2	
		time [h]	scaling	time [h]	scaling
DNA <sub>1</sub>	625	0.16	-	0.23	-
DNA <sub>2</sub>	1332	6.36	4.87	4.75	4.02
DNA <sub>4</sub>	2746	231.63	4.97	53.22	3.34
DNA <sub>8</sub>	5574	-	-	449.53	3.01

Table 3. CPU times on a single CPU core and scaling behavior for conventional RI-MP2 as well as RI-CDD-MP2 calculations on model DNA systems in a def2-SVP basis. The index of the DNA systems denotes the number of A-T base pairs. For full details and additional performance data see Ref. [148]

### 3. Wave function methods

#### 3.1. *Perturbative methods*

Second order Møller-Plesset perturbation theory [142, 143] is widely used as the simplest and most computationally inexpensive wave function treatment of dynamic correlation. Q-CHEM's workhorse implementation based on resolution-of-the-identity (RI) algorithms for the energy and gradient [144, 145] is highly efficient for small and medium-sized molecules. For greater efficiency in larger basis sets, energies [133] and gradients [146] are also available for the dual basis RI-MP2 method. For larger molecules, an efficient cubic-scaling MP2 method has been implemented in Q-CHEM. The method is grounded on the atomic orbital-based MP2 formulation and uses a Cholesky decomposition of pseudo-density matrices (CDD) [147, 148] in combination with integral screening procedures using QQR integral estimates [148–150]. Using the RI approach and efficient sparse matrix algebra, the RI-CDD-MP2 method shows a fairly small prefactor for a reduced scaling method. Due to the asymptotically cubic scaling of the computational cost of the RI-CDD-MP2 method with the size of the molecule the approach is faster for larger systems than the conventional fifth-order scaling RI-MP2 method. The crossover between RI-CDD-MP2 and conventional RI-MP2 is found already for systems as small as, e.g., two DNA base pairs as shown by the timings in Table 3.

Whilst MP2 greatly improves on the mean-field reference in many cases, it also has some well-known weaknesses. These include need for large basis sets, overestimation of intermolecular interactions, and susceptibility to spin-contamination. Q-CHEM contains a variety of recently developed methods that partially lift some of these limitations. For ground state treatment of intermolecular interactions, Q-CHEM contains newly developed attenuated MP2 methods, which offer remarkable improvements in accuracy for small and medium-sized basis sets. Attenuated MP2 [151–153] is available with the Dunning aug-cc-pVDZ (small) and aug-cc-pVTZ (medium) basis sets. This approach works by canceling the overestimation of intermolecular interactions by attenuation of the long-range part of the correlation energy. A summary of the RMS errors (kcal/mol) obtained for a series of inter and intramolecular non-bonded interactions is given in Table 4. Consistent improvement relative to unattenuated MP2 is found for databases of hydrogen-bonded, dispersion, and mixed interactions (Divalent Sulfur, A24, S22, S66, and L7). Relative conformational energies for sulfate-water clusters, alkane conformers (ACONF), cysteine conformers (CYCONF), sugar conformers (SCONF), and dipeptide and tripeptide conformers (P76) are in good agreement with benchmarks.

As a further evolution of spin-component scaled MP2 methods for systems susceptible to spin-contamination, the orbital optimized opposite spin (O2) method is available (energies [165] and gradients [166]). Relative to full OO-MP2, which exhibits systematic overbinding, O2 yields higher accuracy by virtue of its single semi-empirical scaling parameter, and also lower computational cost ( $O(M^4)$  vs  $O(M^5)$ )

	MP2/aDZ	MP2(terfc, aDZ)	MP2/aTZ	MP2(terfc, aTZ)	MP2/CBS
Divalent Sulfur	1.25	0.28	0.80	0.16	0.41
A24	0.52	0.26	0.31	0.18	0.21
S22	3.91	0.61	2.5	0.48	1.39
S66	2.66	0.43	1.53	0.25	0.73
L7	24.14	1.10	14.00	1.87	8.78
SW49(bind)	1.23	1.03	0.84	0.36	0.34
SW49(rel)	0.49	0.34	0.34	0.39	0.10
ACONF	0.31	0.29	0.24	0.08	0.11
CYCONF	0.20	0.28	0.30	0.21	0.25
SCONF	0.28	0.52	0.22	0.12	0.21
P76	1.06	0.33	0.59	0.31	0.42

Table 4. Root mean squared errors (in kcal/mol) for databases of nonbonded interactions, grouped by intermolecular or intramolecular interactions. Only equilibrium geometries were examined from the Divalent Sulfur database [154]. Complete basis set estimates (CBS) for MP2 were taken from references for the Divalent Sulfur, SW49 [155–157], ACONF [158], CYCONF [159], and SCONF [160] databases. MP2/CBS results for the S22 [82, 83], S66 [84, 85], L7 [161], and P76 [162] databases were obtained from the Benchmark Energy and Geometry DataBase (BEGDB) [163]. MP2/CBS results for the A24 databases [164] were generated for this work.

by virtue of containing no same spin contribution [167]. In addition to cleaning up spin-contamination problems [165], O2 also avoids the n-representability and force discontinuity issues of MP2 [168]. At higher computational cost than O2 (same cost as OO-MP2), the recently introduced  $\delta$ -OO-MP2 method [169] simultaneously solves the problems of over-estimating correlation effects and divergences from vanishing denominators in small-gap systems by using a regularization, or level shift, parameter.

Beyond ground states, the corresponding second order correction to single excitation CI for excited states [170], CIS(D), offers similar advantages to MP2 and suffers from very similar limitations. Within Q-CHEM, more computationally efficient excited state scaled opposite spin methods are available, that, like SOS-MP2 and O2 scale as  $O(M^4)$ . SOS-CIS(D), a non-degenerate method [171], is available for excited state energies. SOS-CIS(D0), a quasidegenerate approach, which is therefore more robust at the cost of some additional computation, has both energies [172] and analytic gradients [173, 174] available.

### 3.2. Coupled cluster methods

Q-CHEM 4 features a wide variety of computational methods for the ground and excited states based on coupled-cluster theory [175, 176]. These methods are among the most versatile and accurate electronic structure approaches. Equation-of-motion (EOM) approach extends single-reference coupled-cluster methods to various multi-configurational wave functions. Q-CHEM 4 includes EOM-CC methods for electronically excited states (EOM-EE), ionized/electron-attached ones (EOM-IP/EA), as well as doubly-ionized (EOM-DIP) [177] and spin-flip (EOM-SF and EOM-2SF) [178, 179] extensions that enable robust and reliable treatment of bond-breaking, diradicals/triradicals, and other selected multi-configurational wave functions. Gradient and properties calculations (including interstate properties) are available for most CC/EOM-CC methods.

Q-CHEM 4 offers an efficient multi-core parallel implementation of these methods based on a general purpose tensor library [180]. The library provides a convenient tensor expressions C++ interface that aids new developments.

In order to reduce computational requirement for the CC methods and improve parallel performance we exploited two reduced-rank approaches based on resolution of the identity (RI) and Cholesky decomposition (CD) of two-electron repulsion integrals [181]. The equations were rewritten to eliminate the storage of the largest

Table 5. Timings of one CD-CCSD iteration (in hours) for  $(mU)_2\text{-H}_2\text{O}$  (test 4 in Ref. [181]) using  $1E-2$  threshold for Cholesky decomposition. This calculation takes 12 CCSD iterations to converge.

Method	Basis	# Basis functions	Memory limit	Wall time
CD-CCSD	6-31+G(d,p)	489	100 GB	5.1
CD-CCSD/FNO	6-31+G(d,p)	489	100 GB	1.4
cc-pVTZ/FNO	cc-pVTZ	882	300 GB	12.2

four-dimensional intermediates leading to a significant reduction in disk storage requirements, reduced I/O penalties, and, as a result, improved parallel performance. For medium-size examples, RI/CD calculations are approximately 40-50% faster compared with the canonical implementation. More significant speedups (2–5 fold) are obtained in larger bases, e.g., cc-pVTZ.

Even more considerable speedups (6–7-fold) are achieved by combining RI/CD with the frozen natural orbitals approach [182]. Importantly, with Q-CHEM, one can perform CC/EOM-CC calculations for relatively large systems (up to  $\sim 1000$  basis functions) on main-stream single-node servers. Detailed performance benchmarks are available in Refs. [180, 181]. Table 5 shows selected timings obtained on a single 16-core Xeon-Dell node for dimethyl-uracyl dimer solvated by one water molecule ( $(mU)_2\text{-H}_2\text{O}$ , C1 symmetry, 158 electrons). FNO calculations in Table 5 used an occupation threshold of 99.5%. As an example, for the 6-31+G(d,p) basis, this corresponds to 292 active virtual orbitals and 118 frozen virtuals. Using FNO leads to errors in IEs that are less than 0.02 eV relative to the full calculation, which is typical for this threshold [182].

While conventional coupled-cluster and equation-of-motion methods allow one to tackle electronic structure ranging from well-behaved closed shell molecules to various open-shell and electronically excited species [176], metastable electronic states, so-called resonances, present a difficult case for theory. By using complex scaling and complex absorbing potential techniques, we extended these powerful methods to describe autoionizing states, such as transient anions, highly excited electronic states, and core-ionized species [183–185]. In addition, users can employ stabilization techniques using charged sphere and scaled atomic charges options [186]. Various improvements of iterative diagonalization algorithms enable access to high-lying interior eigenvalues.

### 3.3. Algebraic diagrammatic construction (ADC) methods

Algebraic diagrammatic construction (ADC) methods constitute a series of methods for the calculation of excited states which derive from the perturbation expansion of the polarisation propagator [187, 188]. Each method differs in the approximation to the Hamiltonian matrix for which the eigenvalue problem has to be solved, as well as in the way state properties and transition properties are computed from the eigenvectors. In first order, the ADC(1) eigenvalue problem is identical to CIS, but additional terms enter in the computation of transition moments. The second order approximation ADC(2) provides excitation energies (and transition properties) comparable to those obtained with CIS(D) [170] and CC2 [189, 190]. An extension to the second order scheme ADC(2)-x adds additional terms to the Hamiltonian matrix which put more weight on doubly excited configurations. As result, the excitation energies are shifted to lower energies, in particular if the respective states possess strong double excitation character. Accordingly, the comparison of ADC(2)-x and ADC(2) results can yield useful insights about the importance of double excitations in the spectrum [191]. With the third order method ADC(3) the accuracy of the excitation energies improves further getting close to the results

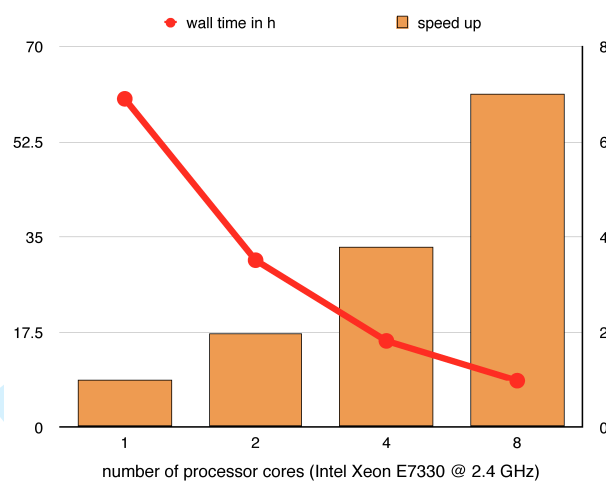


Figure 2. Timings and parallel speed-up of an ADC(3) calculation of the benzene molecule using aug-cc-pVTZ basis set.

obtained by CC3 calculations, though at computational costs which are an order of magnitude smaller.

In Q-CHEM, ADC methods up to third order are available for the computation of excited states [192]. They have been implemented based on the same general purpose tensor library [180] as the coupled cluster methods offering shared-memory parallelisation and a LaTeX style programming interface for new equations. The implementation allows for the calculation of excitation energies and transition properties from the ground state, as usual. In addition, excited state properties and transition properties between excited states can be computed on request. From those, two-photon absorption cross-sections can be deduced via sum-over-states expressions. Alternatively, the two-photon absorption cross-section can be obtained by inversion of the ADC matrix [193]. For visualisation of the excited states, transition densities or attachment and detachment densities may be exported as grid data for later display by standard visualisation tools.

Furthermore, Q-CHEM features spin-opposite scaled (SOS) ADC variants for both second order schemes ADC(2) and ADC(2)-x [194]. They follow the idea of SOS-MP2 to reduce computational costs and improve the resulting energies. Therefore, same-spin contributions in the ADC matrix are neglected, while opposite spin contributions are scaled using appropriate semi-empirical parameters. SOS-ADC(2) requires two scaling parameters  $c_{os}$  and  $c_c$ , while for SOS-ADC(2)-x another parameter  $c_x$  is needed. The parameter  $c_{os} = 1.3$  is inherited from SOS-MP2 for the scaling of the  $T_2$  amplitudes, while the parameters  $c_c$  and  $c_x$  are used to scale the ph/2p2h block and the off-diagonal part of the 2p2h/2p2h block of the ADC matrix, respectively. For SOS-ADC(2) the optimal value of  $c_c = 1.17$  was determined by fitting against the Thiel benchmark set [195]. A similar fit for SOS-ADC(2)-x yielded  $c_c = 1.0$  and  $c_x = 0.9$  as optimal values [194]. With these parameters, a mean absolute error of 0.14 eV in the excitation energies is achieved by SOS-ADC(2) for the Thiel benchmark set. For SOS-ADC(2)-x the mean absolute error for predominantly single excitations becomes 0.17 eV, while for states with large double excitation character it is 0.21 eV.

Another set of ADC variants in Q-CHEM uses the core-valence separation (CVS) approximation [196] to calculate core excitations. In general, the calculation of core-excited states is quite difficult, since with standard implementations the valence excited states need to be calculated before any core-excited state can be obtained. The CVS approximation solves this problem by decoupling core and valence ex-

1 citations in the ADC Hamiltonian. Thereby, it makes use of the fact that the  
2 interactions between core and valence excitations are negligible due to the strong  
3 localisation of the core orbitals and the large energy separation between core and  
4 valence orbitals. As result, core-excited states can be computed independently from  
5 the core excitation part of the ADC Hamiltonian which significantly reduces the  
6 computational costs compared to the calculation of valence-excited states. CVS  
7 variants for ADC(1), ADC(2), and ADC(2)-x are available with CVS-ADC(2)-x  
8 showing excellent agreement with experimental data [197].  
9

### 10 11 12 **3.4. Density matrix renormalization group**

13 Q-CHEM now includes an interface to the density matrix renormalization group  
14 (DMRG) code of Sharma and Chan (“Block”) [198–201]. The density matrix renor-  
15 malization group [198–211] is a variational wavefunction method based on a class  
16 of wavefunctions known as matrix product states (MPS) [208, 212]. The DMRG  
17 allows for unique kinds of quantum chemical calculations to be performed. The ac-  
18 curacy of the DMRG can be continuously tuned based on a single parameter, the  
19 number of renormalized states, denoted  $M$ . In typical calculations  $M$  ranges from  
20 1000-10000. By increasing  $M$  it is possible to push DMRG calculations to yield  
21 highly accurate energies (e.g. to within 10-100 microHartrees of the exact result)  
22 for systems much larger than can be treated with FCI [213–215]. While convergence  
23 with  $M$  is system dependent, as a guide, for modest number of electrons (10-20)  
24 high accuracy can be achieved for more than 100 orbitals, while for larger number  
25 of electrons (e.g. up to 40) high accuracy can be achieved for about 40 orbitals,  
26 using  $M$  up to 10000.  
27

28 Further, because the MPS is not built on an excitation expansion around a Slater  
29 determinant, DMRG calculations are well suited to describe *strong* or *multirefer-*  
30 *ence* correlation, as found in transition metals or excited states [208]. Here, the  
31 DMRG is often used to replace a complete active space calculation [205, 216, 217].  
32 Active spaces with up to 40 orbitals can be treated reliably, and the DMRG has  
33 been applied to bioinorganic complexes with as many as 4 transition metal ions,  
34 such as the  $Mn_4Ca$  cluster of photosystem II [218], and [4Fe-4S] clusters. Finally,  
35 the MPS mathematically represents one-dimensional chain-like correlations very  
36 efficiently. The DMRG can thus be used with great effect in treating correlations  
37 in  $\pi$ -systems of many conjugated molecules [216, 219, 220].  
38

39 The version of Block included with Q-CHEM can be run in an entirely black-box  
40 fashion; orbital ordering, one of the more unusual inputs into a DMRG calculation,  
41 can be determined automatically using a graph-theoretical algorithm, or a genetic  
42 algorithm optimization. The user need only specify the final number of states  $M$   
43 desired. The DMRG module is also completely parallelized; larger calculations as  
44 described above should be run on 10-100 cores.  
45  
46  
47  
48

### 49 **3.5. Active space spin flip methods**

50 This is a family of methods capable of treating strong correlations via an active  
51 space at lower computational cost than CASSCF type methods, and with greater  
52 ease of use. A molecule with strong correlations requires multi-configurational wave  
53 functions to be even qualitatively correct. For 2 strongly correlated electrons, the  
54 first such approach is the spin-flip extended single configuration interaction (SF-  
55 XCIS) model [221]. For general numbers of strongly correlated electrons (though  
56 computational cost increases exponentially with the number of spin flips), two  
57 implementations [222, 223] of the restricted active space spin flip (RAS-SF) model  
58  
59  
60



[224, 225] are available. These methods start from a high spin restricted open shell Hartree-Fock determinant, where the strongly correlated electrons are initially all high spin. The target low-spin strongly correlated states are accessed by flipping the spins of half the high spin levels (which define the active space), and performing a full CI calculation in the active space, augmented by single excitations into and out of the active space. These additional “particle” (p) and “hole” (h) excitations provide state-specific relaxation of the orbitals.

The efficient implementation of RAS-SF (i.e. spin-flipping in the RAS-CI formalism) has enabled detailed electronic structure studies of singlet fission in dimers plus environment models of pentacene and tetracene crystals [226–229]. Relevant electronic states include delocalized excitonic states, with a variable admixture of charge-resonance configurations, interacting with a dark multi-exciton state of a doubly excited character. Importantly, RAS-2SF method allows one to treat all electronic states within the same computational framework in dimers and even trimers of relevant compounds (tetracene, pentacene, hexacene, etc). RAS-SF calculations enabled investigations of the effect of morphology on the state couplings.

Very recently, the efficiency of the methods has been increased by treating the excitations into and out of the active space perturbatively, to define the SF-CAS(h,p) method [230]. The basic idea is that if the states of interest are predominantly described by active space configurations, then the small state-specific relaxations that are accounted for by the particle and hole excitations in RAS-SF can be accurately approximated by perturbation theory at much lower computational cost. The perturbative framework also permits treatment of extended single excitations that go from the hole space to the particle space (i.e. “hole-particle” excitations), as the active space is rearranged, defining the SF-CAS(S) method [231]. SF-CAS(S) is a method that contains physics that goes beyond RAS-SF, and therefore begins to account for effects that we would normally identify as being associated with dynamic correlation.

As an example of the performance of the newest SF-CAS methods, one may consider the simultaneous bond dissociation of  $\text{H}_2\text{O}$ . In the aug-cc-pVTZ basis set, CCSD(T) provides a binding energy of 231 kcal/mol, with 75 kcal/mol attributed to dynamical electron correlation. In Figure 3, the computed bond dissociation curves for the SF-CAS, SF-CAS(h,p)<sub>1</sub>, and SF-CAS(S)<sub>1</sub> methods are compared. In general, a single spin-flip takes care of a single bond dissociation. In this example, two bonds are broken, requiring two spin-flips from the quintet ROHF reference.

While all the methods smoothly dissociate to correct products without spin-contamination, the binding energy for SF-CAS is significantly less than even that of UHF, reflecting the biasing of quintet orbitals against the bound singlet state. The perturbative treatment of hole and particle states in SF-CAS(h,p)<sub>1</sub> improves this binding (-174 kcal/mol) to a value that slightly better than the uncorrelated UHF method, while avoiding any spin-contamination or kinks in the PES. Adding the full singles correction perturbatively, SF-CAS(S)<sub>1</sub> significantly increases the binding, to 208 kcal/mol, which corresponds to recovering a considerable fraction of the dynamical correlation energy.

### 3.6. Coupled cluster valence bond

The Perfect Pairing (PP) approximation [232, 233] treats a molecular system as a collection of semi-independent electron pairs. In fact, this treatment is quite compatible with the classic Lewis dot structure picture of bonds and lone pairs. When neighboring covalent bonds are broken, resulting in open-shell fragments, they can become strongly coupled to each other, invalidating the semi-independence assigned

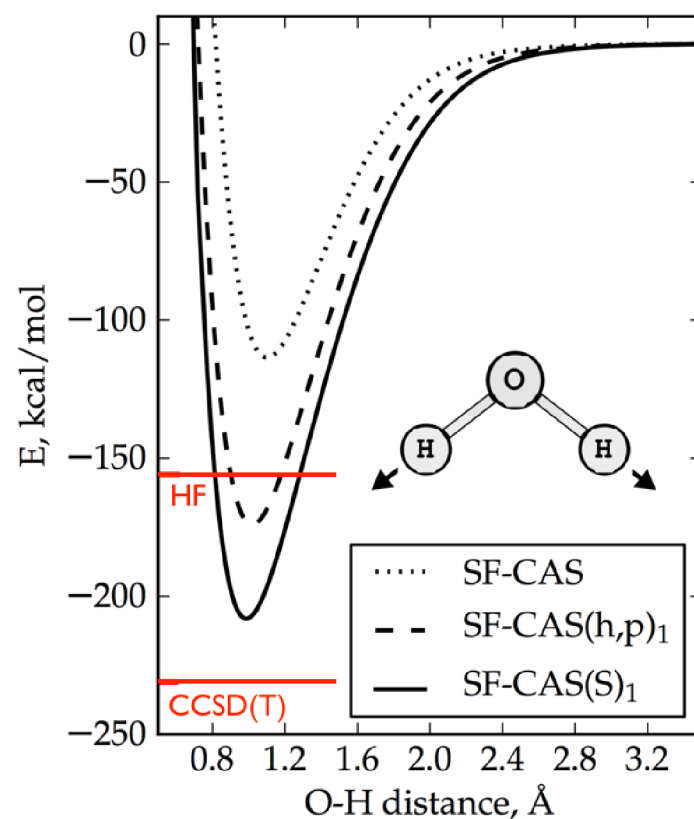


Figure 3.  $\text{H}_2\text{O}$  potential energy surfaces for double dissociation in the aug-cc-pVTZ basis set. SF-CAS is the dotted line, SF-CAS(h,p)<sub>1</sub> is the dashed line, and SF-CAS(S)<sub>1</sub> is solid line. The upper red line is the HF binding energy (no correlation), and the lower red line is the CCSD(T) binding energy (nearly complete treatment of correlation effects at equilibrium vs dissociation).

to them by PP. This is true for double and triple bonds, for example, and in such cases the PP energy will lie far above the sum of the energies of the dissociated fragments. The Coupled Cluster Valence Bond (CCVB) approximation [234] was introduced to account for this strong coupling, while retaining the simple Lewis picture of PP. CCVB possesses exact spin symmetry, will give correct energy profiles in these sorts of bond dissociations, and incurs only a modest computational cost (the number of variables describing the strong correlations between pairs smaller than the number of MO coefficients). CCVB can treat both open and closed-shell systems. CCVB is particularly useful for the lowest energy state of each spin multiplicity for systems with strong spin correlations, such as the example discussed below. The main limitation of CCVB is that, effectively, it models only one Lewis dot structure at a time, and this can result in irregularities in situations where resonance effects are significant, as discussed in more detail elsewhere [235].

As an example of the application of CCVB, we have computed the potential energy surface for the dissociation of  $\text{Cr}_2$ . The  $\text{Cr}_2$  molecule has a formal sextuple bond, amounting to 6 strongly correlated electron pairs, and it is well recognized as a difficult multireference problem in which static and dynamic correlation effects are both important [236]. The canonical multireference approach for  $\text{Cr}_2$  is to employ a 12 electrons in 12 orbitals complete active space, which entails many thousands of configurations (the naive number is  $(^{12}C_6)^2$ ). In contrast, the CCVB wavefunction for this case is built from only 21 parameters. We have included CASSCF and unrestricted Hartree Fock (UHF) results, and all calculations used the Wachters+f basis set.[237–239] The energies are relative to 2 times the septet-spin Cr energy.

The results of our calculations are given in Fig 4. The principal purpose is to

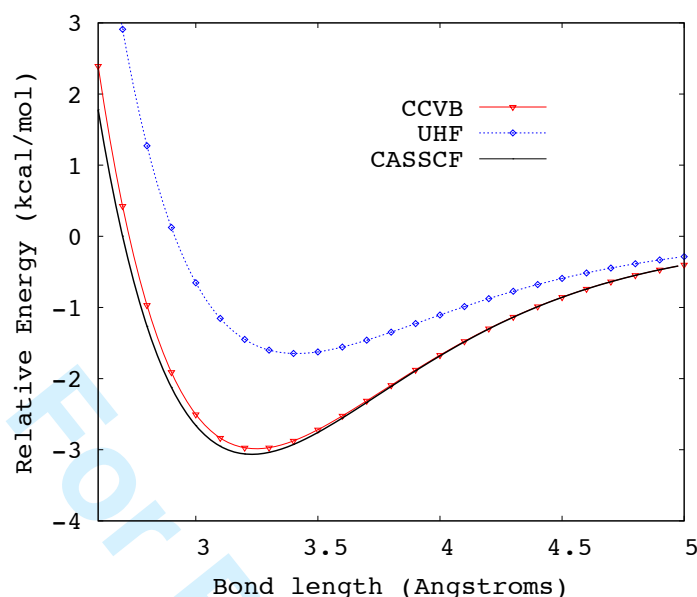


Figure 4. A plot of the potential curve for  $\text{Cr}_2$  molecule, treated by the CASSCF method using 12 electrons in 12 orbitals, by CCVB correlating 6 electron pairs, and by the spin-polarized UHF method. The difference between UHF and CASSCF can be viewed as defining the strength of static correlations in this molecule.

illustrate the ability of CCVB to capture the important static correlations associated with bond-breaking in this system. Such correlations are so important that the UHF wave function is spin-unrestricted at all bond lengths shown: the restricted solution is not stable anywhere in the range shown! For static correlation, CASSCF represents exact solution of the (12,12) Schrodinger equation, and is the benchmark against which CCVB can be tested. Across the range of bond lengths shown, CCVB is remarkably close to CASSCF, while UHF, with its spin contamination error, is clearly inferior. Furthermore, the optimal bond lengths are 3.23, 3.25, and 3.41 Å, for CASSCF, CCVB, and UHF, respectively. Finally it should be remembered that the experimentally derived equilibrium bond length of  $\text{Cr}_2$  is only 1.7 Å, and the binding energy is about 35 kcal/mol, which indicates the key role of dynamic correlation, which is not considered in CCVB (or CASSCF).

#### 4. Advanced computing capabilities

Shared memory parallel routines for density functional theory and Hartree-Fock energies and gradients have been recently implemented in Q-CHEM by Zhengting Gan. The key computational bottlenecks that require special programming are matrix element evaluation, both analytical two-electron integral formation, and numeral exchange correlation quadrature. As an illustration of the usefulness of the resulting algorithms for small-scale (single node or workstation) parallel calculations, Figure 5 shows the CPU timings and parallel speedups for a B3LYP/6-311G(3df,3pd) calculation on the glutamine molecule. Note that upon going from 1 core to 2 cores, the speedup is super linear: this reflects algorithmic improvements in the integral code that were made in the process of developing the parallel code.

OpenMP parallel capabilities have also been added for RI-MP2 calculations [153]. A novel algorithm that minimizes disk transfers in the shared memory environment is employed, and all steps scaling higher than quadratic in system size are parallelized. Combining the OpenMP SCF and OpenMP parallel capabilities permits low elapsed job times for even quite large molecules in medium-sized basis sets.

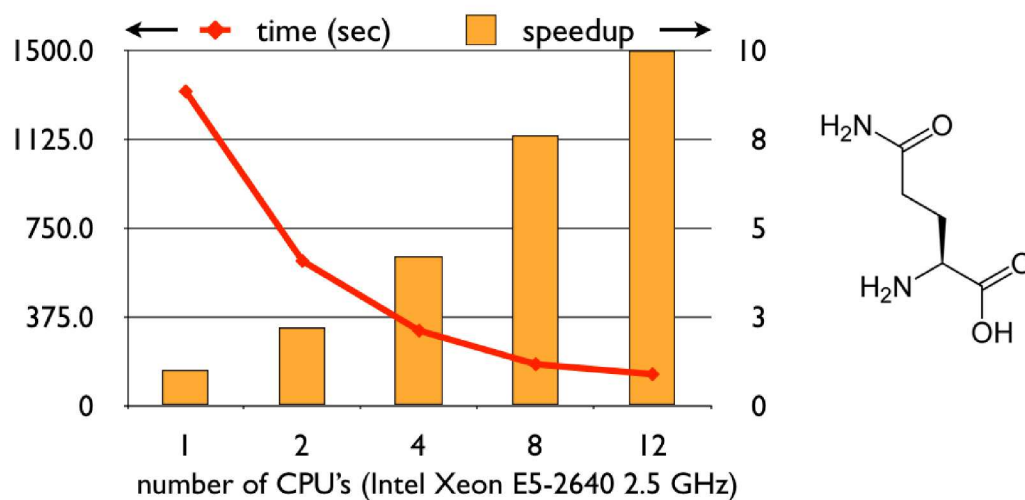


Figure 5. A plot of the computer timings and parallel speedups for calculations on the glutamine molecule (see 2-d structure at the right of the figure), for energy evaluation at the B3LYP/6-311(3df,3pd) level of theory.

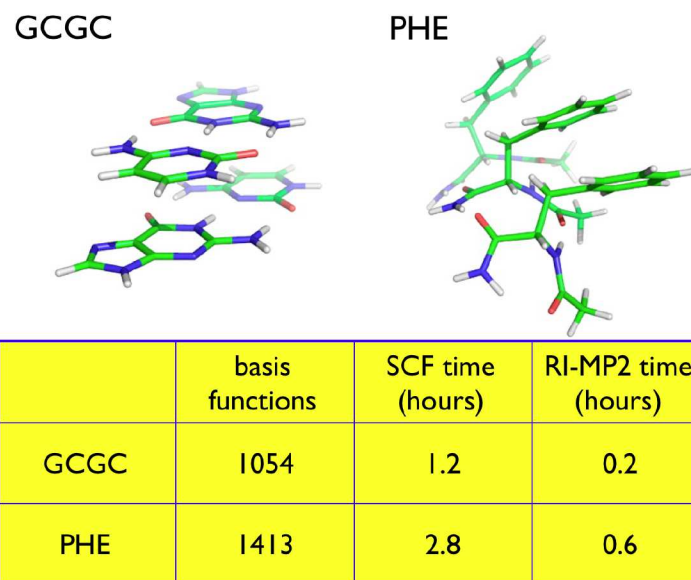


Figure 6. Elapsed times for SCF and MP2 energy evaluation on two large complexes from the L7 database [161], using the aug-cc-pVDZ basis set, with integral thresholds of  $10^{-14}$  and an SCF convergence criterion of  $10^{-10}$ . The calculations were performed on a 64 core 2.3 GHz AMD Opteron 6300 series node.

As an example of the usefulness of these algorithms for practical applications, Figure 6 shows two large molecular complexes from the L7 database [161]. The first, GCGC, is two guanine-cytosine base pairs that are arranged in a stacked Watson-Crick hydrogen-bonded arrangement as in DNA. The second, PHE, is a trimer of phenylalanine residues in a mixed hydrogen-bonded-stacked conformation. Figure 6 also shows the elapsed timings for the SCF and MP2 steps on a 64 core 2.3 GHz AMD Opteron 6300 series node, which indicate that the MP2 calculation is still less computationally demanding than the SCF step in these quite extended systems. These large 1000-1400 basis function calculations with high precision (integral thresholds of  $10^{-14}$  and SCF convergence of  $10^{-10}$ ) show elapsed times of only 2-3 hours. Additionally, graphical processing unit (GPU) code has been added for RI-MP2 energies [240, 241] and gradients.

## 5. Walking on potential energy surfaces

In quantum chemistry codes, it has been common practice to provide sophisticated local optimization methods [242] that permit optimization to minima with emphasis on requiring as few gradient evaluations as possible, both by effective choice of coordinates, as well as guesses for hessian, in addition to the optimization procedure itself. Extensions of local optimizers, such as the partitioned rational function optimization (P-RFO) method [243], are provided for converging to transition structures. Such methods, which are local optimizations to saddle points, walking downhill in all directions but the reaction coordinate, in which the walk is uphill. The P-RFO approach (and related methods) is very computationally efficient given an excellent initial guess, and an associated hessian [244]. Recent developments provide additional sophisticated techniques that supplement these established tools, as discussed in the following subsections.

### 5.1. Growing and freezing string methods

If the initial guess for a transition structure is poor so that the associated hessian has the incorrect character, then transition structure optimizations are quite likely to fail, and the cycle of guess structure, run search, fail, guess again, etc, can be labor intensive and frustrating. This difficulty can be substantially overcome if the reactant and product geometries, corresponding to initial and final minima, are known. In that case, automatic path-finding tools, such as the growing and freezing string methods, can characterize a reaction coordinate joining the end-points. The highest point on the pathway becomes an excellent initial guess for subsequent refinement of the transition structure.

The growing string method (GSM) is an iterative algorithm [245] for determining a set of intermediate structures that connect the reactant and the product via the intrinsic reaction coordinate (IRC). The GSM has been reimplemented recently [246], with the use of linear synchronous transit [247] to improve initial guessing. Whilst formally very attractive, the GSM is still computationally quite expensive compared to the cost of a local optimization to a transition structure. The freezing string method [248] provides a much less expensive algorithm for determining a path with a specified number of intermediate structures (nodes) connecting reactant and product, starting like the GSM from both ends of the path, and adding nodes irreversibly until the two ends join. As a result of its non-iterative nature, the FSM cannot guarantee an IRC, but it is typically a quite reliable way to obtain a good initial guess for a transition structure that can then be refined by conventional local search.

Neither the FSM or GSM require Hessians. To further avoid the high cost of exact hessian evaluation, additional new tools [249] have been added that provide two more important capabilities. First, algorithms that combine the known reaction coordinate and its curvature from the FSM (and refined by subsequent iterative diagonalization using only gradients) enable the automatic construction of an initial hessian for transition structure refinement at the end of an FSM calculation. Second, when a local optimization has completed, the characterization of the stationary point can also be performed by iterative diagonalization using only gradients, to avoid hessian evaluation at this step also. An example of the use of these tools is given at the end of this section.



## 5.2. *Classical and quasiclassical trajectories*

Q-CHEM has contained ab initio classical trajectory methods for some years, based on an efficient Fock matrix interpolation strategy [250]. For some purposes, however, purely classical dynamics are inadequate. As a simple example, consider simulating the infrared spectrum of a high frequency mode such as an OH stretch in water clusters [251]: the vibrational amplitude would be orders of magnitude too small at room temperature by classical dynamics. Some (though not all!) of the limitations of classical trajectories may be overcome through the use of quasi-classical trajectories [252, 253], which is now available in Q-CHEM [254]. An old but useful idea, quasiclassical trajectories are initialized with kinetic energy corresponding approximately to the appropriate quantum distributions based on normal mode analysis. The trajectories are run classically. Useful information can be obtained at short times (while at long times energy artificially flows from high frequency modes to low frequency ones), and a particularly useful case is the exploration of short trajectories that are launched from the highest energy intermediate transition structures in complex chemical reactions. As an example, quasiclassical trajectory studies of hydrocarbon cracking in zeolites have shown that a single high energy transition structure can lead to multiple products (rather than a single path) [255].

## 5.3. *Basin hopping for low-lying minima of clusters*

In many chemical problems it is necessary to identify the global or low lying minima on a complex potential energy surface. Characterization of the structure of molecular clusters is one example that presents a challenge for standard structural optimization techniques. The basin hopping method [256] is a combination of a Metropolis Monte Carlo sampling technique and a local search method, which has the effect of sampling energy basins instead of sampling configuration space. In Q-CHEM the basin hopping search also incorporates “jumping” which allows the search to escape from a minimum by unconditionally accepting a series of moves.

Performing a basin hopping search in conjunction with quantum chemical methods removes the need to have a suitable empirical force field available and allows systems with more complex electronic structure or changes in electronic structure to be studied. Molecular clusters comprising water and methanol clusters have been studied at the B3LYP+D/6-31+G\* level of theory [257]. The structures corresponding to the global minimum for the  $(\text{H}_2\text{O})_7$  and  $(\text{H}_2\text{O})_3(\text{CH}_3\text{OH})_4$  clusters are illustrated in Figure 7, which shows the structures to be similar with the methyl groups of methanol occupying the sites of free hydrogens in the  $(\text{H}_2\text{O})_7$  cluster. Other studies have considered radical cation clusters including water [258, 259] with a combination of DFT and MP2 methods. Low energy structures that correspond to different characteristic structural motifs can be identified. Figure 7 also shows the two lowest energy isomers of the  $(\text{H}_2\text{O})_8^+$  cluster. Both of these isomers conform to a separated ion-radical pair structure, with  $\text{H}_3\text{O}^+$  and OH that are not directly attached to each other. Also shown are the computed infrared spectra for the O-H stretching region. The spectrum for the lowest energy isomer is in excellent agreement with the spectrum measured by experiment [260], confirming that the correct isomer has been identified.

## 5.4. *Case study: ethane dehydrogenation transition structure in H-MFI zeolite*

Cracking and dehydrogenation are competing reactions that alkanes undergo at Brønsted-acid sites within acidic zeolites. These monomolecular reactions can be

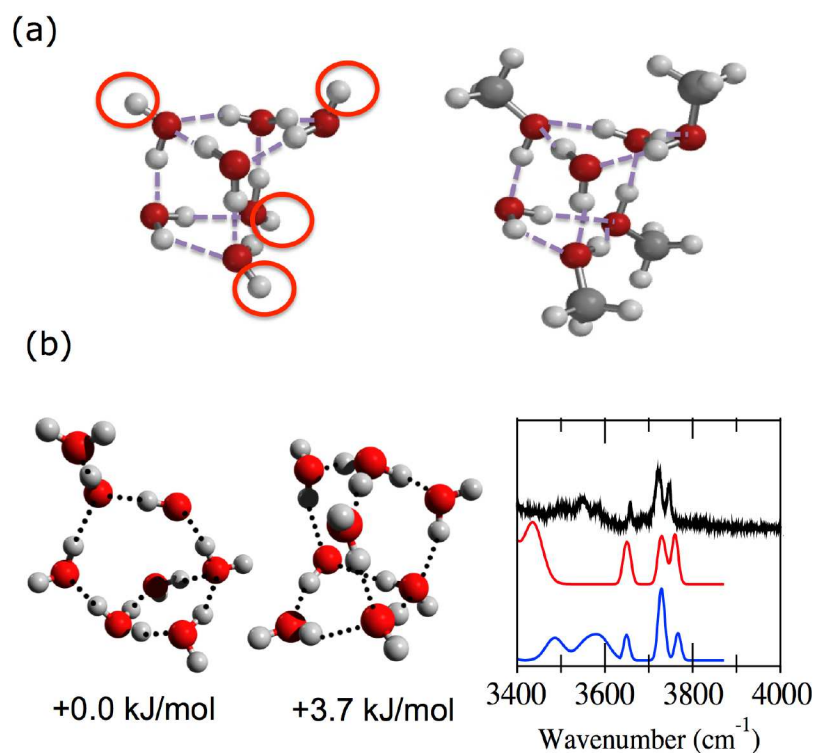


Figure 7. (a) The global minimum energy structures of the  $(\text{H}_2\text{O})_7$  and  $(\text{H}_2\text{O})_3(\text{CH}_3\text{OH})_4$  clusters. (b) the structures of the two lowest energy  $(\text{H}_2\text{O})_8^+$  clusters with the infrared spectra. The spectrum for the lowest energy isomer is shown in blue and the experimental spectrum is shown in black.

used to probe the shape-selective behavior in zeolite pores. There is a very large literature on electronic structure calculations on such systems, and prior to the development of economical methods for automatically locating transition structures, such as the freezing string method (FSM), the location of transition structures was labor intensive. In this example, the FSM TS search beginning with reactant and product geometries is used.

A cluster model consisting of 12 tetrahedral (T) atoms terminated with H is used, with the acid site located at the T12 position. The reactant state consists of ethane physisorbed at this acid site, and the product state consists of physisorbed ethene and H<sub>2</sub>. The T5 cluster consisting of the Al atom and 4 surrounding Si atoms is allowed to relax, and the remaining zeolite framework is fixed. The system is treated at the B3LYP/3-21G level of theory. The transition structure that is located is illustrated in Fig. 8.

The first step in this method is the generation of a guess to the TS. The freezing string method (FSM) is used with 20 nodes along the string, and 3 gradient relaxation steps per node. The maximum energy point along the FSM string is taken as the TS guess. The second step involves refining this guess to the correct TS using the partitioned-rational function optimization (P-RFO) method. For TS search, P-RFO is more reliable if the hessian at the TS guess is used as input. In order to avoid full hessian calculation, which can be expensive for large systems such as zeolite clusters, an approximate hessian can be generated from the FSM output. The TS guess and the approximate reaction coordinate generated by the FSM can be used to iteratively calculate the lowest eigenvalue and corresponding eigenvector of the exact hessian using a finite difference implementation of the Davidson method. This information can then be incorporated into a guess matrix as described elsewhere.

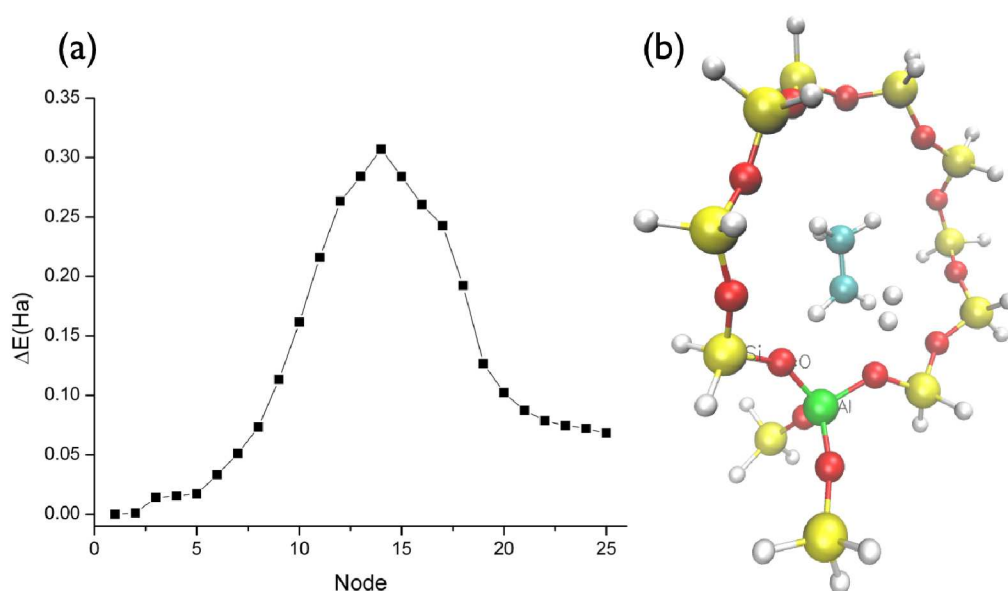


Figure 8. Illustration of a Freezing String Method (FSM) calculation on the transition structure for ethane dehydrogenation to ethene in the zeolite, H-MFI, modeled by a T12 cluster as described in the text. In panel (a), the relative energies of the calculated nodes of the FSM pathway are shown, beginning from the optimized structures of the reactant and the product. In panel (b), the final optimized transition structure is shown, which was calculated starting from the highest energy node on the FSM pathway.

The first step, generation of the FSM reaction path, requires 83 gradients. An additional 10 gradients are required to generate the lowest eigenvalue and eigenvector of the hessian to initiate the TS refinement, which itself required 167 gradients to converge to good tolerances. The first key point to be made is that the automatic generation of the TS guess via the FSM does not greatly affect the cost of the overall search (less than twice as expensive), yet has the great advantage of removing the need to generate the guess by hand (possibly multiple times, if first attempts are inadequate). A second point is that the automatic generation of a Hessian with the correct structure requires only 10 gradients vs the equivalent of about 62 gradients done analytically. The third point is that the approximate Hessian performs comparably to the exact one in the TS search itself (it requires 186 gradients for the same convergence from the same guess using the exact Hessian).

## 6. Modeling extended environment

Classical modeling of an extended environment (a solvent, or a macromolecular framework for example) is an important aspect of modern quantum chemistry calculations. Q-CHEM provides a variety of low-cost methods, of varying complexity and sophistication, for incorporating a classical environment into a quantum-mechanical calculation of the molecule or region of primary interest. These methods include several dielectric continuum-based descriptions of a liquid solvent; mixed quantum mechanics/molecular mechanics (QM/MM) calculations that can be performed using Q-CHEM as a stand-alone program or else via an interface [261] with the widely-used “CHARMM” molecular mechanics program [262]; and the effective fragment potential (EFP) method [263], which can be used to parameterize a polarizable force field, in an automated way based on quantum chemistry calculations. In addition to these quantum/classical approaches, several fragment-based quantum chemistry models are also available [264], in which the entire (super)system is ultimately described quantum-mechanically, but in order to reduce the cost this is



1 done one subsystem at a time, using a variety of methods to describe the coupling  
2 between different subsystems.  
3

### 6.1. Continuum solvation

7 Dielectric continuum models of liquid solution have a long history in quantum  
8 chemistry calculations [265], where they are usually known as *polarizable contin-*  
9 *uum models* (PCMs). PCMs model bulk electrostatics by treating the solvent as  
10 a homogeneous dielectric continuum characterized by a single parameter,  $\epsilon$ : the  
11 dielectric constant. Q-CHEM includes several of the most recent innovations in this  
12 area, including a sophisticated treatment of continuum electrostatics that is known  
13 variously as the *integral equation formalism* (IEF-PCM) [266] or the *surface and*  
14 *simulation of volume polarization for electrostatics* [SS(V)PE] model [267]. (The  
15 two are formally equivalent at the level of integral equations [268, 269], but there  
16 are subtle yet important implementation differences, as discussed in Ref. [270].)  
17

18 For high-dielectric solvents such as water, the much simpler conductor-like model  
19 (C-PCM) [271, 272] affords nearly identical solvation free energies as compared to  
20 IEF-PCM/SS(V)PE, differing formally only by terms of order  $\mathcal{O}(\epsilon^{-1})$  that are  
21 negligible for  $\epsilon \gtrsim 50$  [270]. Mathematically, C-PCM has the form [272]  
22

$$23 \quad \mathbf{S}\mathbf{q} = -f(\epsilon) \mathbf{v} \quad (1)$$

24 where  $\mathbf{S}\mathbf{q}$  (the self-interaction of the induced surface charge) is proportional to  $\mathbf{v}$ ,  
25 the solute's electrostatic potential at the solute/continuum interface. The propor-  
26 tionality factor,  
27

$$28 \quad f(\epsilon) = \frac{\epsilon - 1}{\epsilon + x}, \quad (2)$$

29  
30  
31  
32  
33 has been a source of much discussion in the literature [272–275], specifically with  
34 respect to whether the optimal choice is  $x = 0$  [273] (consistent with the Born  
35 model) and  $x = 1/2$  [276] (a compromise between Born's model of a charge in  
36 a sphere and Onsager's model of a dipole in a sphere). The choice is obviously  
37 inconsequential in high-dielectric ( $\epsilon \gg 1$ ) solvents, but in non-polar solvents the  
38 choice  $x = 1/2$  proves to be somewhat more accurate as compared to experiment,  
39 at least when non-electrostatic terms are included as well [272]. Equation (1), with  
40  $x = 1/2$ , was originally suggested by Klamt and Schüürmann [276], who called  
41 it the *conductor-like screening model* (COSMO). Nowadays, however, "COSMO"  
42 implies a model based on Eq. (1) but with an explicit correction for outlying  
43 charge [274, 275]. (On the other hand, even C-PCM includes an *implicit* correction  
44 for outlying charge, as shown by Chipman [268].)  
45

46 A C-PCM description of the solvent is available for excited-state TD-DFT cal-  
47 culations as well [130], including its analytic gradient and Hessian. Together, these  
48 methods facilitate efficient solution-phase geometry optimizations and harmonic  
49 frequency calculations for molecules in excited electronic states.  
50

51 One crucial aspect of the implementation of any PCM is the construction of  
52 a molecule-shaped "cavity" that defines the interface between the atomistic so-  
53 lute and the continuum solvent. A formally appealing way to construct the cav-  
54 ity is to let it coincide with an isocontour of the quantum-mechanical solute  
55 electron density [277], and such a construction is available in Q-CHEM for use  
56 with SS(V)PE [278]. Unfortunately, the analytic energy gradient for such a con-  
57 struction has yet to be developed, and at present, carefully-parameterized, bond-  
58 connectivity-dependent atomic radii can surpass the accuracy of an isodensity cav-  
59 e  
60

solute class	no. data points	SM8 MUE (kcal/mol)
all neutrals	940	0.6
all ions	332	4.3
all cations	124	3.9
all anions	208	4.6
aq. neutrals	274	0.6
nonaq. neutrals	666	0.6
aq. ions	112	3.2
nonaq. ions	220	4.9

Table 6. Mean unsigned errors (MUEs, in kcal/mol) for solvation free energies in water and in 17 organic solvents, from Ref. 287.

ity when it comes to computing solvation free energies [279]. (Recent attempts to incorporate non-electrostatic terms into the isodensity construction show great promise for high accuracy with minimal parameterization [280, 281], but these corrections are not yet available in Q-CHEM.)

For these reasons, the vast majority of PCM calculations use a cavity construction that is based in some way on atom-centered van der Waals spheres. Because these spheres must be discretized onto a grid for practical calculations, such an approach suffers from discontinuities in the energy and forces as the atoms are allowed to move, *e.g.*, in a geometry optimization [282]. This ubiquitous problem is avoided by Q-CHEM’s intrinsically smooth implementation of both IEF-PCM and C-PCM [270, 282, 283]. This implementation passes the stringent test of conserving energy in *ab initio* molecular dynamics simulations of solution-phase molecules, even for difficult cases involving such as intramolecular proton transfer in aqueous glycine, where the shape of the cavity changes drastically as the proton is shuffled between carboxylate and amino moieties [283].

The aforementioned PCMs, however, treat only the electrostatic contributions to solvation, neglecting other contributions such as dispersion, exchange repulsion, and solute-induced changes in the solvent structure. Although non-electrostatic corrections to PCMs can be put in “by hand” [284, 285] to obtain accurate free energies of solvation [286], a more universal approach is offered by the so-called SM $x$  models developed by Cramer and Truhlar [287]. The SM $x$  models use a variety of macroscopic solvent descriptors (surface tension, refractive index, acid/base parameters, etc.) to parameterize non-electrostatic corrections to a Generalized Born treatment of bulk electrostatics [288, 289], and are designed to work in a black-box way for any solvent. Q-CHEM includes two of the more recent versions of the SM $x$  approach: SM8 [290] and SM12 [291]. Both models afford similar statistical errors in solvation energies [291], but SM12 does lift an important restriction on the level of electronic structure that can be combined with these models. Specifically, the Generalized Born model for electrostatics that is employed in SM8 is based upon a variant of Mulliken-style atomic charges, and is therefore parameterized only for a few small basis sets, *e.g.*, 6-31G\*, whereas SM12 uses charges that are stable with respect to basis-set expansion and is therefore available at any level of electronic structure theory.

Mean statistical errors in solvation free energies ( $\Delta G_{298}$ ) versus experiment are shown in Tables 6 and 7 for several implicit solvent models. Results in Table 6 demonstrate that the SM8 model achieves sub-kcal/mol accuracy for neutral molecules, although average errors for ions are more like  $\sim 4$  kcal/mol [287]. Non-electrostatic terms appropriate for IEF-PCM are available for a few solvents [284, 285], and when these are included the “IEF-PCM+non-elst.” errors (Ta-



solute class	no. data points	MUE (kcal/mol)		
		IEF-PCM+ non-elst. <sup>a</sup>	COSMO- RS <sup>b</sup>	SM8
all neutral <sup>c</sup>	2346		0.5	0.6
17 organic solvents	960		0.6	0.6
3 organic solvents <sup>d</sup>	960	0.6		0.6
aq. solvation	284	1.0	0.6	0.6

<sup>a</sup>Includes non-electrostatic terms [284, 285]

<sup>b</sup>Requires the COSMOTHERM software in addition to Q-CHEM

<sup>c</sup>Includes all 91 solvents and 2,346 data points used to parameterize SM8

<sup>d</sup>Octanol, CHCl<sub>3</sub>, and CCl<sub>4</sub>

Table 7. Mean unsigned errors (MUEs, in kcal/mol) for solvation free energies, for models that include non-electrostatic interactions. (Adapted from Ref. 286; copyright 2009 American Chemical Society.)

ble 7) are comparable to those obtained using SM8 [286]. Also shown in Table 7 are results from the COSMO-RS model (where RS stands for “real solvent”) [292, 293]. This model yields error statistics that are essentially identical to those exhibited by SM8, but requires external software in addition to Q-CHEM.

## 6.2. QM/MM and fragment methods

For serious QM/MM applications, significant developments have also occurred with respect to Q-CHEM’s ability to interface with external classical simulation packages, particularly the CHARMM program. Firstly, major strides were made in the area of QM/MM normal mode analysis. In 2009, full QM/MM analytic second derivatives were implemented in Q-CHEM (stand-alone and coupled to CHARMM) [294]; both restricted and unrestricted HF and DFT methods are supported. This was closely followed by the parallelization of these full QM/MM Hessian calculations and extension to the Mobile Block Hessian (MBH) formalism; significantly reducing CPU and memory requirements for these intensive calculations [295]. Complementing Q-CHEM/CHARMM support for QM/MM dielectric approaches (see also QM/MM/PCM below), the solvent macromolecule boundary potential (SMBP) method has also been interfaced to Q-CHEM [296, 297]. Last, but not least, a user-friendly Web interface that facilitates the graphical setup of QM/MM calculations (i.e., Q-CHEM/CHARMM) was also developed [298]. It is anticipated that this will receive significant enhancements in the near future and tie closely into IQMOL, which is discussed in Sec. 9.

In addition, major progress has been made since v. 3.0 towards making Q-CHEM a versatile, stand-alone QM/MM program [38, 299], without the need to interface with CHARMM or any other classical MD package. Notable features of the stand-alone QM/MM package include the availability of several widely-used force fields (AMBER, CHARMM, OPLS) with an option to add user-definable force field parameters. QM/MM functionality is available for all QM models implemented in Q-CHEM, including excited-state methods insofar as correlated post-Hartree-Fock wave function models or time-dependent DFT can be based on a reference determinant that has been polarized by the MM environment. For ground-state calculations, periodic boundary conditions are available based on a novel implementation of Ewald summation for QM/MM calculations [299]. Alternatively, the PCM solvation models discussed in Section 6.1 can be used as boundary conditions for a QM/MM calculation. In this case, the solute/continuum interface is defined by the (potentially sizable) MM region of the calculation, such that the cubic-scaling

method	HB	DISP	MIXED	ALL
EFP	1.97	0.48	0.34	0.91
Force fields				
Amber	4.79	0.98	0.98	2.16
OPLSAA	4.59	1.04	0.57	2.02
MMFF94	3.75	0.88	0.59	1.70
HF and DFT				
HF	3.29	7.24	3.15	4.56
B3LYP	1.77	6.22	2.64	3.54
PBE	1.13	4.53	1.66	2.44
M05	1.26	3.16	1.09	1.84
M06	0.89	0.99	0.67	0.85
M06-2X	0.73	0.36	0.32	0.47
BLYP-D3				0.23
$\omega$ B97X-D				0.22
Correlated methods				
MP2	0.24	1.69	0.61	0.88
SCS-MP2	1.54	0.55	0.37	0.80
SCS-CCSD	0.40	0.23	0.08	0.24
XSAPT-based methods				
XSAPT(KS)+D1	0.73	0.38	0.52	0.53
XSAPT(KS)+D2	0.72	1.18	0.52	0.82
XSAPT(KS)+D3	0.76	0.67	0.38	0.61
sd-XSAPT	0.33	0.30	0.32	0.32

Table 8. Mean unsigned errors (in kcal/mol) of the total interaction energies for hydrogen bonded (HB), dispersion dominated (DISP), mixed (MIXED) complexes and the whole group (ALL) of the S22 dataset by EFP, molecular mechanics force fields, HF, DFT, and ab initio methods. From Ref. 305 and references therein, except for the XSAPT values [306, 307].

PCM equations potentially become the bottleneck of the calculation, outpacing the QM cost! To facilitate large-scale QM/MM/PCM calculations, Q-CHEM therefore includes a linear-scaling, scalable-parallel conjugate gradient solver for the PCM equations [300]. Significant progress toward enhancing the stand-alone QM/MM functionality is anticipated in the near future.

Q-CHEM also provides a more sophisticated way to account for environment effects on the electronic structure of a solute, by using the Effective Fragment Potential (EFP) method. The EFP method is a first-principles-based model that was originally designed to describe aqueous environment [301, 302]. It was later extended to general solvents and biological environments [263, 303, 304]. The interaction energy between EFP fragments is modeled as a sum of Coulomb, polarization, dispersion, and exchange-repulsion terms, all of which are derived as truncated expansions in terms of intermolecular distance and overlap integrals. The accuracy of the EFP method was tested on the S22 and S66 datasets for non-covalent interactions [305]. The results shown in Table 8 demonstrate that EFP is similar in accuracy to MP2 and the M06 density functional and is superior to classical force fields and most density functionals not corrected for dispersion interactions.

EFP is interfaced with the SCF, CIS/TD-DFT, and CCMAN/CCMAN2 modules, allowing ground and excited state calculations in a presence of polarizable environment [308–310]. Electrostatic and polarization EFP terms in QM/EFP calculations modify the electronic Hamiltonian of the quantum region to affect the shapes and energies of the molecular orbitals of a solute. Each excited state interacts differently with the polarizable environment. This effect is accounted for by

1 computing additive energy corrections to the excitation energies [308]. The com-  
 2 bination of first-principle polarizable explicit solvent with the EOM-CC family of  
 3 methods is a unique feature of QChem enabling state-of-the art calculations of  
 4 solvatochromic effects and redox processes [310, 311]. To sum up, the major dif-  
 5 ferences between the QM/EFP and QM/MM schemes are: (i) more accurate and  
 6 detailed description of the electrostatic interactions in EFP using distributed mul-  
 7 tipoles up to octopoles versus the partial charge representation used in typical  
 8 MM; (ii) polarizable environment in EFP induces self-consistent response to the  
 9 electronic wave function of the quantum region, while most classical force fields are  
 10 not polarizable.

11 EFP is a fragment-based rather than atom-based potential. Each effective frag-  
 12 ment contains a set of pre-defined parameters. Parameters for any fragment may be  
 13 generated in the GAMESS package [312] in a special type of run (MAKEFP run).  
 14 The Q-CHEM distribution contains a library of fragments with prepared and tested  
 15 potentials (typical solvents, DNA bases, molecules from S22 and S66 datasets). Ef-  
 16 fective fragments are kept rigid in all computations. The QM/EFP formalism can  
 17 be extended to biological systems. For that, a biological polymer is split into and  
 18 represented by a set of individual effective fragments. Scripts automating prepara-  
 19 tion of the fragments and parameters are provided within the Q-CHEM distribution.  
 20 The Q-CHEM implementation of the EFP method is based on the stand-alone EFP  
 21 library *libefp* [313] and will benefit from all future updates and improvements to  
 22 the EFP algorithms.

23 Other fragment-based methods for non-covalent interactions that are available in  
 24 Q-CHEM include an electrostatically-embedded many-body expansion [314]. This  
 25 method is based on a truncation of the traditional many-body expansion,

$$E = \sum_I E_I + \sum_I \sum_{J>I} \Delta E_{IJ} + \sum_I \sum_{J>I} \sum_{K>J} \Delta E_{IJK} + \dots, \quad (3)$$

26 in which  $E_I$  represents the energy of monomer  $I$ ,  $\Delta E_{IJ} = E_{IJ} - E_I - E_J$  is a  
 27 two-body correction for dimer  $IJ$ , etc. The idea is to truncate Eq. (3) at some  
 28 number of “bodies”  $n \ll N$ , and to accelerate convergence (with respect to  $n$ ) by  
 29 performing the monomer ( $E_I$ ), dimer ( $E_{IJ}$ ), trimer ( $E_{IJK}$ ), ... calculations in a  
 30 point-charge representation of the remaining monomer units. These point charges  
 31 can be obtained, *e.g.*, as Mulliken charges or as charges fitted to the monomer elec-  
 32 trostatic potentials (ChElPG charges [315]). Due to the highly nonlinear scaling of  
 33 quantum chemistry methods, the cost of performing, *e.g.*,  $N(N-1)(N-2)/6$  dis-  
 34 tinct trimer calculations,  $N(N-1)/2$  distinct dimer calculations, and  $N$  distinct  
 35 monomer calculations may be far less than the cost of performing an electronic  
 36 structure calculation on the entire non-covalent supersystem. The subsystem cal-  
 37 culations can be performed at any level of theory, and electrostatically-embedded  
 38 two- and three-body expansions are often reasonably faithful to supersystem results  
 39 computed at the same level of theory [264, 314, 316].

40 A fragment-based method for non-covalent interactions that is currently unique  
 41 to Q-CHEM is an extended (cluster) version of symmetry-adapted perturbation  
 42 theory [264, 306, 307, 317, 318]. This so-called XSAPT method generalizes the tra-  
 43 ditional SAPT methodology [319] to clusters of arbitrary size, treating many-body  
 44 polarization effects in a self-consistent way but approximating other non-covalent  
 45 interactions (exchange and dispersion) in a pairwise-additive but *ab initio* fashion.  
 46 XSAPT extends SAPT-style energy decomposition analysis to clusters contain-  
 47 ing more than two monomer units [307]. For a cluster consisting of  $N$  monomer  
 48 units, the cost of an XSAPT calculation is about the same as  $N(N-1)/2$  second-  
 49 order

Method	Basis Set	S22		S66		CHB15	
		MUE	Max	MUE	Max	MUE	Max
XSAPT(KS)+D1	ha-DZ <sup>a</sup>	0.53	(1.16)	0.29	(1.07)	0.98	(1.96)
XSAPT(KS)+D2	ha-TZVPP <sup>b</sup>	0.82	(4.23)	0.39	(3.32)	1.43	(4.30)
XSAPT(KS)+D3	hp-TZVPP <sup>c</sup>	0.61	(1.91)	0.45	(1.96)	0.89	(2.39)
sd-XSAPT(KS)	6-31G(d,2p)	0.32	(0.72)	0.37	(0.97)	0.77	(2.21)

<sup>a</sup>cc-pVDZ for hydrogen and aug-cc-pVDZ for other atoms.

<sup>b</sup>def2-TZVPP, with diffuse functions from aug-cc-pVTZ for non-hydrogen atoms.

<sup>c</sup>def2-TZVPP, with diffuse functions from 6-311+G for non-hydrogen atoms.

Table 9. Mean unsigned errors (MUEs) and maximum errors, both in kcal/mol, with respect to CCSD(T)/CBS benchmarks for the S22 [82, 83], S66 [84, 85], and CHB15 data sets [320], using three generations of XSAPT(KS)+D as well as XSAPT(KS) with scaled second-order dispersion, sd-XSAPT(KS). The Kohn-Sham functional used is LRC- $\omega$ PBE [37], with  $\omega$  tuned in a monomer-specific way to achieve the condition that  $\epsilon_{\text{HOMO}}$  equals minus the ionization potential 307.

order dimer SAPT calculations, each of which is MP2-like in cost. Second-order SAPT works well for non-covalent clusters whose interactions are dominated by polarization (induction) and electrostatics, but inherits MP2's problems with overestimating dispersion energies in the basis-set limit. For dispersion-bound systems, good results are only obtained by carefully choosing a small basis set to exploit error cancellation [317, 318].

This unhappy state of affairs is remedied by replacing the MP2-like dispersion and exchange-dispersion terms in SAPT with empirical atom-atom dispersion potentials, which also has the effect of reducing the cost from fifth-order to third-order scaling [306, 307]! The resulting method is called XSAPT(KS)+D, where the "KS" refers to the fact that Kohn-Sham DFT is used for the monomers. The cost therefore scales like DFT with respect to the size of the monomer units [306], while scaling only quadratically with respect to the number of monomer units, making it cheaper than supersystem DFT already for as few as  $N = 2$  monomers [306]. At the same time, the method exhibits sub-kcal/mol accuracy (relative to complete-basis CCSD(T) benchmarks) for non-covalent interactions [306, 307], as shown in Table 9 for three successively-improved versions of the empirical dispersion potential (D1, D2, and D3). Also shown are very recent results in which second-order dispersion is retained but empirically scaled, as suggested in Ref. 321. MUEs for various subsets of the S22 data set are shown in Table 8, from which it is clear that these methods provide outstanding performance for both systems that are dominated by electrostatics and induction (the HB subset) as well as those whose binding is dominated by dispersion.

## 7. Energy and electron transfer

### 7.1. Energy transfer: direct Coulomb and exchange couplings

Excitation energy transfer (EET) is a process where one electronically excited molecule or fragment passes its excitation energy to another. In the singlet states, it is the widely used Förster energy transfer [322]. EET in triplet states is seen in triplet quenching processes [323], as well as artificial light-emitting systems utilizing phosphorescence [324, 325]. Fermi's Golden rule has the rates of these processes proportional to the square of an electronic coupling factor, which is the off-diagonal Hamiltonian matrix element for the diabatic states (i.e. locally excited states [326]).

Computational schemes that offer total EET couplings such as the Fragment Excitation Difference and the Fragment Spin Difference has been available in Q-

CHEM for several years [327–329]. In this revision, we have included the option to compute the Coulomb and exchange couplings to further dissect the total coupling and derive physical insights into its origin [330]. In the derivation of the coupling for singlet EET, [322, 331–333] a first-order perturbation expansion is often used. It can be shown that the electronic coupling for singlet EET contains three contributions,

$$V^{\text{SEET}} = V^{\text{Coul}} + V^{\text{exch}} + V^{\text{ovlp}}, \quad (4)$$

while the corresponding break-down for triplet EET is [329]:

$$V^{\text{TEET}} = V^{\text{exch}} + V^{\text{ovlp}}. \quad (5)$$

In Eq. (4),  $V^{\text{Coul}}$  is the Coulomb coupling that arises from the Coulomb interaction between electronic transitions,

$$V^{\text{Coul}} = \iint d\mathbf{r}_1 d\mathbf{r}_2 \frac{\rho_{\text{D}}^{\text{tr}*}(\mathbf{r}_1) \rho_{\text{A}}^{\text{tr}}(\mathbf{r}_2)}{|\mathbf{r}_1 - \mathbf{r}_2|}. \quad (6)$$

$V^{\text{exch}}$  in both Eqs. (4) and (5) is the exchange coupling,

$$V^{\text{exch}} = - \iint d\mathbf{r}_1 d\mathbf{r}_2 \frac{\gamma_{\text{D}}^{\text{tr}*}(\mathbf{r}_1, \mathbf{r}_2) \gamma_{\text{A}}^{\text{tr}}(\mathbf{r}_1, \mathbf{r}_2)}{|\mathbf{r}_1 - \mathbf{r}_2|}, \quad (7)$$

which is the Dexter exchange coupling that arises from the indistinguishability of the electrons in many-electron wavefunctions[331].  $\gamma^{\text{tr}}(\mathbf{r}, \mathbf{r}')$  in Eq. (7) is a one-particle transition density matrix.  $\rho^{\text{tr}}(\mathbf{r})$  in Eq. (6) contains diagonal elements of the transition density matrix:  $\rho^{\text{tr}}(\mathbf{r}) \equiv \gamma^{\text{tr}}(\mathbf{r}, \mathbf{r})$ . The remaining contributions to EET couplings, such as the term  $V^{\text{ovlp}}$  arising from the overlap of donor-acceptor orbitals, and the influence of ionic-configuration interactions have also been discussed in the literature [330, 334, 335].

In the condensed phase, the polarizability of surrounding molecules affects the Coulomb part of the EET coupling of the chromophores. A quantum mechanical model was formulated through a general TDDFT framework [333] for the polarizability effect in SEET coupling. The solvent effect on the Coulomb coupling was treated with a continuum solvent model [336]. Such solvent effects has been studied for photosynthetic light-harvesting systems [337, 338].

Q-CHEM's direct coupling scheme for electron transfer coupling is now extended for the Coulomb and Exchange couplings in EET ( $V^{\text{Coul}}$  and  $V^{\text{exch}}$  Eqs. (6) and (7)). The donor and acceptor transition densities are calculated separately from CIS or TDDFT calculations, and the Coulomb and Exchange couplings are calculated using the efficient 2-electron integrals in Q-CHEM. The solvent polarization effect on the Coulomb coupling is also implemented in this revision, using the efficient PCM kernel in Q-CHEM (Sec. 6.1). Such results allow one to analyze the physical contributions to the EET coupling [327, 329, 330].

## 7.2. Constrained DFT

To accurately treat energy- and electron-transfer one always needs to construct appropriate diabatic states [339]. In the context of DFT, one appealing way to do this is through *constrained* DFT (CDFT) [340]. One minimizes the energy of the system subject to chemically or physically-motivated constraints on the density [341, 342]. For example, in electron transfer, one might constrain the net charge on



1 a fragment of the molecule [343, 344], or for magnetic systems one might constrain  
 2 the net spin [345]. These states then provide a basis for describing reactant- and  
 3 product-like states for electronic reactions. From the computational point of view,  
 4 because CDFT is variational, the energies and analytic forces are easily computed  
 5 at a cost that is not much higher than standard DFT. Q-CHEM has the ability to  
 6 apply multiple simultaneous constraints to the system for any density functional.  
 7 The result is that, in addition to specifying the atomic coordinates, one also has  
 8 the ability to specify the net charges and/or spins on multiple fragments within a  
 9 molecule or supramolecular assembly.

10 In addition to energies of these diabatic-like states, one also would like to be  
 11 able to compute the electronic coupling between two CDFT states. This can be  
 12 done using a simple approximation involving the Kohn-Sham orbitals[346]. The  
 13 resulting electronic coupling can then be computed in a fraction of the time of  
 14 the CDFT calculations themselves. The CDFT idea can also be applied in many  
 15 contexts beyond electron transfer. Notably, the CDFT solutions bear a strong  
 16 resemblance to valence bond configurations, which leads to the realization that  
 17 CDFT states can be a good way of using DFT for problems that are inherently  
 18 multi-reference [347, 348]. The basic idea is to converge several CDFT states (that  
 19 play the role of the active space in an MCSCF or CASSCF calculation) and then  
 20 build the Hamiltonian as a matrix, using the energies of the states and the couplings  
 21 between them. One then does a small configuration interaction (CI) calculation to  
 22 account for the influence of these different valence-bond like states on the total wave  
 23 function. This CDFT-CI method is able to describe conical intersections between  
 24 the excited state and the ground state [349] and recently analytic gradients of this  
 25 method have also been implemented [350].

### 31 7.3. Localized diabaticization

32 As an alternative to direct coupling or constrained DFT, meaningful diabatic states  
 33 can also be computed via localized diabaticization. In particular, Q-CHEM now allows  
 34 the user to transform CIS or TD-DFT/TDA adiabatic excited states according  
 35 to either Boys[351] or Edmiston-Ruedenberg[352] localized diabaticization. Diabatic  
 36 states  $\{|\Xi_I\rangle\}$  can be generated from multiple ( $N_{states} \geq 2$ ) adiabatic states

$$37 \quad |\Xi_I\rangle = \sum_{J=1}^{N_{states}} |\Phi_J\rangle U_{ji} \quad I = 1 \dots N_{states}, \quad (8)$$

38 and the user must decide only which adiabatic states  $\{|\Phi_I\rangle\}$  should be transformed.  
 39 In analogy to orbital localization, Boys localized diabaticization prescribes maximiz-  
 40 ing the charge separation between diabatic state centers, whereas ER localized di-  
 41 abaticization prescribes maximizing the total self-interaction energy. Note, however,  
 42 that both methods are completely invariant to choice of orbitals. These methods  
 43 can be justified by assuming a slow solvent coordinate that is moderately coupled  
 44 to an electronic subsystem. Boys localization then assumes that the solvent coordi-  
 45 nate yields an electric field that is linear in space (and, in effect, is a multi-state  
 46 generalization of generalized Mulliken-Hush [351]), while ER localization assumes  
 47 that solvent takes the form of an isotropic linear dielectric medium. While Boys  
 48 localization can be applied safely for ET, ER localization can be applied safely  
 49 for both ET and EET. Q-CHEM also allows a third option, BoysOV[353], specif-  
 50 ically for EET; according to BoysOV, one performs Boys localized diabaticization  
 51 separately for the virtual (particle) and occupied (hole) components of the dipole  
 52 operator.  
 53  
 54  
 55  
 56  
 57  
 58  
 59  
 60

Finally, for energy transfer, it can be helpful to understand the origin of the diabatic couplings. Thus, for adiabatic CIS excited states, Q-CHEM now provides the functionality to decompose the diabatic coupling between diabatic states into Coulomb (J), Exchange (K) and one-electron (O) components[354]:

$$\begin{aligned}
 |\Xi_I\rangle &\equiv \sum_{ia} t_i^{Ia} |\Phi_i^a\rangle \\
 \langle \Xi_P | H | \Xi_Q \rangle &= \underbrace{\sum_{iab} t_i^{Pa} t_j^{Qb} F_{ab}}_O - \underbrace{\sum_{ija} t_i^{Pa} t_j^{Qa} F_{ij}}_+ + \underbrace{\sum_{ijab} t_i^{Pa} t_j^{Qb} (ia|jb)}_J - \underbrace{\sum_{ijab} t_i^{Pa} t_j^{Qb} (ij|ab)}_K
 \end{aligned}$$

#### 7.4. Derivative couplings

As one last tool for studying electronic relaxation and nonadiabatic dynamics, Q-CHEM now provides the functionality to compute derivative couplings between CIS excited states,  $d_{IJ}^\alpha \equiv \langle \Phi_I | \frac{\partial}{\partial R^\alpha} | \Phi_J \rangle$ . Within the context of an adiabatic representation, derivative couplings are the leading terms that break the Born-Oppenheimer approximation[355]; indeed, they are infinite at a conical intersection. As detailed in Ref. [356], these couplings can be computed with or without electron translation factors; without electron translation factors, the derivative couplings are not translationally invariant. Q-CHEM provides derivative couplings for the user with and without such factors.

#### 7.5. Transport and molecular electronics

Molecular scale electronics, where either one or a few molecules bridge two conducting electrodes is a focus of considerable research activity. These large scale efforts have led to impressive advances in the fabrication of molecular bridges, measurement of current-voltage relations, and associated computational modeling [357–365]. Much of the interest stems from the prospect of fabricating electronic devices that are tunable at the molecular level.

In molecular bridges the electronic density is affected by the coupling to biased electrodes. Accordingly, the electrodes' electronic band structure is projected onto the otherwise discrete electronic levels of the molecules. Most computational approaches to model electron transport are based on viewing the conductivity as due to scattering events through the molecule, where electrons are transmitted to the bridge broadened electronic states [366–370]. This picture of current follows the seminal work of Landauer, where the quantum transport function is integrated over the energies around the Fermi level as set by the voltage bias [371–373]. In state-of-the-art treatments, the electronic density of an electrode-coupled system is evaluated by the single particle Green's function (GF) formalism with density functional theory (DFT) for describing the electronic interactions within the bridge. The GF formalism is then used to calculate the transmission function [374, 375]. The same approach can be extended to treat biasing conditions by a self consistent procedure for calculating the electronic density coupled to the biased electrodes using non-equilibrium GF formalism [369, 376, 377].

The quantum transport utility in Q-CHEM (called T-CHEM) can calculate the transmission function at any implemented variational level. T-CHEM implements

1 the Green's function expressions used for calculating the transmission function  
2 [378–390]. An important modeling aspect is to set the self-energies (SEs) that  
3 represent the coupling to the extended system posed by the electrodes. Here, the  
4 extent of the electronic screening has to be decided. Namely, the molecular bridge  
5 region is usually defined to include several repeating units of the electrode beyond  
6 the surface layer [391, 392]. In T-CHEM the SE can be based on precalculated  
7 electrode models or on subregions within the supermolecule that are provided in  
8 the *\$molecule* section which are calculated on the fly. While the flexibility in setting  
9 the SE models is a great advantage, it has to be used with great care to avoid  
10 artifacts.[391, 392].  
11  
12

## 13 8. Analysis

### 14 8.1. Energy decomposition analysis

15 Understanding the origin of intermolecular or intra-molecular interactions in terms  
16 of physically interpretable components is the goal of energy decomposition analy-  
17 sis (EDA) methods. Such components typically include permanent electrostatics,  
18 corresponding to interactions between charges and/or multipole moments, induced  
19 electrostatics associated with polarization, Pauli repulsions associated with inter-  
20 actions between filled orbitals, and dative or donor acceptor interactions associated  
21 with interactions between filled and empty orbitals. By far the best-known EDA  
22 approach is the Natural Bond Orbital (NBO) suite of methods due to Weinhold  
23 and co-workers [393–396], which Q-CHEM supports via a standard interface to the  
24 current version of the NBO package.  
25

26 In addition, Q-CHEM contains the absolutely localized molecular orbital (ALMO)  
27 EDA [397], as a built-in method. The ALMO EDA is a descendent of the Kitaura-  
28 Morokuma EDA [398] (which is perhaps the first EDA method), and uses the  
29 same definition of the frozen interactions. It is also closely related to the Block-  
30 Localized Wave function (BLW) EDA [399, 400] because both approaches use the  
31 same variational definition of the polarization energy that is an upper limit to the  
32 true extent of polarization [401]. A distinctive advantage of the ALMO-EDA is  
33 that the charge-transfer contribution is separated into pairwise additive contribu-  
34 tions associated with forward and back-donation, and a non-pairwise decomposable  
35 higher order contribution, which is very small for typical intermolecular interac-  
36 tions. The ALMO-EDA is implemented for open shell [402] as well as closed shell  
37 fragments [397], and uses the efficient ALMO-SCF method [403] as its underlying  
38 computational engine.  
39

40 In addition to the energy decomposition, the ALMO-EDA provides a means to  
41 automatically generate the pairs of orbitals (donor and acceptor) that are responsi-  
42 ble for dative interactions, which can be visualized and chemically interpreted [404].  
43 As an example of the application of the ALMO-EDA, Figure 9 shows the princi-  
44 pal intermolecular interactions associated with the trimeric complex between vinyl  
45 alcohol cation, water and formaldehyde. This triplex was recently identified by com-  
46 putational and experimental evidence [405] as being the principal intermediate that  
47 results from photoionization of the glycerol molecule, before fragmentation occurs.  
48 The remarkable stability of the complex is due to two very strong intermolecu-  
49 lar interactions. The first one has the character of a very short, strong hydrogen  
50 bond, involving charge transfer from a water lone pair towards the vinyl alcohol  
51 cation, in addition to strong polarization effects. The second one is primarily an  
52 electrostatic interaction, involving both permanent and induced components, be-  
53 tween vinyl alcohol cation and formaldehyde. The strength of the ALMO-EDA is  
54  
55  
56  
57  
58  
59  
60

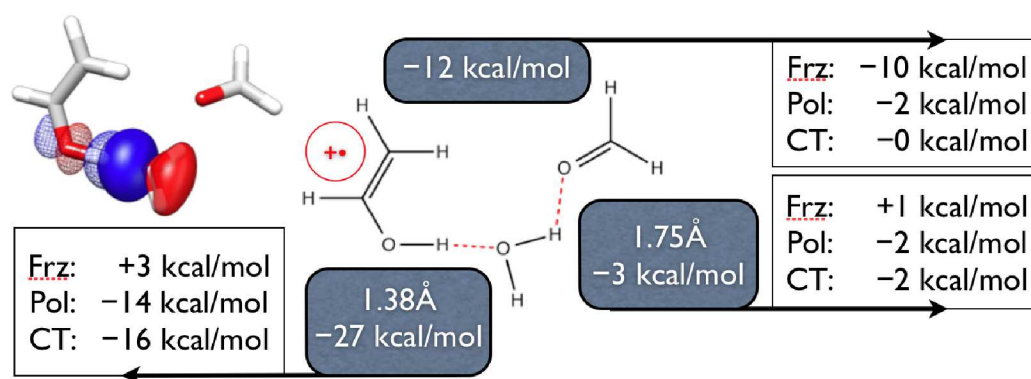


Figure 9. EDA results (from large basis DFT calculations) for the ternary complex of vinyl alcohol cation, formaldehyde, and water that results from photoionizing glycerol, HOCH<sub>2</sub>-CHOH-CH<sub>2</sub>OH. Its stability arises from 2 strong interactions. The largest is a 27 kcal/mol H-bond between water and vinyl alcohol cation. This type of H-bridged ion-molecule interaction is often assumed to be electrostatic, but the EDA shows it is at least 50% CT in origin. The O lone pair donor orbital (bold), and HO  $\sigma^*$  acceptor orbital (faint) pair are shown at the top left. The second strong interaction is a longer-range electrostatic (charge-dipole, frozen-dominated) interaction between vinyl alcohol cation and formaldehyde with little CT (see top right).

in clearly distinguishing the different character of the two strongest interactions.

## 8.2. Natural transition orbitals

The canonical MOs are seldom a good basis for conceptual understanding of electronic transitions, especially for Hartree-Fock (as opposed to Kohn-Sham) MOs, where the virtual orbitals formally describe electron-attached states rather than bound excitations, leading to significant mixing of the canonical MOs in the excited-state wave function. Density differences or attachment/detachment densities [406], both long available in Q-CHEM, are often more helpful, but densities lack the nodal structure that sometimes provides important information about the character of an excited state. An important class of examples are the Frenkel exciton states in a system composed of multiple, electronically-coupled chromophore units. These excitons are delocalized over more than one chromophore unit, leading to attachment and detachment densities that are both highly delocalized, and each of which occupies approximately the same region of space. Nodal information is extremely useful in interpreting the character of such an excited state, which is often (at a qualitative level) simply a linear combination of optically-allowed transitions on the monomer units [38].

Analysis of these and other excited states is greatly simplified by constructing *natural transition orbitals* (NTOs) [407–409]. For a given excited state, these orbitals amount to the unitary transformations of the occupied and virtual MOs that provide the best possible particle/hole picture of that state, in the sense of having a dominant occupied/virtual transition. The attachment/detachment densities are recovered as the sum of the squares of the particle/hole NTOs, but the NTOs are orbitals (not densities) and thus contain phase information. This is helpful in assigning diabatic character ( $\pi\pi^*$ ,  $n\pi^*$ , etc.) to excited states in complex systems. An example is shown in Fig. 10, which depicts both NTOs and attachment/detachment densities for a particular exciton-type state of a nine-chromophore model of a self-assembling organic nanotube [410]. Both the attachment and detachment densities are delocalized over essentially the same four chromophores. Inspection of the four occupied/virtual NTO pairs with largest amplitudes, however, immediately reveals how this excitation can be understood as electronic coupling between four different



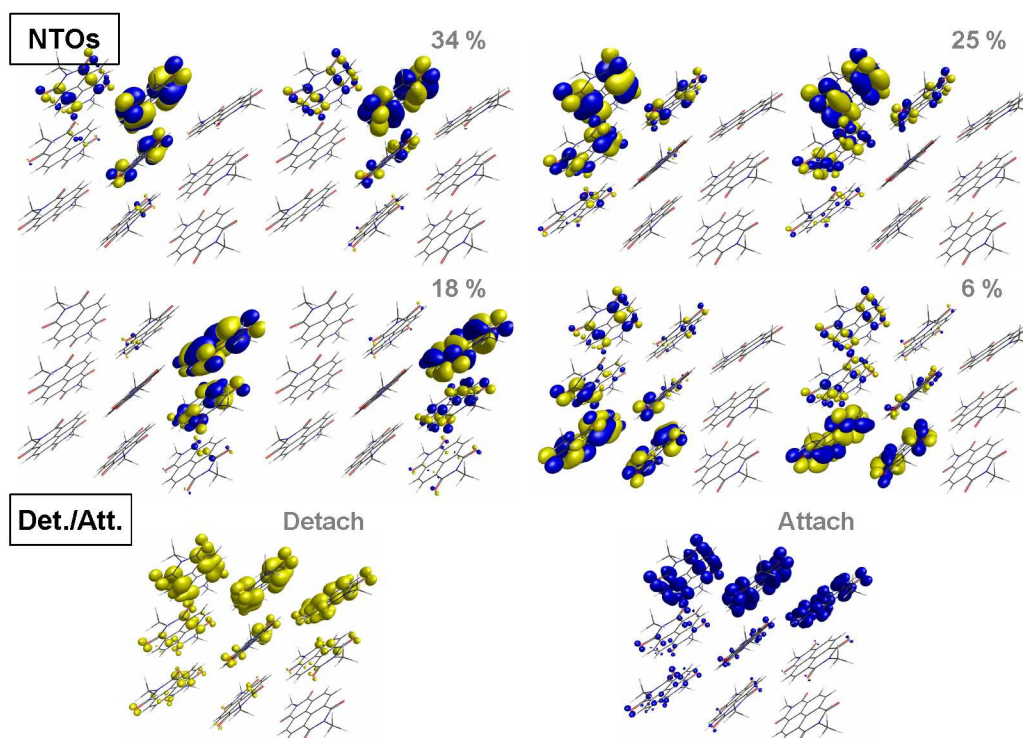


Figure 10. NTOs with largest amplitude, and attachment/detachment densities, for a Frenkel exciton state in a nine-unit model of the self-assembling nanotube described in Ref. 410. The chromophore unit is a derivative of naphthalenetetracarboxylic acid diimide.

localized  $\pi \rightarrow \pi^*$  excitations on each of four different chromophores. In systems not displaying excitonic character, a single occupied  $\rightarrow$  virtual transition in the NTO basis often accounts for  $\gtrsim 95\%$  of the total excitation amplitude.

## 9. Graphical user interfaces

### 9.1. IQmol

IQMOL is an open source molecular editor and visualization package that has been written to work with the Q-CHEM package. It provides a single integrated environment for building molecules, setting up and submitting Q-CHEM calculations, and analysing the resulting output.

IQMOL has a flexible and easy to use free-form molecular builder that allows structures to be built from a variety of building blocks including atoms, functional groups and entire molecular fragments. It also allows the user to add effective fragment potential (EFP) fragments for use in EFP calculations [411]. The functional groups, molecular fragments and EFPs are obtained from an internal library that is loaded at start up and that can be easily extended by the user. Structures can be optimized using a range of molecular mechanics (MM) force fields available in the Open Babel library [412] including MMFF94, UFF, Ghemical and Gaff. Constraints can be applied to the structure and these are applied in the MM minimization as well as being passed through to Q-CHEM for any subsequent geometry optimization. Structures can also be symmetrized using the integrated SYMMOL [413] routine which recovers the full point-group symmetry of the molecule to within a given tolerance.

Q-CHEM jobs can be configured using the built-in job set up panel which includes most of the Q-CHEM job options presented in a logical and hierarchical way. Each



option has a separate control which has tool-tip documentation associated with it which summarizes its use and details what settings are valid, thus reducing the need to constantly check the Q-CHEM user's manual. Multiple Q-CHEM servers can be configured allowing jobs to be submitted directly from IQMOL. These servers can correspond to either the local machine or a remote server running PBS or SGE queueing software. In the case of remote servers, all communication is carried out securely via SSH channels. Apart from ensuring Q-CHEM is properly installed, no other server-side configuration is required for job submission from IQMOL, allowing it to be used on servers where the user has limited access permissions.

IQMOL's analysis package can read data from a variety of file formats including Q-CHEM input/output, xyz, formatted checkpoint and cube data files. Isovalue surfaces can be plotted for a range of properties based on an SCF wave function including densities, spin-densities and molecular orbitals. Promolecule and van der Waal surfaces are also available for systems where the wave function information is not available. All surfaces can be colored based on a scalar property such as the electrostatic potential, or arbitrary data from a cube file. The animation module is capable of animating vibrational frequencies as well as intrinsic reaction coordinate (IRC) and optimization pathways. Animations of molecular surfaces are also possible. Key frames are loaded from separate cube files and then a configurable number of interpolated surfaces are generated to provide a smooth transition between the key frames. Animations can be recorded and saved as a movie file for later viewing.

## 9.2. *Spartan*

Starting in 2000, Q-CHEM has provided back-end source code to Wavefunction Inc ([www.wavefun.com](http://www.wavefun.com)) that provides high performance SCF-level and correlated calculations as part of its advanced user interface within the Spartan Pro and Spartan Student packages. The Spartan environment includes not only highly developed graphics, but also advanced database capabilities and a rich suite of conformational searching and modeling tools that complement Q-CHEM's focus on ab initio methods.

## 9.3. *Other interfaces*

Q-CHEM is also interfaced with a variety of other public domain user interfaces, including Avogadro [414], Molden [415], and WebMO [416].

## 10. Summary

In this review, we have summarized the main technical features that have been incorporated into the Q-CHEM program since the last major review of its capabilities [17]. The main reason that such an extensive range of developments can be reported is the size and level of activity of our developer community, as captured by the authorship list of the paper. Looking to the future, Q-CHEM will continue to try to serve the academic needs of our developers by providing a state of the art development platform, which in turn serves the needs of our users by the creation of new electronic structure capabilities and algorithms. With our open team-ware model, we continue to encourage new developers to join us in creating future advances.

## 11. Acknowledgements

Electronic structure software development at Q-CHEM has been supported during the period reviewed in this paper by SBIR grants from the National Institutes of Health (2R44GM073408, 2R44GM069255, 1R43GM086987, 2R44GM076847, 2R44GM081928, 2R44GM084555, and 1R43GM096678). In addition, the academic research groups that have contributed to Q-CHEM have been supported within the U.S. by grants from the Department of Energy, the National Science Foundation and other Federal agencies, and by corresponding national agencies in other countries. Several co-authors of this paper (P.M.W. Gill, M. Head-Gordon, J.M. Herbert, and A.I. Krylov) are part-owners of Q-CHEM, Inc.

## References

- [1] G. T. Velde, F. M. Bickelhaupt, E. J. Baerends, C. F. Guerra, S. J. A. Van Gisbergen, J. G. Snijders and T. Ziegler, *J. Comput. Chem.*, 2001, **22**, 931–967.
- [2] M. J. Frisch, G. W. Trucks, H. B. Schlegel, G. E. Scuseria, M. A. Robb, J. R. Cheeseman, F. Scalmani, V. Barone, B. Mennucci, G. A. Petersson, H. Nakatsuji, M. Caricato, X. Li, H. P. Hratchian, A. F. Izmaylov, J. Bloino, G. Zheng, J. L. Sonnenberg, M. Hada, M. Ehara, K. Toyota, R. Fukuda, J. Hasegawa, M. Ishida, T. Nakajima, Y. Honda, O. Kitao, H. Nakai, T. Vreven, J. A. Montgomery, Jr., J. E. Peralta, F. Ogliaro, M. Bearpark, J. J. Heyd, E. Brothers, K. N. Kudin, V. N. Staroverov, T. Keith, R. Kobayashi, J. Normand, K. Raghavachari, A. Rendell, J. C. Burant, S. S. Iyengar, J. Tomasi, M. Cossi, N. Rega, J. M. Millam, M. Klene, J. E. Knox, J. B. Cross, V. Bakken, C. Adamo, J. Jaramillo, R. Gomperts, R. E. Stratmann, O. Yazyev, A. J. Austin, R. Cammi, C. Pomelli, J. W. Ochterski, R. L. Martin, K. Morokuma, V. G. Zakrzewski, G. A. Voth, P. Salvador, J. J. Dannenberg, S. Dapprich, A. D. Daniels, O. Farkas, J. B. Foresman, J. V. Ortiz, J. Cioslowski and D. J. Fox, *Gaussian 09, Revision B.01*, 2009.
- [3] A. D. Bochevarov, E. Harder, T. F. Hughes, J. R. Greenwood, D. A. Braden, D. M. Philipp, D. Rinaldo, M. D. Halls, J. Zhang and R. A. Friesner, *Int. J. Quantum Chem.*, 2013, **113**, 2110–2142.
- [4] F. Aquilante, T. B. Pedersen, V. Veryazov and R. Lindh, *Wiley Interdiscip. Rev.: Comput. Mol. Sci.*, 2013, **3**, 143–149.
- [5] H. J. Werner, P. J. Knowles, G. Knizia, F. R. Manby and M. Schutz, *WIREs Comput. Mol. Sci.*, 2012, **2**, 242–253.
- [6] R. Ahlrichs, M. Bar, M. Haser, H. Horn and C. Kolmel, *Chem. Phys. Lett.*, 1989, **162**, 165–169.
- [7] F. Furche, R. Ahlrichs, C. Hättig, W. Klopper, M. Sierka and F. Weigend, *Wiley Interdiscip. Rev.: Comput. Mol. Sci.*, 2014, **4**, 91.
- [8] V. Lotrich, N. Flocke, M. Ponton, A. D. Yau, A. Perera, E. Deumens and R. J. Bartlett, *J. Chem. Phys.*, 2008, **128**, 194104.
- [9] M. E. Harding, T. Metzroth, J. Gauss and A. A. Auer, *J. Chem. Theor. Comput.*, 2008, **4**, 64–74.
- [10] K. Aidas, C. Angeli, K. L. Bak, V. Bakken, R. Bast, L. Boman, O. Christiansen, R. Cimiraglia, S. Coriani, P. Dahle, E. K. Dalskov, U. Ekström, T. Enevoldsen, J. J. Eriksen, P. Etenhuber, B. Fernández, L. Ferrighi, H. Fliegl, L. Frediani, K. Hald, A. Halkier, C. Hättig, H. Heiberg, T. Helgaker, A. C. Hennum, H. Hettrema, E. Hjertenaes, S. Høst, I.-M. Høyvik, M. F. Iozzi, B. Jansík, H. J. A. Jensen, D. Jonsson, P. Jørgensen, J. Kauczor, S. Kirpekar, T. Kjaergaard, W. Klopper, S. Knecht, R. Kobayashi, H. Koch, J. Kongsted, A. Krapp, K. Kristensen, A. Ligabue, O. B. Lutnaes, J. I. Melo, K. V. Mikkelsen, R. H. Myhre, C. Neiss, C. B. Nielsen, P. Norman, J. Olsen, J. M. H. Olsen, A. Osted, M. J. Packer, F. Pawłowski, T. B. Pedersen, P. F. Provasi, S. Reine, Z. Rinkevicius, T. A. Ruden, K. Ruud, V. V. Rybkin, P. Salek, C. C. M. Samson, A. S. de Merás, T. Saue, S. P. A. Sauer, B. Schimmelpfennig, K. Sneskov, A. H. Steindal, K. O. Sylvester-Hvid, P. R. Taylor, A. M. Teale, E. I. Tellgren, D. P. Tew, A. J. Thorvaldsen, L. Thøgersen, O. Vahtras, M. A. Watson, D. J. D. Wilson, M. Ziolkowski and H. Ågren, *Wiley Interdiscip. Rev.: Comput. Mol. Sci.*, 2014, **4**, 269–284.
- [11] M. W. Schmidt, K. K. Baldrige, J. A. Boatz, S. T. Elbert, M. S. Gordon, J. H. Jensen, S. Koseki, N. Matsunaga, K. A. Nguyen, S. Su, T. L. Windus, M. Dupuis and J. A. Mont-

- gomery, Jr., *J. Comput. Chem.*, 1983, **14**, 1347.
- [12] M. F. Guest, I. J. Bush, H. J. J. Van Dam, P. Sherwood, J. M. H. Thomas, J. H. Van Lenthe, R. W. A. Havenith and J. Kendrick, *Mol. Phys.*, 2005, **103**, 719–747.
- [13] M. Valiev, E. J. Bylaska, N. Govind, K. Kowalski, T. P. Straatsma, H. J. J. Van Dam, D. Wang, J. Nieplocha, E. Apra, T. L. Windus and W. de Jong, *Comput. Phys. Commun.*, 2010, **181**, 1477–1489.
- [14] J. M. Turney, A. C. Simmonett, R. M. Parrish, E. G. Hohenstein, F. A. Evangelista, J. T. Fermann, B. J. Mintz, L. A. Burns, J. J. Wilke, M. L. Abrams, N. J. Russ, M. L. Leininger, C. L. Janssen, E. T. Seidl, W. D. Allen, H. F. Schaefer, R. A. King, E. F. Valeev, C. D. Sherrill and T. D. Crawford, *WIREs Comput. Mol. Sci.*, 2012, **2**, 556–565.
- [15] J. Kong, C. A. White, A. I. Krylov, D. Sherrill, R. D. Adamson, T. R. Furlani, M. S. Lee, A. M. Lee, S. R. Gwaltney, T. R. Adams, C. Ochsenfeld, A. T. B. Gilbert, G. S. Kedziora, V. A. Rassolov, D. R. Maurice, N. Nair, Y. H. Shao, N. A. Besley, P. E. Maslen, J. P. Dombroski, H. Daschel, W. M. Zhang, P. P. Korambath, J. Baker, E. F. C. Byrd, T. Van Voorhis, M. Oumi, S. Hirata, C. P. Hsu, N. Ishikawa, J. Florian, A. Warshel, B. G. Johnson, P. M. W. Gill, M. Head-Gordon and J. A. Pople, *J. Comput. Chem.*, 2000, **21**, 1532.
- [16] J. Pople, *Rev. Mod. Phys.*, 1999, **71**, 1267–1274.
- [17] Y. Shao, L. F. Molnar, Y. Jung, J. Kussmann, C. Ochsenfeld, S. T. Brown, A. T. B. Gilbert, L. V. Slipchenko, S. V. Levchenko, D. P. O’Neill, R. A. DiStasio Jr., R. C. Lochan, T. Wang, G. J. O. Beran, N. A. Besley, J. M. Herbert, C. Y. Lin, T. Van Voorhis, S. H. Chien, A. Sodt, R. P. Steele, V. A. Rassolov, P. E. Maslen, P. P. Korambath, R. D. Adamson, B. Austin, J. Baker, E. F. C. Byrd, H. Dachsel, R. J. Doerksen, A. Dreuw, B. D. Dunietz, A. D. Dutoi, T. R. Furlani, S. R. Gwaltney, A. Heyden, S. Hirata, C.-P. Hsu, G. Kedziora, R. Z. Khaliullin, P. Klunzinger, A. M. Lee, M. S. Lee, W. Liang, I. Lotan, N. Nair, B. Peters, E. I. Proynov, P. A. Pieniazek, Y. M. Rhee, J. Ritchie, E. Rosta, C. D. Sherrill, A. C. Simmonett, J. E. Subotnik, H. L. Woodcock III, W. Zhang, A. T. Bell, A. K. Chakraborty, D. M. Chipman, F. J. Keil, A. Warshel, W. J. Hehre, H. F. Schaefer III, J. Kong, A. I. Krylov, P. M. W. Gill and M. Head-Gordon, *Phys. Chem. Chem. Phys.*, 2006, **8**, 3172.
- [18] A. I. Krylov and P. Gill, *WIREs Comput Mol Sci*, 2013, **3**, 317–326.
- [19] W. Kohn, A. D. Becke and R. G. Parr, *J. Phys. Chem.*, 1996, **100**, 12974.
- [20] L. Goerigk and S. Grimme, *Phys. Chem. Chem. Phys.*, 2011, **13**, 6670–6688.
- [21] N. Mardirossian, J. A. Parkhill and M. Head-Gordon, *Phys. Chem. Chem. Phys.*, 2011, **13**, 19325–19337.
- [22] R. Sedlak, T. Janowski, M. Pitonak, J. Rezac, P. Pulay and P. Hobza, *J. Chem. Theory Comput.*, 2013, **9**, 3364–3374.
- [23] R. Peverati and D. G. Truhlar, *Phil. Trans. Royal Soc. A*, 2014, **372**, 20120476.
- [24] J. P. Perdew, A. Ruzsinszky, L. A. Constantin, J. W. Sun and G. I. Csonka, *J. Chem. Theory Comput.*, 2009, **5**, 902–908.
- [25] A. J. Cohen, P. Mori-Sanchez and W. T. Yang, *Chem. Rev.*, 2012, **112**, 289–320.
- [26] A. D. Becke, *J. Chem. Phys.*, 1993, **98**, 1372.
- [27] Y. Zhao and D. G. Truhlar, *Theor. Chem. Acc.*, 2008, **120**, 215.
- [28] R. Peverati and D. G. Truhlar, *J. Phys. Chem. Lett.*, 2011, **2**, 2810.
- [29] R. Peverati and D. G. Truhlar, *J. Phys. Chem. Lett.*, 2012, **3**, 117.
- [30] J. Tao, J. P. Perdew, V. N. Staroverov and G. E. Scuseria, *Phys. Rev. Lett.*, 2003, **91**, 146401.
- [31] T. Bally and G. N. Sastry, *J. Phys. Chem. A*, 1997, **101**, 7923–7925.
- [32] A. D. Dutoi and M. Head-Gordon, *Chem. Phys. Lett.*, 2006, **422**, 230–233.
- [33] A. Dreuw, J. L. Weisman and M. Head-Gordon, *J. Chem. Phys.*, 2003, **119**, 2943.
- [34] A. Dreuw and M. Head-Gordon, *J. Am. Chem. Soc.*, 2004, **126**, 4007–4016.
- [35] T. M. Henderson, B. G. Janesko and G. E. Scuseria, *J. Chem. Phys.*, 2008, **128**, 194105.
- [36] M. A. Rohrdanz and J. M. Herbert, *J. Chem. Phys.*, 2008, **129**, 034107.
- [37] M. A. Rohrdanz, K. M. Martins and J. M. Herbert, *J. Chem. Phys.*, 2009, **130**, 054112.
- [38] A. W. Lange and J. M. Herbert, *J. Am. Chem. Soc.*, 2009, **131**, 124115.
- [39] J.-D. Chai and M. Head-Gordon, *J. Chem. Phys.*, 2008, **128**, 084106.
- [40] J.-D. Chai and M. Head-Gordon, *Phys. Chem. Chem. Phys.*, 2008, **10**, 6615.
- [41] J.-D. Chai and M. Head-Gordon, *J. Chem. Phys.*, 2009, **131**, 174105.
- [42] N. Mardirossian and M. Head-Gordon, *Phys. Chem. Chem. Phys.*, 2014, **16**, 9904–9924.
- [43] R. Baer and D. Neuhauser, *Phys. Rev. Lett.*, 2005, **94**, 043002.
- [44] E. Livshits and R. Baer, *Phys. Chem. Chem. Phys.*, 2007, **9**, 2932.
- [45] U. Salzner and R. Baer, *J. Chem. Phys.*, 2009, **131**, 231101.
- [46] R. Baer, E. Livshits and U. Salzner, *Annu. Rev. Phys. Chem.*, 2010, **61**, 85.
- [47] Y. Zhao, N. E. Schultz and D. G. Truhlar, *J. Chem. Theory Comput.*, 2006, **2**, 364.

- 1 [48] N. A. Besley, M. J. G. Peach and D. J. Tozer, *Phys. Chem. Chem. Phys.*, 2009, **11**, 10350.  
2 [49] S. Kristyian and P. Pulay, *Chem. Phys. Lett.*, 1994, **229**, 175–180.  
3 [50] J. Klimes and A. Michaelides, *J. Chem. Phys.*, 2012, **137**, 120901.  
4 [51] S. Grimme, *J. Comput. Chem.*, 2006, **27**, 1787.  
5 [52] S. Grimme, J. Antony, S. Ehrlich and H. Krieg, *J. Chem. Phys.*, 2010, **132**, 154104.  
6 [53] A. D. Becke and E. R. Johnson, *J. Chem. Phys.*, 2005, **122**, 154104.  
7 [54] E. R. Johnson and A. D. Becke, *J. Chem. Phys.*, 2005, **123**, 024101.  
8 [55] J. Kong, Z. Gan, E. Proynov, M. Freindorf and T. Furlani, *Phys. Rev. A*, 2009, **79**, 042510.  
9 [56] M. Dion, H. Rydberg, E. Schröder, D. C. Langreth and B. I. Lundqvist, *Phys. Rev. Lett.*,  
10 2004, **92**, 246401.  
11 [57] K. Lee, E. D. Murray, L. Kong, B. I. Lundqvist and D. C. Langreth, *Phys. Rev. B*, 2010,  
12 **82**, 081101.  
13 [58] O. A. Vydrov and T. Van Voorhis, *Phys. Rev. Lett.*, 2009, **103**, 063004.  
14 [59] O. A. Vydrov and T. Van Voorhis, *J. Chem. Phys.*, 2010, **133**, 244103.  
15 [60] S. Grimme, *J. Chem. Phys.*, 2006, **124**, 034108.  
16 [61] T. Schwabe and S. Grimme, *Phys. Chem. Chem. Phys.*, 2007, **9**, 3397.  
17 [62] Y. Zhang, X. Xu and W. A. Goddard III, *Proc. Natl. Acad. Sci. USA*, 2009, **106**, 4963.  
18 [63] J. D. Chai and S. P. Mao, *Chem. Phys. Lett.*, 2012, **538**, 121–125.  
19 [64] I. Zhang, X. Xu, Y. Jung and W. Goddard, *Proc. Natl. Acad. Sci. U. S. A.*, 2011, **108**,  
20 19896–19900.  
21 [65] H. Ji, Y. Shao, W. A. Goddard and Y. Jung, *J. Chem. Theory Comput.*, 2013, **9**, 1971.  
22 [66] A. D. Becke, *J. Chem. Phys.*, 2003, **119**, 2972–2977.  
23 [67] A. D. Becke, *J. Chem. Phys.*, 2005, **122**, 064101.  
24 [68] A. D. Becke and M. R. Roussel, *Phys. Rev. A*, 1989, **39**, 3761–3767.  
25 [69] A. D. Becke, *J. Chem. Phys.*, 1988, **88**, 1053–1062.  
26 [70] A. D. Becke, *Int. J. Quantum Chem.*, 1994, **52**, 625–632.  
27 [71] E. Proynov, Y. Shao and J. Kong, *Chem. Phys. Lett.*, 2010, **493**, 381.  
28 [72] E. Proynov, F. Liu, Y. Shao and J. Kong, *J. Chem. Phys.*, 2012, **136**, 034102.  
29 [73] N. Mardirossian and M. Head-Gordon, *J. Chem. Phys.*, 2014, **140**, 18A527.  
30 [74] A. Karton, S. Daon and J. M. Martin, *Chem. Phys. Lett.*, 2011, **510**, 165–178.  
31 [75] A. Karton, D. Gruzman and J. M. L. Martin, *J. Phys. Chem. A*, 2009, **113**, 8434–8447.  
32 [76] J. Zheng, Y. Zhao and D. G. Truhlar, *J. Chem. Theory Comput.*, 2007, **3**, 569–582.  
33 [77] A. Karton, A. Tarnopolsky, J.-F. Lamère, G. C. Schatz and J. M. L. Martin, *J. Phys.*  
34 *Chem. A*, 2008, **112**, 12868–12886.  
35 [78] J. Zheng, Y. Zhao and D. G. Truhlar, *J. Chem. Theory Comput.*, 2009, **5**, 808–821.  
36 [79] L. A. Curtiss, K. Raghavachari, G. W. Trucks and J. A. Pople, *J. Chem. Phys.*, 1991, **94**,  
37 7221–7230.  
38 [80] L. Goerigk and S. Grimme, *Phys. Chem. Chem. Phys.*, 2011, **13**, 6670–6688.  
39 [81] K. L. Copeland and G. S. Tschumper, *J. Chem. Theory Comput.*, 2012, **8**, 1646–1656.  
40 [82] P. Jurečka, J. Šponer, J. Černý and P. Hobza, *Phys. Chem. Chem. Phys.*, 2006, **8**, 1985–1993.  
41 [83] T. Takatani, E. G. Hohenstein, M. Malagoli, M. S. Marshall and C. D. Sherrill, *J. Chem.*  
42 *Phys.*, 2010, **132**, 144104.  
43 [84] J. Řezáč, K. E. Riley and P. Hobza, *J. Chem. Theory Comput.*, 2011, **7**, 2427.  
44 [85] J. Řezáč, K. E. Riley and P. Hobza, *J. Chem. Theory Comput.*, 2011, **7**, 3466.  
45 [86] J. Řezáč and P. Hobza, *J. Chem. Theory Comput.*, 2013, **9**, 2151–2155.  
46 [87] J. Řezáč, K. E. Riley and P. Hobza, *J. Chem. Theory Comput.*, 2012, **8**, 4285–4292.  
47 [88] B. J. Mintz and J. M. Parks, *J. Phys. Chem. A*, 2012, **116**, 1086–1092.  
48 [89] J. Kussmann, M. Beer and C. Ochsenfeld, *Wiley Interdiscip. Rev.: Comput. Mol. Sci.*, 2013,  
49 **3**, 614.  
50 [90] C. Ochsenfeld, J. Kussmann and F. Koziol, *Angew. Chem. Int. Ed. Engl.*, 2004, **43**, 4485–9.  
51 [91] W. Pisula, Z. Tomovic, M. D. Watson, K. Müllen, J. Kussmann, C. Ochsenfeld, T. Metzroth  
52 and J. Gauss, *J. Phys. Chem. B*, 2007, **111**, 7481–7487.  
53 [92] D. Flaig, M. Beer and C. Ochsenfeld, *J. Chem. Theory Comput.*, 2012, **8**, 2260–2271.  
54 [93] J. Kussmann and C. Ochsenfeld, *J. Chem. Phys.*, 2007, **127**, 054103.  
55 [94] C. Ochsenfeld, J. Kussmann and F. Koziol, *Angew. Chem.*, 2004, **116**, 4585.  
56 [95] S. P. Karna and M. Dupuis, *J. Comput. Chem.*, 1991, **12**, 487–504.  
57 [96] H. Sekino and R. J. Bartlett, *J. Chem. Phys.*, 1993, **98**, 3022–3037.  
58 [97] J. Kussmann and C. Ochsenfeld, *J. Chem. Phys.*, 2007, **127**, 204103.  
59 [98] C. A. White, B. G. Johnson, P. M. W. Gill and M. Head-Gordon, *Chem. Phys. Lett.*, 1994,  
60 **230**, 8.  
[99] C. Ochsenfeld, C. A. White and M. Head-Gordon, *J. Chem. Phys.*, 1998, **109**, 1663.  
[100] C. Ochsenfeld, *Chem. Phys. Lett.*, 2000, **327**, 216.



- 1 [101] C. V. Sumowski and C. Ochsenfeld, *J. Phys. Chem. A*, 2009, **113**, 11734–11741.  
2 [102] C. V. Sumowski, B. B. T. Schmitt, S. Schweizer and C. Ochsenfeld, *Angew. Chem.*, 2010,  
3 **122**, 10147–10151.  
4 [103] T. Helgaker, M. Watson and N. C. Handy, *J. Chem. Phys.*, 2000, **113**, 9402.  
5 [104] V. Sychrovsky, J. Gräfenstein and D. Cremer, *J. Chem. Phys.*, 2000, **113**, 3530.  
6 [105] A. Luenser, J. Kussmann and C. Ochsenfeld, 2014, in preparation.  
7 [106] S. N. Maximoff, J. E. Peralta, V. Barone and G. E. Scuseria, *J. Chem. Theory Comput.*,  
8 2005, **1**, 541–545.  
9 [107] T. Bally and P. R. Rablen, *J. Org. Chem.*, 2011, **76**, 4818–30.  
10 [108] P. F. Provasi, G. A. Aucar and S. P. A. Sauer, *J. Chem. Phys.*, 2001, **115**, 1324.  
11 [109] F. Jensen, *J. Chem. Theory Comput.*, 2006, **2**, 1360.  
12 [110] F. Jensen, *Theor. Chem. Acc.*, 2009, **126**, 371.  
13 [111] U. Benedikt, A. A. Auer and F. Jensen, *J. Chem. Phys.*, 2008, **129**, 064111.  
14 [112] N. Matsumori, D. Kaneno, M. Murata, H. Nakamura and K. Tachibana, *J. Org. Chem.*,  
15 1999, **64**, 866–876.  
16 [113] G. Bifulco, P. Dambruoso, L. Gomez-Paloma and R. Riccio, *Chem. Rev.*, 2007, **107**, 3744–79.  
17 [114] M. Karplus, *J. Chem. Phys.*, 1959, **30**, 11.  
18 [115] M. Karplus, *J. Phys. Chem.*, 1960, **64**, 1793–1798.  
19 [116] M. Karplus, *J. Am. Chem. Soc.*, 1963, **85**, 2870–2871.  
20 [117] M. Barfield and B. Chakrabarti, *Chem. Rev.*, 1969, **69**, 757–778.  
21 [118] A. J. Dingley, F. Cordier and S. Grzesiek, *Concepts Magnetic Res.*, 2001, **13**, 103.  
22 [119] A. Sodt and M. Head-Gordon, *J. Chem. Phys.*, 2006, **125**, 074116.  
23 [120] A. Sodt and M. Head-Gordon, *J. Chem. Phys.*, 2008, **128**, 104106.  
24 [121] J. Kong, S. T. Brown and L. Fusti-Molnar, *J. Chem. Phys.*, 2006, **124**, 094109.  
25 [122] C.-M. Chang, N. J. Russ and J. Kong, *Phys. Rev. A*, 2011, **84**, 022504.  
26 [123] N. J. Russ, C.-M. Chang and J. Kong, *Can. J. Chem.*, 2011, **89**, 657.  
27 [124] L. Fusti-Molnar and J. Kong, *J. Chem. Phys.*, 2005, **122**, 074108.  
28 [125] S. Hirata and M. Head-Gordon, *Chem. Phys. Lett.*, 1999, **314**, 291.  
29 [126] F. Liu, Z. Gan, Y. Shao, C.-P. Hsu, A. Dreuw, M. Head-Gordon, B. T. Miller, B. R. Brooks,  
30 J.-G. Yu, T. R. Furlani and J. Kong, *Mol. Phys.*, 2010, **108**, 2791.  
31 [127] D. Maurice and M. Head-Gordon, *Mol. Phys.*, 1999, **96**, 1533.  
32 [128] J. Liu and W. Liang, *J. Chem. Phys.*, 2011, **135**, 014113.  
33 [129] J. Liu and W. Liang, *J. Chem. Phys.*, 2011, **135**, 184111.  
34 [130] J. Liu and W. Liang, *J. Chem. Phys.*, 2013, **138**, 024101.  
35 [131] W. Z. Liang and M. Head-Gordon, *J. Phys. Chem. A*, 2004, **108**, 3206.  
36 [132] R. P. Steele, Y. Shao, R. A. DiStasio, Jr. and M. Head-Gordon, *J. Phys. Chem. A*, 2006,  
37 **110**, 13915.  
38 [133] R. P. Steele, R. A. DiStasio, Jr., Y. Shao, J. Kong and M. Head-Gordon, *J. Chem. Phys.*,  
39 2006, **125**, 074108.  
40 [134] R. P. Steele, R. A. DiStasio, Jr. and M. Head-Gordon, *J. Chem. Theory Comput.*, 2009, **5**,  
41 1560.  
42 [135] J. Deng, A. T. B. Gilbert and P. M. W. Gill, *J. Chem. Phys.*, 2009, **130**, 231101.  
43 [136] J. Deng, A. T. B. Gilbert and P. M. W. Gill, *J. Chem. Phys.*, 2009, **133**, 044116.  
44 [137] J. Deng, A. T. B. Gilbert and P. M. W. Gill, *Phys. Chem. Chem. Phys.*, 2010, **12**, 10759.  
45 [138] A. J. W. Thom and M. Head-Gordon, *Phys. Rev. Lett.*, 2008, **101**, 193001.  
46 [139] A. J. W. Thom and M. Head-Gordon, *J. Chem. Phys.*, 2009, **131**, 124113.  
47 [140] E. J. Sundstrom and M. Head-Gordon, *J. Chem. Phys.*, 2014, **140**, 114103.  
48 [141] K. U. Lao and J. M. Herbert, *J. Chem. Phys.*, 2013, **139**, 034107.  
49 [142] C. Møller and M. S. Plesset, *Phys. Rev.*, 1934, **46**, 618.  
50 [143] J. A. Pople, J. S. Binkley and R. Seeger, *Int. J. Quantum Chem.*, 1976, **S10**, 1–19.  
51 [144] Y. M. Rhee, R. A. DiStasio Jr., R. C. Lochan and M. Head-Gordon, *Chem. Phys. Lett.*,  
52 2006, **426**, 197–203.  
53 [145] R. A. DiStasio, Jr., R. P. Steele, Y. M. Rhee, Y. Shao and M. Head-Gordon, *J. Comput.*  
54 *Chem.*, 2007, **28**, 839.  
55 [146] R. A. DiStasio, Jr., R. P. Steele and M. Head-Gordon, *Mol. Phys.*, 2007, **105**, 27331.  
56 [147] J. Zienau, L. Clin, B. Doser and C. Ochsenfeld, *J. Chem. Phys.*, 2009, **130**, 204112.  
57 [148] S. A. Maurer, L. Clin and C. Ochsenfeld, *J. Chem. Phys.*, 2014, **140**, 224112.  
58 [149] S. A. Maurer, D. S. Lambrecht, D. Flaig and C. Ochsenfeld, *J. Chem. Phys.*, 2012, **136**,  
59 144107.  
60 [150] S. A. Maurer, D. S. Lambrecht, J. Kussmann and C. Ochsenfeld, *J. Chem. Phys.*, 2013,  
**138**, 014101.  
[151] M. Goldey and M. Head-Gordon, *J. Phys. Chem. Lett.*, 2012, **3**, 3592.



- 1 [152] M. Goldey, A. Dutoi and M. Head-Gordon, *Phys. Chem. Chem. Phys.*, 2013, **15**, 15869.
- 2 [153] M. Goldey, R. A. Distasio Jr., Y. Shao and M. Head-Gordon, *Mol. Phys.*, 2014, **112**, 836–
- 3 843.
- 4 [154] B. J. Mintz and J. M. Parks, *J. Phys. Chem. A*, 2012, **116**, 1086–1092.
- 5 [155] D. S. Lambrecht, G. N. I. Clark, T. Head-Gordon and M. Head-Gordon, *J. Phys. Chem. A*,
- 6 2011, **115**, 11438–11454.
- 7 [156] D. S. Lambrecht, L. McCaslin, S. S. Xantheas, E. Epifanovsky and M. Head-Gordon, *Mol.*
- 8 *Phys.*, 2012, **110**, 2513–2521.
- 9 [157] N. Mardirossian, D. S. Lambrecht, L. McCaslin, S. S. Xantheas and M. Head-Gordon, *J.*
- 10 *Chem. Theory Comput.*, 2013, **9**, 1368–1380.
- 11 [158] D. Gruzman, A. Karton and J. M. L. Martin, *J. Phys. Chem. A*, 2009, **113**, 11974–11983.
- 12 [159] J. J. Wilke, M. C. Lind, H. F. Schaefer, A. G. Csaszar and W. D. Allen, *J. Chem. Theory*
- 13 *Comput.*, 2009, **5**, 1511–1523.
- 14 [160] G. I. Csonka, A. D. French, G. P. Johnson and C. A. Stortz, *J. Chem. Theory Comput.*,
- 15 2009, **5**, 679–692.
- 16 [161] R. Sedlak, T. Janowski, M. Pitoňák, J. Rezac, P. Pulay and P. Hobza, *J. Chem. Theory*
- 17 *Comput.*, 2013, **9**, 3364–3374.
- 18 [162] H. Valdes, K. Pluhackova, M. Pitoňák, J. Řezáč and P. Hobza, *Phys. Chem. Chem. Phys.*,
- 19 2008, **10**, 2747–2757.
- 20 [163] J. Řezáč, P. Jurecka, K. E. Riley, J. Cerny, H. Valdes, K. Pluhackova, K. Berka, T. Řezáč,
- 21 M. Pitoňák, J. Vondrasek and P. Hobza, *Collect. Czech. Chem. C.*, 2008, **73**, 1261–1270.
- 22 [164] J. Řezáč and P. Hobza, *J. Chem. Theory Comput.*, 2013, **9**, 2151–2155.
- 23 [165] R. C. Lochan and M. Head-Gordon, *J. Chem. Phys.*, 2007, **126**, 164101.
- 24 [166] W. Kurlancheek, R. Lochan, K. Lawler and M. Head-Gordon, *J. Chem. Phys.*, 2012, **136**,
- 25 054113.
- 26 [167] Y. Jung, R. C. Lochan, A. D. Dutoi and M. Head-Gordon, *J. Chem. Phys.*, 2004, **121**, 9793.
- 27 [168] W. Kurlancheek and M. Head-Gordon, *Mol. Phys.*, 2009, **107**, 1223–1232.
- 28 [169] D. Stuck and M. Head-Gordon, *J. Chem. Phys.*, 2013, **139**,
- 29 [170] M. Head-Gordon, R. J. Rico, M. Oumi and T. J. Lee, *Chem. Phys. Lett.*, 1994, **219**, 21.
- 30 [171] Y. M. Rhee and M. Head-Gordon, *J. Phys. Chem. A*, 2007, **111**, 5314.
- 31 [172] D. Casanova, Y. M. Rhee and M. Head-Gordon, *J. Chem. Phys.*, 2008, **128**, 164106.
- 32 [173] Y. M. Rhee, D. Casanova and M. Head-Gordon, *J. Chem. Theor. Comput.*, 2009, **5**, 1224–
- 33 1236.
- 34 [174] Y. Rhee, D. Casanova and M. Head-Gordon, *J. Phys. Chem. A*, 2009, **113**, 10564–10576.
- 35 [175] R. J. Bartlett and M. Musial, *Rev. Mod. Phys.*, 2007, **79**, 291–352.
- 36 [176] A. I. Krylov, *Annu. Rev. Phys. Chem.*, 2008, **59**, 433.
- 37 [177] T. Kuš and A. I. Krylov, *J. Chem. Phys.*, 2011, **135**, 084109.
- 38 [178] A. I. Krylov, *Acc. Chem. Res.*, 2006, **39**, 83.
- 39 [179] D. Casanova, L. V. Slipchenko, A. I. Krylov and M. Head-Gordon, *J. Chem. Phys.*, 2009,
- 40 **130**, 044103.
- 41 [180] E. Epifanovsky, M. Wormit, T. Kuš, A. Landau, D. Zuev, K. Khistyayev, P. Manohar, I. Kali-
- 42 man, A. Dreuw and A. Krylov, *J. Comput. Chem.*, 2013, **34**, 2293–2309.
- 43 [181] E. Epifanovsky, D. Zuev, X. Feng, K. Khistyayev, Y. Shao and A. Krylov, *J. Chem. Phys.*,
- 44 2013, **139**, 134105.
- 45 [182] A. Landau, K. Khistyayev, S. Dolgikh and A. I. Krylov, *J. Chem. Phys.*, 2010, **132**, 014109.
- 46 [183] T.-C. Jagau, K. B. D. Zuev, E. Epifanovsky and A. Krylov, *J. Phys. Chem. Lett.*, 2014, **5**,
- 47 310–315.
- 48 [184] K. B. Bravaya, D. Zuev, E. Epifanovsky and A. I. Krylov, *J. Chem. Phys.*, 2013, **138**,
- 49 124106.
- 50 [185] D. Zuev, T.-C. Jagau, K. Bravaya, E. Epifanovsky, Y. Shao, E. Sundstrom, M. Head-Gordon
- 51 and A. Krylov, *J. Chem. Phys.*, 2014, **141**, 024102.
- 52 [186] T. Kuš and A. I. Krylov, *J. Chem. Phys.*, 2012, **136**, 244109.
- 53 [187] J. Schirmer, *Phys. Rev. A*, 1982, **26**, 2395.
- 54 [188] A. B. Trofimov, G. Stelter and J. Schirmer, *J. Chem. Phys.*, 1999, **111**, 9982.
- 55 [189] O. Christiansen, H. Koch and P. Jørgensen, *Chem. Phys. Lett.*, 1995, **243**, 409.
- 56 [190] C. Hattig and F. Weigend, *J. Chem. Phys.*, 2000, **113**, 5154–5161.
- 57 [191] J. H. Starcke, M. Wormit, J. Schirmer and A. Dreuw, *Chem. Phys.*, 2006, **329**, 39–49.
- 58 [192] M. Wormit, D. R. Rehn, P. H. P. Harbach, J. Wenzel, C. M. Krauter, E. Epifanovsky and
- 59 A. Dreuw, *Mol. Phys.*, 2014, **112**, 774.
- 60 [193] S. Knippenberg, D. R. Rehn, M. Wormit, J. H. Starcke, I. L. Rusakova, A. B. Trofimov and
- A. Dreuw, *J. Chem. Phys.*, 2012, **136**, 064107.
- [194] C. M. Krauter, M. Pernpointner and A. Dreuw, *J. Chem. Phys.*, 2013, **138**, 044107.

- [195] M. Schreiber, M. R. Silva-Junior, S. P. A. Sauer and W. Thiel, *J. Chem. Phys.*, 2008, **128**, 134110.
- [196] L. S. Cederbaum, W. Domcke and J. Schirmer, *Phys. Rev. A*, 1980, **22**, 206.
- [197] J. Wenzel, M. Wormit and A. Dreuw, 2014, submitted for publication.
- [198] G. K.-L. Chan and M. Head-Gordon, *J. Chem. Phys.*, 2002, **116**, 4462–4476.
- [199] G. K.-L. Chan, *J. Chem. Phys.*, 2004, **120**, 3172–3178.
- [200] D. Ghosh, J. Hachmann, T. Yanai and G. K.-L. Chan, *J. Chem. Phys.*, 2008, **128**, 144117.
- [201] S. Sharma and G. K.-L. Chan, *J. Chem. Phys.*, 2012, **136**, 124121.
- [202] S. R. White *et al.*, *Phys. Rev. Lett.*, 1992, **69**, 2863–2866.
- [203] S. R. White, *Phys. Rev. B*, 1993, **48**, 10345.
- [204] S. R. White and R. L. Martin, *J. Chem. Phys.*, 1999, **110**, 4127–4130.
- [205] K. H. Marti, I. M. Ondík, G. Moritz and M. Reiher, *J. Chem. Phys.*, 2008, **128**, 014104.
- [206] Ö. Legeza and J. Sólyom, *Phys. Rev. B*, 2003, **68**, 195116.
- [207] A. Mitrushenkov, R. Linguerri, P. Palmieri and G. Fano, *J. Chem. Phys.*, 2003, **119**, 4148–4158.
- [208] G. K.-L. Chan and S. Sharma, *Annu. Rev. Phys. Chem.*, 2011, **62**, 465–481.
- [209] D. Zgid and M. Nooijen, *J. Chem. Phys.*, 2008, **128**, 144116.
- [210] T. Yanai, Y. Kurashige, D. Ghosh and G. K. Chan, *Int. J. Quantum Chem.*, 2009, **109**, 2178–2190.
- [211] T. Yanai, Y. Kurashige, E. Neuscammen and G. K.-L. Chan, *J. Chem. Phys.*, 2010, **132**, 024105.
- [212] G. K. Chan, *Wiley Interdiscip. Rev.: Comput. Mol. Sci.*, 2012, **2**, 907–920.
- [213] G. K.-L. Chan and M. Head-Gordon, *J. Chem. Phys.*, 2003, **118**, 8551–8554.
- [214] G. K.-L. Chan, M. Kállay and J. Gauss, *J. Chem. Phys.*, 2004, **121**, 6110–6116.
- [215] S. Sharma, T. Yanai, G. H. Booth, C. J. Umrigar and G. K.-L. Chan, *J. Chem. Phys.*, 2014, **140**, 104112.
- [216] J. Hachmann, J. J. Dorando, M. Avilés and G. K.-L. Chan, *J. Chem. Phys.*, 2007, **127**, 134309.
- [217] Y. Kurashige and T. Yanai, *J. Chem. Phys.*, 2011, **135**, 094104.
- [218] Y. Kurashige, G. K.-L. Chan and T. Yanai, *Nature Chem.*, 2013, **5**, 660–666.
- [219] J. Hachmann, W. Cardoen and G. K.-L. Chan, *J. Chem. Phys.*, 2006, **125**, 144101.
- [220] W. Mizukami, Y. Kurashige and T. Yanai, *J. Chem. Phys.*, 2010, **133**, 091101.
- [221] D. Casanova and M. Head-Gordon, *J. Chem. Phys.*, 2008, **129**, 064104.
- [222] P. M. Zimmerman, F. Bell, M. Goldey, A. T. Bell and M. Head-Gordon, *J. Chem. Phys.*, 2012, **137**, 164110.
- [223] D. Casanova, *J. Comput. Chem.*, 2013, **34**, 720.
- [224] D. Casanova and M. Head-Gordon, *Phys. Chem. Chem. Phys.*, 2009, **11**, 9779.
- [225] F. Bell, P. M. Zimmerman, D. Casanova, M. Goldey and M. Head-Gordon, *Phys. Chem. Chem. Phys.*, 2013, **15**, 358.
- [226] P. M. Zimmerman, F. Bell, D. Casanova and M. Head-Gordon, *J. Am. Chem. Soc.*, 2011, **133**, 19944.
- [227] P. Zimmerman, C. Musgrave and M. Head-Gordon, *Acc. Chem. Res.*, 2013, **46**, 1339–1347.
- [228] X. Feng, A. Luzanov and A. Krylov, *J. Phys. Chem. Lett.*, 2013, **4**, 3845–3852.
- [229] A. Kolomeisky, X. Feng and A. Krylov, *J. Phys. Chem. C*, 2014, **118**, 5188–5195.
- [230] N. J. Mayhall, M. Goldey and M. Head-Gordon, *J. Chem. Theory Comput.*, 2014, **10**, 589–599.
- [231] N. Mayhall and M. Head-Gordon, *J. Chem. Phys.*, 2014, **141**, 044112.
- [232] J. Cullen, *Chem. Phys.*, 1996, **202**, 217.
- [233] G. J. O. Beran, B. Austin, A. Sodt and M. Head-Gordon, *J. Phys. Chem. A*, 2005, **109**, 9183.
- [234] D. W. Small and M. Head-Gordon, *J. Chem. Phys.*, 2009, **130**, 084103.
- [235] D. W. Small and M. Head-Gordon, *Phys. Chem. Chem. Phys.*, 2011, **13**, 19285.
- [236] Y. Kurashige and T. Yanai, *J. Chem. Phys.*, 2011, **135**, 094104.
- [237] A. J. H. Wachters, *J. Chem. Phys.*, 1970, **52**, 1033.
- [238] A. J. H. Wachters, IBM Tech. Rept. RJ584 (1969).
- [239] C. W. Bauschlicher, Jr., S. R. Langhoff and L. A. Barnes, *J. Chem. Phys.*, 1989, **91**, 2399.
- [240] L. Vogt, R. Olivares-Amaya, S. Kermes, Y. Shao, C. Amador-Bedolla and A. Aspuru-Guzik, *J. Phys. Chem. A*, 2008, **112**, 2049–2057.
- [241] M. Watson, R. Olivares-Amaya, R. G. Edgar and A. Aspuru-Guzik, *Comput. Sci. Eng.*, 2010, **12**, 40–51.
- [242] H. Schlegel, *J. Comput. Chem.*, 2003, **24**, 1514–1527.
- [243] A. Banerjee, N. Adams, J. Simons and R. Shepard, *J. Phys. Chem.*, 1985, **89**, 52.

- 1 [244] A. Heyden, A. T. Bell and F. J. Keil, *J. Chem. Phys.*, 2005, **123**, 224101.  
2 [245] B. Peters, A. Heyden, A. T. Bell and A. Chakraborty, *J. Chem. Phys.*, 2004, **120**, 7877.  
3 [246] A. Behn, P. M. Zimmerman, A. T. Bell and M. Head-Gordon, *J. Chem. Theory Comput.*,  
4 2011, **7**, 4019–4025.  
5 [247] T. A. Halgren and W. N. Lipscomb, *Chem. Phys. Lett.*, 1977, **49**, 225–232.  
6 [248] A. Behn, P. M. Zimmerman, A. T. Bell and M. Head-Gordon, *J. Chem. Phys.*, 2011, **135**,  
7 224108.  
8 [249] S. M. Sharada, P. M. Zimmerman, A. T. Bell and M. Head-Gordon, *J. Chem. Theory*  
9 *Comput.*, 2012, **8**, 5166.  
10 [250] J. M. Herbert and M. Head-Gordon, *Phys. Chem. Chem. Phys.*, 2005, **7**, 3269.  
11 [251] E. Ramos-Cordoba, D. S. Lambrecht and M. Head-Gordon, *Faraday Discuss.*, 2011, **150**,  
12 345–362.  
13 [252] M. Karplus, R. N. Porter and R. D. Sharma, *J. Chem. Phys.*, 1965, **43**, 3259.  
14 [253] R. Porter, L. Raff and W. H. Miller, *J. Chem. Phys.*, 1975, **63**, 2214.  
15 [254] D. S. Lambrecht, G. N. I. Clark, T. Head-Gordon and M. Head-Gordon, *J. Phys. Chem. A*,  
16 2011, **115**, 5928.  
17 [255] P. M. Zimmerman, D. C. Tranca, J. Gomes, D. S. Lambrecht, M. Head-Gordon and A. T.  
18 Bell, *J. Am. Chem. Soc.*, 2012, **134**, 19468–19476.  
19 [256] D. Wales and J. Doye, *J. Phys. Chem. A*, 1997, **101**, 5111–5116.  
20 [257] H. Do and N. A. Besley, *J. Chem. Phys.*, 2012, **137**, 134106.  
21 [258] H. Do and N. A. Besley, *J. Phys. Chem. A*, 2013, **117**, 5385–5391.  
22 [259] H. Do and N. A. Besley, *Phys. Chem. Chem. Phys.*, 2013, **15**, 16214–16219.  
23 [260] K. Mizuse, J. Kuo and A. Fujii, *Chem. Sci.*, 2011, **2**, 868–876.  
24 [261] H. L. Woodcock, M. Hodoscek, A. T. B. Gilbert, P. M. W. Gill, H. F. Schaefer III and B. R.  
25 Brooks, *J. Comput. Chem.*, 2007, **28**, 1485.  
26 [262] B. R. Brooks, C. L. Brooks III, A. D. Mackerell, Jr., L. Nilsson, R. J. Petrella, B. Roux,  
27 Y. Won, G. Archontis, C. Bartels, S. Boresch, A. Caffisch, L. Caves, C. Qui, A. R. Din-  
28 ner, M. Feig, S. Fischer, J. Gao, M. Hodoscek, W. Im, K. Kuczera, T. Lazaridis, J. Ma,  
29 V. Ovchinnikov, E. Paci, R. W. Pastor, C. B. Post, J. Z. Pu, M. Schaefer, B. Tidor, R. M.  
30 Venable, H. L. Woodcock, X. Wu, W. Yang, D. M. York and M. Karplus, *J. Comput. Chem.*,  
31 2009, **30**, 1545.  
32 [263] D. Ghosh, D. Kosenkov, V. Vanovschi, C. F. Williams, J. M. Herbert, M. S. Gordon, M. W.  
33 Schmidt, L. V. Slipchenko and A. I. Krylov, *J. Phys. Chem. A*, 2010, **114**, 12739.  
34 [264] L. D. Jacobson, R. M. Richard, K. U. Lao and J. M. Herbert, *Annu. Rep. Comp. Chem.*,  
35 2013, **9**, 25.  
36 [265] J. Tomasi, B. Mennucci and R. Cammi, *Chem. Rev.*, 2005, **106**, 2999.  
37 [266] J. Tomasi, B. Mennucci and E. Cancès, *J. Mol. Struct. (Theochem)*, 1999, **464**, 211.  
38 [267] D. M. Chipman, *Theor. Chem. Acc.*, 2002, **107**, 80.  
39 [268] D. M. Chipman, *J. Chem. Phys.*, 2000, **112**, 5558.  
40 [269] E. Cancès and B. Mennucci, *J. Chem. Phys.*, 2001, **114**, 4744.  
41 [270] A. W. Lange and J. M. Herbert, *Chem. Phys. Lett.*, 2011, **509**, 77.  
42 [271] V. Barone and M. Cossi, *J. Phys. Chem. A*, 1998, **102**, 1995.  
43 [272] M. Cossi, N. Rega, G. Scalmani and V. Barone, *J. Comput. Chem.*, 2003, **24**, 669.  
44 [273] T. N. Truong and E. V. Stefanovich, *Chem. Phys. Lett.*, 1995, **240**, 253.  
45 [274] A. Klamt and V. Jonas, *J. Chem. Phys.*, 1996, **105**, 9972.  
46 [275] K. Baldrige and A. Klamt, *J. Chem. Phys.*, 1997, **106**, 6622.  
47 [276] A. Klamt and G. Schüürmann, *J. Chem. Soc. Perkin Trans. 2*, 1993, 799.  
48 [277] J. B. Foresman, T. A. Keith, K. B. Wiberg, J. Snoonian and M. J. Frisch, *J. Phys. Chem.*,  
49 1996, **100**, 16098.  
50 [278] D. M. Chipman and M. Dupuis, *Theor. Chem. Acc.*, 2002, **107**, 90.  
51 [279] V. Barone, M. Cossi and J. Tomasi, *J. Chem. Phys.*, 1997, **107**, 3210.  
52 [280] A. Pomogaeva and D. M. Chipman, *J. Chem. Theory Comput.*, 2011, **7**, 3952.  
53 [281] A. Pomogaeva and D. M. Chipman, *J. Chem. Theory Comput.*, 2014, **10**, 211.  
54 [282] A. W. Lange and J. M. Herbert, *J. Phys. Chem. Lett.*, 2010, **1**, 556.  
55 [283] A. W. Lange and J. M. Herbert, *J. Chem. Phys.*, 2010, **133**, 244111.  
56 [284] C. Curutchet, M. Orozco and F. J. Luque, *J. Comput. Chem.*, 2001, **22**, 1180.  
57 [285] I. Soteras, C. Curutchet, A. Bidon-Chanal, M. Orozco and F. J. Luque, *J. Mol. Struct.*  
58 *(Theochem)*, 2005, **727**, 29.  
59 [286] A. Klamt, B. Mennucci, J. Tomasi, V. Barone, C. Curutchet, M. Orozco and F. J. Luque,  
60 *Acc. Chem. Res.*, 2009, **42**, 489.  
[287] C. J. Cramer and D. G. Truhlar, *Acc. Chem. Res.*, 2008, **41**, 760.  
[288] W. C. Still, A. Tempczyk, R. C. Hawley and T. Hendrickson, *J. Am. Chem. Soc.*, 1990,

- 1  
2  
3  
4  
5  
6  
7  
8  
9  
10  
11  
12  
13  
14  
15  
16  
17  
18  
19  
20  
21  
22  
23  
24  
25  
26  
27  
28  
29  
30  
31  
32  
33  
34  
35  
36  
37  
38  
39  
40  
41  
42  
43  
44  
45  
46  
47  
48  
49  
50  
51  
52  
53  
54  
55  
56  
57  
58  
59  
60
- 112, 6127.
- [289] C. J. Cramer and D. G. Truhlar, *J. Am. Chem. Soc.*, 1991, **113**, 8305.
- [290] A. V. Marenich, R. M. Olson, C. P. Kelly, C. J. Cramer and D. G. Truhlar, *J. Chem. Theory Comput.*, 2007, **3**, 2011.
- [291] A. V. Marenich, C. J. Cramer and D. G. Truhlar, *J. Chem. Theory Comput.*, 2013, **9**, 609.
- [292] A. Klamt, *J. Phys. Chem.*, 1995, **99**, 2225.
- [293] A. Klamt, F. Eckert and W. Arlt, *Annu. Rev. Chem. Biomol. Eng.*, 2010, **1**, 101–122.
- [294] H. L. Woodcock, W. Zheng, A. Ghysels, Y. Shao, J. Kong and B. R. Brooks, *J. Chem. Phys.*, 2008, **129**, 214109.
- [295] A. Ghysels, H. L. Woodcock, J. D. Larkin, B. T. Miller, Y. Shao, J. Kong, D. V. Neck, V. V. Speybroeck, M. Waroquier and B. R. Brooks, *J. Chem. Theory Comput.*, 2011, **7**, 496–514.
- [296] T. Benighaus and W. Thiel, *J. Chem. Theory Comput.*, 2009, **5**, 3114–3128.
- [297] J. Zienau and Q. Cui, *J. Phys. Chem. B*, 2012, **116**, 12522–12534.
- [298] B. T. Miller, R. P. Singh, J. B. Klauda, M. Hodoscek, B. R. Brooks and H. L. Woodcock III, *J. Chem. Inf. Model.*, 2008, **48**, 1920.
- [299] Z. C. Holden, R. M. Richard and J. M. Herbert, *J. Chem. Phys.*, 2013, **139**, 244108.
- [300] J. M. Herbert and A. W. Lange, in *Many-Body Effects and Electrostatics in Multi-Scale Computations of Biomolecules*, ed. Q. Cui, P. Ren and M. Meuwly, 2014.
- [301] P. N. Day, J. H. Jensen, M. S. Gordon, S. P. Webb, W. J. Stevens, M. Krauss, D. Garmer, H. Basch and D. Cohen, *J. Chem. Phys.*, 1996, **105**, 1968.
- [302] M. S. Gordon, M. A. Freitag, P. Bandyopadhyay, J. H. Jensen, V. Kairys and W. J. Stevens, *J. Phys. Chem. A*, 2001, **105**, 293.
- [303] M. S. Gordon, L. V. Slipchenko, H. Li and J. H. Jensen, *Annual Rep. Comp. Chem.*, 2007, **3**, 177–193.
- [304] M. S. Gordon, D. G. Fedorov, S. R. Pruitt and L. V. Slipchenko, *Chem. Rev.*, 2012, **112**, 632.
- [305] J. C. Flick, D. Kosenkov, E. G. Hohenstein, C. D. Sherrill and L. V. Slipchenko, *J. Chem. Theory Comput.*, 2012, **8**, 2835.
- [306] K. U. Lao and J. M. Herbert, *J. Phys. Chem. Lett.*, 2012, **3**, 3241.
- [307] K. U. Lao and J. M. Herbert, *J. Chem. Phys.*, 2013, **139**, 034107.
- [308] L. V. Slipchenko, *J. Phys. Chem. A*, 2010, **114**, 8824.
- [309] D. Kosenkov and L. V. Slipchenko, *J. Phys. Chem. A*, 2011, **115**, 392.
- [310] D. Ghosh, O. Isayev, L. Slipchenko and A. Krylov, *J. Phys. Chem. A*, 2011, **115**, 6028–6038.
- [311] D. Ghosh, A. Roy, R. Seidel, B. Winter, S. Bradforth and A. Krylov, *J. Phys. Chem. B*, 2012, **116**, 7269–7280.
- [312] M. Gordon and M. Schmidt, in *Advances in Electronic Structure Theory: GAMESS a Decade Later*, Elsevier, 2005, ch. 41.
- [313] I. A. Kaliman and L. V. Slipchenko.
- [314] E. Dahlke and D. G. Truhlar, *J. Chem. Theory Comput.*, 2007, **3**, 46.
- [315] C. M. Breneman and K. B. Wiberg, *J. Comput. Chem.*, 1990, **11**, 361.
- [316] R. M. Richard and J. M. Herbert, *J. Chem. Phys.*, 2012, **137**, 064113.
- [317] L. D. Jacobson and J. M. Herbert, *J. Chem. Phys.*, 2011, **134**, 094118.
- [318] J. M. Herbert, L. D. Jacobson, K. U. Lao and M. A. Rohrdanz, *Phys. Chem. Chem. Phys.*, 2012, **14**, 7679.
- [319] B. Jeziorski, R. Moszynski and K. Szalewicz, *Chem. Rev.*, 1994, **94**, 1887.
- [320] J. Řezáč and P. Hobza, *J. Chem. Theory Comput.*, 2012, **8**, 141.
- [321] S. A. Maurer, M. Beer, D. S. Lambrecht and C. Ochsenfeld, *J. Chem. Phys.*, 2013, **139**, 184104.
- [322] T. Förster, *Ann. Phys. (Leipzig)*, 1948, **2**, 55–75.
- [323] Z.-Q. You and C.-P. Hsu, *J. Phys. Chem. A*, 2011, **115**, 4092–4100.
- [324] M. A. Baldo, S. Lamansky, P. E. Burrows, M. E. Thompson and S. R. Forrest, *Appl. Phys. Lett.*, 1999, **75**, 4–6.
- [325] *Highly Efficient OLEDs with Phosphorescent Materials*, ed. H. Yersin, Wiley-VCH, 2008.
- [326] P. A. M. Dirac, *Proc. R. Soc. Lond. A*, 1927, **114**, 243–265.
- [327] C.-P. Hsu, Z.-Q. You and H.-C. Chen, *J. Phys. Chem. C*, 2008, **112**, 1204.
- [328] C.-P. Hsu, *Acc. Chem. Res.*, 2009, **42**, 509–518.
- [329] Z.-Q. You and C.-P. Hsu, *J. Chem. Phys.*, 2010, **133**, 074105.
- [330] Z.-Q. You and C.-P. Hsu, *Int. J. Quan. Chem.*, 2014, **114**, 102–115.
- [331] D. L. Dexter, *J. Chem. Phys.*, 1953, **21**, 836–850.
- [332] R. McWeeny, *Methods of Molecular Quantum Mechanics*, Academic Press, New York, 2nd edn., 1992.
- [333] C.-P. Hsu, G. R. Fleming, M. Head-Gordon and T. Head-Gordon, *J. Chem. Phys.*, 2001,



- 114, 3065–3072.
- [334] S.-I. Choi, J. Jortner, S. A. Rice and R. Silbey, *J. Chem. Phys.*, 1964, **41**, 3294–3306.
- [335] R. D. Harcourt, G. D. Scholes and K. P. Ghiggino, *J. Chem. Phys.*, 1994, **101**, 10521–10525.
- [336] M. F. Iozzi, B. Mennucci, J. Tomasi and R. Cammi, *J. Chem. Phys.*, 2004, **120**, 7029–7040.
- [337] G. D. Scholes, C. Curutchet, B. Mennucci, R. Cammi and J. Tomasi, *J. Phys. Chem. B*, 2007, **111**, 6978–6982.
- [338] C. Curutchet, G. D. Scholes, B. Mennucci and R. Cammi, *J. Phys. Chem. B*, 2007, **111**, 13253–13265.
- [339] T. Van Voorhis, T. Kowalczyk, B. Kaduk, L. P. Wang, C. L. Cheng and Q. Wu, *Ann. Rev. Phys. Chem.*, 2010, **61**, 149–170.
- [340] B. Kaduk, T. Kowalczyk and T. Van Voorhis, *Chem. Rev.*, 2012, **112**, 321–370.
- [341] P. H. Dederichs, S. Blügel, R. Zeller and H. Akai, *Phys. Rev. Lett.*, 1984, **53**, 2512–2515.
- [342] Q. Wu and T. Van Voorhis, *Phys. Rev. A*, 2005, **72**, 024502.
- [343] Q. Wu and T. Van Voorhis, *J. Chem. Theo. Comp.*, 2006, **2**, 765–774.
- [344] Q. Wu and T. Van Voorhis, *J. Phys. Chem. A*, 2006, **110**, 9212–9218.
- [345] I. Rudra, Q. Wu and T. Van Voorhis, *J. Chem. Phys.*, 2006, **24**, 024103.
- [346] Q. Wu and T. Van Voorhis, *J. Chem. Phys.*, 2006, **125**, 164105.
- [347] Q. Wu, C. L. Cheng and T. Van Voorhis, *J. Chem. Phys.*, 2007, **127**, 164119.
- [348] Q. Wu, B. Kaduk and T. Van Voorhis, *J. Chem. Phys.*, 2009, **130**, 034109.
- [349] B. Kaduk and T. Van Voorhis, *J. Chem. Phys.*, 2010, **133**, 061102.
- [350] B. Kaduk, T. Tsuchimochi and T. Van Voorhis, *J. Chem. Phys.*, 2014, **140**, 18A503.
- [351] J. E. Subotnik, S. Yeganeh, R. J. Cave and M. A. Ratner, *J. Chem. Phys.*, 2008, **129**, 244101.
- [352] J. E. Subotnik, R. J. Cave, R. P. Steele and N. Shenvi, *J. Chem. Phys.*, 2009, **130**, 234102.
- [353] J. E. Subotnik, J. Vura-Weis, A. Sodt and M. A. Ratner, *J. Phys. Chem. A*, 2010, **114**, 8665.
- [354] J. Vura-Weis, M. Wasielewski, M. D. Newton and J. E. Subotnik, *J. Phys. Chem. C*, 2010, **114**, 20449.
- [355] D. R. Yarkony, in *Conical Intersections: Electronic Structure, Dynamics and Spectroscopy*, ed. W. Domcke, D. R. Yarkony and H. Koppel, World Scientific Publishing Co., New Jersey, 2004, pp. 41–128.
- [356] S. Fatehi, E. Alguire, Y. Shao and J. E. Subotnik, *J. Chem. Phys.*, 2011, **135**, 234105.
- [357] C. P. Collier, G. Mattersteig, E. W. Wong, Y. Luo, K. Beverly, J. Sampaio, F. M. Raymo, J. F. Stoddart and J. R. Heath, *Science*, 2000, **289**, 1172–1175.
- [358] T. Rueckes, K. Kim, E. Joselevich, G. Y. Tseng, C. L. Cheung and C. M. Lieber, *Science*, 2000, **289**, 94–97.
- [359] J. M. Tour, A. M. Rawlett, M. Kozaki, Y. X. Yao, R. C. Jagessar, S. M. Dirk, D. W. Price, M. A. Reed, C. W. Zhou, J. Chen, W. Y. Wang and I. Campbell, *Chem.-Eur. J.*, 2001, **7**, 5118–5134.
- [360] F. R. F. Fan, J. P. Yang, L. T. Cai, D. W. Price, S. M. Dirk, D. V. Kosynkin, Y. X. Yao, A. M. Rawlett, J. M. Tour and A. J. Bard, *J. Am. Chem. Soc.*, 2002, **124**, 5550–5560.
- [361] J. Park, A. N. Pasupathy, J. I. Goldsmith, C. Chang, Y. Yaish, J. R. Petta, M. Rinkoski, J. P. Sethna, H. D. Abruna, P. L. McEuen and D. C. Ralph, *Nature*, 2002, **417**, 722–725.
- [362] W. J. Liang, M. P. Shores, M. Bockrath, J. R. Long and H. Park, *Nature*, 2002, **417**, 725–729.
- [363] Y. Luo, C. P. Collier, J. O. Jeppesen, K. A. Nielsen, E. Delonno, G. Ho, J. Perkins, H. R. Tseng, T. Yamamoto, J. F. Stoddart and J. R. Heath, *ChemPhysChem*, 2002, **3**, 519.
- [364] R. M. Metzger, *Chem. Rev.*, 2003, **103**, 3803–3834.
- [365] A. Nitzan and M. A. Ratner, *Science*, 2003, **300**, 1384–1389.
- [366] W. Tian, S. Datta, S. Hong, R. Reifengerger, J. I. Henderson and C. P. Kubiak, *J. Chem. Phys.*, 1998, **109**, 2874–2882.
- [367] S. N. Yaliraki, A. E. Roitberg, C. Gonzalez, V. Mujica and M. A. Ratner, *J. Chem. Phys.*, 1999, **111**, 6997–7002.
- [368] M. Di Ventra, S. T. Pantelides and N. D. Lang, *Phys. Rev. Lett.*, 2000, **84**, 979–982.
- [369] Y. Xue, S. Datta and M. A. Ratner, *Chem. Phys*, 2002, **281**, 151–170.
- [370] K. Stokbro, J. Taylor, M. Brandbyge, J. L. Mozos and P. Ordejon, *Comput. Mater. Sci*, 2002, **27**, 151–160.
- [371] R. Landauer, *Philos. Mag.*, 1970, **21**, 863.
- [372] P. F. Bagwell and T. P. Orlando, *Phys. Rev. B*, 1989, **40**, 1456–1464.
- [373] Y. Imry and R. Landauer, *Rev. Mod. Phys.*, 1999, **71**, S306–S312.
- [374] S. Datta, *Electronic Transport in Mesoscopic Systems*, Cambridge University Press, New York, 1995.



- [375] M. P. Samanta, W. Tian, S. Datta, J. I. Henderson and C. P. Kubiak, *Phys. Rev. B*, 1996, **53**, R7626–R7629.
- [376] J. Taylor, H. Guo and J. Wang, *Phys. Rev. B*, 2001, **63**, 245407.
- [377] M. Brandbyge, J. L. Mozos, P. Ordejón, J. Taylor and K. Stokbro, *Phys. Rev. B*, 2002, **65**, 165401.
- [378] Y. Chen, A. Prociuk, T. Perrine and B. D. Dunietz, *Phys. Rev. B*, 2006, **74**, 245320.
- [379] M. Das and B. D. Dunietz, *J. Phys. Chem. C*, 2007, **111**, 1535–1540.
- [380] T. Perrine and B. D. Dunietz, *Phys. Rev. B*, 2007, **75**, 195319.
- [381] T. Perrine and B. D. Dunietz, *Nanotechnology*, 2007, **18**, 424003.
- [382] T. M. Perrine, R. G. Smith, C. Marsh and B. D. Dunietz, *J. Chem. Phys.*, 2008, **128**, 154706.
- [383] T. Perrine and B. D. Dunietz, *J. Phys. Chem. A*, 2008, **112**, 2043.
- [384] T. M. Perrine, T. Berto and B. D. Dunietz, *J. Phys. Chem. B*, 2008, **112**, 16070–16075.
- [385] Z. Zhao and B. D. Dunietz, *J. Chem. Phys.*, 2008, **129**, 024702.
- [386] T. Perrine and B. D. Dunietz, *J. Am. Chem. Soc.*, 2010, **132**, 2914–2918.
- [387] B. Ding, V. Washington and B. D. Dunietz, *Mol. Phys.*, 2010, **108**, 2591.
- [388] A. Tan, J. Balachandran, S. Sadat, V. Gavini, B. D. Dunietz, S.-Y. Jang and P. Reddy, *J. Am. Chem. Soc.*, 2011, **133**, 8838–8841.
- [389] R. Balachandran, P. Reddy, B. D. Dunietz and V. Gavini, *J. Phys. Chem. Lett.*, 2012, **3**, 1962.
- [390] R. Balachandran, P. Reddy, B. D. Dunietz and V. Gavini, *J. Phys. Chem. Lett.*, 2013, **4**, 3825–3833.
- [391] A. Prociuk, B. Van Kuiken and B. D. Dunietz, *J. Chem. Phys.*, 2006, **125**, 204717.
- [392] P. Pal and B. D. Dunietz, *J. Chem. Phys.*, 2012, **137**, 194104.
- [393] A. E. Reed, R. B. Weinstock and F. Weinhold, *J. Chem. Phys.*, 1985, **83**, 735–746.
- [394] A. E. Reed, L. A. Curtiss and F. Weinhold, *Chem. Rev.*, 1988, **88**, 899–926.
- [395] F. Weinhold and C. Landis, *Valency and Bonding: A Natural Bond Orbital Donor-Acceptor Perspective*, Cambridge University Press, Cambridge, 2005, p. 760.
- [396] E. D. Glendening, C. R. Landis and F. Weinhold, *WIREs Comput. Mol. Sci.*, 2012, **2**, 1–42.
- [397] R. Z. Khaliullin, E. A. Cobar, R. C. Lochan, A. T. Bell and M. Head-Gordon, *J. Phys. Chem. A*, 2007, **111**, 8753.
- [398] K. Kitaura and K. Morokuma, *Int. J. Quantum Chem.*, 1976, **10**, 325–340.
- [399] Y. R. Mo, J. L. Gao and S. D. Peyerimhoff, *J. Chem. Phys.*, 2000, **112**, 5530–5538.
- [400] Y. Mo, P. Bao and J. Gao, *Phys. Chem. Chem. Phys.*, 2011, **13**, 6760–6775.
- [401] R. J. Azar, P. R. Horn, E. J. Sundstrom and M. Head-Gordon, *J. Chem. Phys.*, 2013, **138**, 084102.
- [402] P. R. Horn, E. J. Sundstrom, T. A. Baker and M. Head-Gordon, *J. Chem. Phys.*, 2013, **138**, 134119.
- [403] R. Z. Khaliullin, M. Head-Gordon and A. T. Bell, *J. Chem. Phys.*, 2006, **124**, 204105.
- [404] R. Z. Khaliullin, A. T. Bell and M. Head-Gordon, *J. Chem. Phys.*, 2008, **128**, 184112.
- [405] F. Bell, Q. N. Ruan, A. Golan, P. R. Horn, M. Ahmed, S. R. Leone and M. Head-Gordon, *J. Am. Chem. Soc.*, 2013, **135**, 14229–14239.
- [406] M. Head-Gordon, A. M. Grana, D. Maurice and C. A. White, *J. Phys. Chem.*, 1995, **99**, 14261.
- [407] A. V. Luzanov, A. A. Sukhorukov and V. E. Umanskii, *Theor. Exp. Chem.*, 1976, **10**, 354.
- [408] R. L. Martin, *J. Chem. Phys.*, 2003, **118**, 4775.
- [409] I. Mayer, *Chem. Phys. Lett.*, 2007, **437**, 284.
- [410] H. Shao, J. Seifert, N. C. Romano, M. Gao, J. J. Helmus, C. P. Jaronec, D. A. Modarelli and J. R. Parquette, *Angew. Chem. Int. Ed. Engl.*, 2010, **49**, 7688–7691.
- [411] D. Ghosh, D. Kosenkov, V. Vanovschi, J. Flick, I. Kaliman, Y. Shao, A. Gilbert, L. Slipchenko and A. Krylov, *J. Comput. Chem.*, 2013, **34**, 1060–1070.
- [412] N. M. O’Boyle, M. Banck, C. A. James, C. Morley, T. Vandermeersch and G. R. Hutchison, *J. Cheminf.*, 2011, **3**, 33.
- [413] T. Pilati and A. Forni, *J. Appl. Cryst.*, 1998, **31**, 503.
- [414] M. D. Hanwell, D. E. Curtis, D. C. Lonie, T. Vandermeersch, E. Zurek and G. R. Hutchinson, *J. Cheminform.*, 2012, **4**, 17.
- [415] G. Schaftenaar and J. H. Noordik, *J. Comput.-Aided Mol. Design*, 2000, **14**, 123.
- [416] WebMO: Schmidt, J.R.; Polik, W.F. WebMO Enterprise, version 14.0; WebMO LLC: Holland, MI, USA, 2014; <http://www.webmo.net>.